SMC-TR-97-10

AEROSPACE REPORT NO.
TR-97(1410)-4

Ground Cloud Dispersion Measurements During The Titan IV Mission #K16 (24 April 1996) at Cape Canaveral Air Station

Volume 1—Test Overview and Data Summary

31 March 1997

Assembled by

Environmental Systems Directorate
Systems Engineering
Space Launch Operations

Prepared for

Launch Programs
SPACE AND MISSILE SYSTEMS CENTER
AIR FORCE MATERIEL COMMAND
2430 E. El Segundo Boulevard
Los Angeles Air Force Base, CA 90245

Space Systems Group

THE AEROSPACE CORPORATION
El Segundo, California

This report was submitted by The Aerospace Corporation, El Segundo, CA 90245-4691, under Contract No. F04701-93-C-0094 with the Space and Missile Systems Center, 2430 E. El Segundo Blvd., Los Angeles Air Force Base, CA 90245. It was reviewed and approved for The Aerospace Corporation by N. F. Dowling Systems Director, Environmental Systems, Systems Engineering Directorate.

This report has been reviewed by the Public Affairs Office (PAS) and is releasable to the National Technical Information Service (NTIS). At NTIS, it will be available to the general public, including foreign nationals.

This technical report has been reviewed and is approved for publication. Publication of this report does not constitute Air Force approval of the report's findings or conclusions. It is published only for the exchange and stimulation of ideas.

R. Reiners, Maj, USAF
SMC/CLN

REPORT DOCUMENTATION PAGE

Form Approved
OMB No. 0704-0188

1. AGENCY USE ONLY (*Leave blank*)	2. REPORT DATE	3. REPORT TYPE AND DATES COVERED
	31 March 1997	

4. TITLE AND SUBTITLE
Ground Cloud Dispersion Measurements During The Titan IV Mission #K16 (24 April 1996) at Cape Canaveral Air Station — Vol. 1 Test Overview and Data Summary

5. FUNDING NUMBERS
F04701-93-C-0094

6. AUTHOR(S)
Environmental Systems Directorate

7. PERFORMING ORGANIZATION NAME(S) AND ADDRESS(ES)
The Aerospace Corporation
Technology Operations
El Segundo, CA 90245-4691

8. PERFORMING ORGANIZATION REPORT NUMBER
TR-97(1410)-4

9. SPONSORING/MONITORING AGENCY NAME(S) AND ADDRESS(ES)
Space and Missile Systems Center
Air Force Materiel Command
2430 E. El Segundo Boulevard
Los Angeles Air Force Base, CA 90245

10. SPONSORING/MONITORING AGENCY REPORT NUMBER
SMC-TR-97-10

11. SUPPLEMENTARY NOTES

12a. DISTRIBUTION/AVAILABILITY STATEMENT
Approved for public release; distribution unlimited

12b. DISTRIBUTION CODE

13. ABSTRACT (*Maximum 200 words*)

Launch plume imagery and aircraft measurement of HCl were accomplished during the launch of Titan IV Mission #K16 at Cape Canaveral Air Station on 24 April 1996. These data will be used to determine the accuracy of the Rocket Exhaust Effluent Diffusion Model. The imagery, recorded at three camera sites, showed a cloud stabilization height of 1023 m above MSL (35% higher than predicted); the height was reached 3.5 min after launch (20% faster than predicted). The cloud had a south-southwesterly trajectory (compared to an east-southeasterly prediction) and an average speed of 3.6 m/s (38% slower than predicted). The imagery documented a large displacement between the upper and lower portions of the ground cloud due to variations in wind speed and direction with altitude. Aircraft measurements, using a modified Geomet instrument in a Piper Seminole aircraft, documented the movement of the lower cloud immediately after launch, the mixing of HCl to altitudes as low as ground level, and the movement of the upper cloud portion first to the southeast and then to the east. The sampling aircraft entered the plume about 3.5 min after launch, made 36 passes, and measured HCl concentrations ranging from 2 to 21 parts per million.

14. SUBJECT TERMS
Toxic launch cloud, Toxic hazard corridors, Atmospheric dispersion models, Launch clouod development and dispersion, Launch cloud imagery, HCl monitoring

15. NUMBER OF PAGES
100

16. PRICE CODE

17. SECURITY CLASSIFICATION OF REPORT	18. SECURITY CLASSIFICATION OF THIS PAGE	19. SECURITY CLASSIFICATION OF ABSTRACT	20. LIMITATION OF ABSTRACT
UNCLASSIFIED	UNCLASSIFIED	UNCLASSIFIED	

Preface

The Air Force Space and Missile Systems Center's Launch Programs Office (SMC/CL) is sponsoring the Atmospheric Dispersion Model Validation Program (MVP). This program is collecting launch cloud dispersion data that will be used to determine the accuracy of atmospheric dispersion models, such as REEDM, in predicting toxic hazard corridors at the launch ranges. This report presents launch cloud dispersion and meteorological measurements performed during the #K16 Titan IV launch at Cape Canaveral Air Station on 24 April 1996.

An MVP Integrated Product Team (IPT) led by Capt. Brian Laine (SMC/CLNM) is directing the MVP effort. Dr. Bart Lundblad of The Aerospace Corporation's Environmental Systems Directorate (ESD) is the MVP technical manager. This report was prepared by Mr. Norm Keegan (ESD) and Dr. Lundblad from materials contributed by personnel participating in the #K16 launch cloud dispersion measurements.

Visible imagery measurements of the launch cloud were made by Dr. Robert Abernathy, Ms. Karen Foster, and Ms. Janet Webb of The Aerospace Corporation's Environmental Monitoring and Technology Department (EMTD). Field assistance was provided by Mr. John Ligda, Mr. Kent Evans, and Mr. James Beardall of the Aerospace Eastern Range Directorate, and Dr. Bart Lundblad. Mr. Doug Schulthess of Aerospace's Eastern Range Directorate coordinated site selection and logistical support with Range organizations. Ms. Foster digitized the imagery data for analysis by Dr. Abernathy. The description of the cloud imagery results was prepared by Dr. Abernathy.

The aircraft-based HCl measurement effort was managed by Mr. Marv Becker and Mr. Pete Mazur of SRS Technologies. The Piper Seminole sampling aircraft is owned and operated by the Florida Institute of Technology. The aircraft was outfitted with a Geomet HCl detector that was modified and calibrated for airborne sampling by Mr. Paul Yocom of the NASA Toxic Vapor Detection/Contamination Monitoring Laboratory. Ms. Jeanne Hawkins of the 45th Medical Group Bioenvironmental Engineering Services (45 AMDS/SGPB) was onboard the aircraft during the sampling measurements to monitor Geomet performance and cockpit contamination. The onboard data logger and GPS system was provided and installed by Mr. Shane Beard of NOAA's Environmental Research Laboratories. The raw aircraft sampling data was processed and analyzed by Dr. Abernathy. Ground sampling of HCl outside of the launch pad area was not conducted during the #K16 launch.

The meteorological data displayed in this report was provided by Mr. Randy Evans of the NASA Applied Meteorology Unit and ENSCO, Inc.

The #K16 mission was the sixth Titan IV launch for which usable launch cloud dispersion data was collected by MVP. The previous missions were #K7, #K23, #K19, #K21, and #K15. It was

the third Titan IV launch to employ an aircraft to collect HCl dispersion data. The previous airborne sampling activities were following the #K23 and #K15 launches.

Contents

Figures

Tables

Executive Summary

This report presents plume imagery and aircraft-based hydrogen chloride (HCl) sampling data documenting the development and dispersion of the Titan IV #K16 launch plume at Cape Canaveral Air Station (CCAS). The HCl is measured in both dry gas and aerosol forms. The report also presents pertinent meteorological data taken from towers and rawinsonde.

The imaging team successfully tracked the trajectory and time evolution of the vehicle's exhaust plume for 55 min following launch using two visible-light video camera systems. A twin-engine Piper Seminole aircraft, equipped with a Geomet total HCl analyzer, was used to measure HCl concentrations within the plume as a function of time for approximately 88 min.

To provide modeling input data, rawinsonde data were measured shortly before launch, and meteorological tower data were measured before launch and during dispersion of the launch plume. These data and similar data on other Titan IV launches (past and future) will be used along with tracer gas release campaigns to determine the accuracy of atmospheric dispersion models such as REEDM in predicting toxic hazard corridors (THCs) at the USAF Eastern and Western Ranges. These THCs, in turn, assess the risk of exposing the public and base personnel to HCl exhaust from solid rocket motors or hypergolic propellant vapors accidentally released during launch operations.

The #K16 launch occurred on 24 April 1996 at 2337 Zulu time. The sampling aircraft entered the plume approximately 3.5 min after launch and made 36 passes through the plume. HCl concentrations from 2 to 21 parts per million (ppm) were measured during these passes.

Imagery from visible-only imagers was obtained at two sites. Reduction of the first 55 min of these data yielded the rise time, stabilization height, dimensions, ground track and speed, and growth rate of the ground cloud. The T–0.7 h REEDM predictions were substantially different from those measured by imagery. According to the quantitative visible imagery from UCS-7 and Press sites, the cloud took 3.5 min to stabilize (20% faster than predicted), stabilized at 1023 m in altitude (35% higher than predicted), moved in a south-southwesterly direction (versus the east-southeasterly prediction), and moved at an average speed of 3.6 m/s (38% slower than predicted).

1. Introduction

There is a strong need to collect launch cloud data that can be used to validate the performance of atmospheric dispersion models used to predict the transport and diffusion of hazardous species that may be released into the atmosphere during Air Force launch vehicle operations. Launch vehicles that employ solid propellant rocket motors release ground clouds into the Eastern Range and Western Range launch areas at Cape Canaveral Air Station (CCAS) and Vandenberg Air Force Base (VAFB), respectively, that contain large amounts of hydrogen chloride (HCl). Large quantities of hazardous hydrazine fuels or the nitrogen tetroxide oxidizer could also be accidentally released at the ranges during propellant transfer operations or due to a launch vehicle failure.

The Air Force launch range safety organizations of the 45th Space Wing at Patrick Air Force Base (45 SPW/SE) and 30th Space Wing at VAFB (30 SPW/SE) are responsible for assuring that launches are carried out only when meteorological conditions are such that nearby communities cannot be exposed to hazardous levels of HCl, the hydrazine fuels, or N_2O_4/NO_2. Predictions of toxic hazard corridors (THCs) that extend into public areas can lead to costly launch delays. The present use of non-validated models requires the use of conservative launch criteria. The development and validation of accurate atmospheric dispersion models is expected to increase launch opportunities and significantly reduce launch costs. The Space and Missile System Center's Launch Programs Office (SMC/CL) established the Atmospheric Dispersion Model Validation Program (MVP). MVP is collecting data to determine the accuracy of current and future atmospheric dispersion and chemical kinetic models in predicting THCs during launches of Titan and other vehicles at CCAS and VAFB.

The MVP effort involves the collection of data during Titan launches at CCAS and VAFB to characterize HCl launch cloud rise, growth, and stabilization, as well as launch cloud transport and diffusion. These data, as well as data from tracer gas releases, will, in particular, be used to determine the capability of the Rocket Exhaust Effluent Diffusion Model (REEDM) for predicting THCs at the launch ranges. REEDM is used at CCAS and VAFB to predict the locations of THCs in support of launch operations. It is applied to large heated sources of toxic air emissions such as nominal launches, catastrophic failure fireballs, and inadvertent ignitions of solid rocket motors. It uses launch vehicle and meteorological data to generate ground-level concentration isopleths of HCl, hydrazine fuels, NO_2, and other toxic launch emissions. Launch holds may occur when REEDM toxic concentration predictions exceed adopted exposure standards. REEDM is a unique and complex model based on relatively simple modeling physics. It has a long developmental history with the Air Force and NASA, but has never been fully validated. Validation of REEDM has been identified as a range safety priority.

The MVP has been organized and is being directed by the MVP Integrated Product Team (IPT). SMC/CL is serving as the IPT leader, while The Aerospace Corporation's Environmental Systems Directorate is the IPT technical manager. The IPT consists of personnel with expertise in atmospheric dispersion modeling, meteorology, and atmospheric concentration field measurements. MVP participants include personnel from 30 and 45 SPW, SMC, The Aerospace Corporation,

NASA, NOAA, and contractors. Key functions include program planning, field data collection, data review and compilation, range coordination, and model validation.

This report presents the results of measurements performed at CCAS during the Titan IV #K16 launch. Visible imagery measurements were made on the launch cloud to monitor its growth, stabilization, and trajectory. An aircraft equipped with an HCl detector was flown through and below the visible cloud to measure HCl concentrations. The imagery results are presented in Section 2. The aircraft sampling results are presented in Section 3. REEDM predictions of ground-cloud stabilization heights and surface concentrations are presented in Appendix A. Measurements of meteorological data are tabulated in Appendix B. A description of the cloud sampling aircraft is presented in Appendix C.

The imagery data obtained show that, for the meteorological conditions present during the launch, the T–0.7 hour REEDM calculation underestimates the cloud's stabilization height (1023m vs. 756 m predicted). REEDM also underestimated the cloud's stabilization time (3.5 min vs. 4.4 min). The results presented in this, as well as previous and subsequent MVP reports, will allow the accuracy of REEDM and other launch range atmospheric dispersion models to be determined over the range of possible meteorological conditions.

2. Imagery of the Titan IV #K16 Ground Cloud

[The material in this section was contributed by R. N. Abernathy, B. P. Kasper, J. Y. Webb, and K. L. Foster of the Environmental Monitoring and Technology Department of The Aerospace Corporation's Space and Environment Technology Center]

2.1 Background

On 24 April 1996, the Titan IV #K16 mission was successfully launched from Space Launch Complex (SLC-41) at Cape Canaveral Air Station (CCAS) at 19:37 EDT (23:37 GMT). The launch window opened at 18:45 EDT. Due to the rupture of a rawinsonde balloon and unacceptable dispersion model predictions, this launch was delayed. This section describes the quantitative exhaust cloud imagery data collected by each of three imagery sites during the 55 min immediately following the launch from Space Launch Complex 41 (SLC-41). This section also describes the data acquisition hardware and analysis software. The two-dimensional cloud images obtained by the various imagery sites were combined in a pairwise fashion to produce stereoscopic 3-D information. This analysis yielded the cloud's rise time, stabilization height, speed, and trajectory.

The quantitative imagery-derived ground cloud data are reported here in several graphical formats to facilitate comparison with REEDM predictions (Appendix A), rawinsonde sounding data (Appendix B), and aircraft-based total HCl measurements (Section 3). For clarity, this chapter includes some data from other chapters and from the appendices. It is apparent from review of this section, that these data are useful for validating current and future dispersion models.

The purpose of this report was to document the quality and quantity of the #K16 exhaust cloud imagery data available for validating dispersion models. However, it is difficult to extract the data for a single instant in time from summary plots that contain many minutes of ground cloud data. Therefore, in order to facilitate the comparison of these data to individual dispersion model runs, a subsequent report will provide a detailed correlation between imagery and aircraft HCl concentration data. This subsequent detailed analysis will provide the data in a format that will allow direct comparison to model runs for specific times, altitudes, and distances from the release site.

The imagery-derived #K16 exhaust cloud imagery data are also available as comma-separated-variable files providing time and position for various ground cloud features. The raw visible imagery data are archived on VCR tapes. The selected visible images analyzed for this report are also archived on magneto-optical disks as digital image files.

2.2 Introduction

This section summarizes the results of quantitative visible imagery of the exhaust cloud from the Titan IV #K16 launch from SLC-41 at CCAS on 24 April 1996 at 19:37 EDT (23:37 GMT). Personnel from the Aerospace Corporation's Environmental Monitoring and Technology Department (EMTD) supported this launch with the deployment of three complete platforms of the Titan IV-dedicated Visible and Infrared Imaging System (VIRIS). For the #K16 evening

launch, three visible imagery systems were used to record imagery from perspectives that would permit post-launch reconstruction of the ground cloud speed and track as a function of time. The imagery sites chosen for the #K16 launch were UCS-7 (north-northwest of the SLC-41 complex), SLC-34 blockhouse (south-southeast of the complex), and the Press Site (east-northeast of the complex). These same sites were employed for the earlier launches of Titan IV #K23 and #K19.

Analysis of the quantitative imagery yielded the stabilization time, the stabilization height, the speed, and the trajectory of the "ground cloud" without recourse to additional data sources. The "ground cloud" is defined as the lower and more concentrated portion of the rocket's exhaust cloud that can diffuse to the ground. The "launch column" is defined as the trail of the rapidly moving rocket that extends above the more spherical "ground cloud."

Rawinsonde wind data were used to run "normal launch" REEDM predictions that were compared to the imagery-derived results. The T–0.7, T–0.5, and T–0.2 hour REEDM predictions are documented in Appendix A and referenced in this section. The T–0.7, T–0.5, and T–0.2 hour rawinsonde pre-launch meteorology data are documented in Appendix B and referenced in this section.

There was a huge wind shear between the upper and lower portions of the ground cloud. This caused the ground cloud to overfill the field of view of the imagers within 6 min of launch even though the imagers continued to pan the extent of the ground cloud until 55 min after launch. Hardware failure at the SLC-34 imaging site prevented the quantitative use of its imagery. Quantitative analysis of the visible imagery from the two fully functional sites for the first 6 min after launch documented the cloud's rise time, stabilization height, trajectory, and speed. These imagery-derived results are compared with rawinsonde data and REEDM predictions in this section and in Appendix A.

2.3 Field Deployment

2.3.1 Planning

The Aerospace Corporation's participants are listed in various subteams below. (Members of the imaging teams for #K16 are indicated with asterisks.)

Technology Operations
- Space and Environment Technology Center
  - Environmental Monitoring and Technology Department
    - R. N Abernathy*
    - K. L. Foster*
    - J. Y. Webb*

Space Launch Operations
- Systems Engineering Directorate
  - Environmental Systems
    - N. F. Dowling, Systems Director
    - H. L. Lundblad*
- Eastern Range
  - Systems Engineering Directorate
    - J. R. Ligda*

D. C. Evans*
J. H. Beardall*
D. R. Schulthess (in control room)

2.3.2 Equipment

The equipment at each site included all the hardware and software necessary to record and document the launch, to communicate between sites, and to supply backup power in case of an outage at the fixed power distribution points. The VIRIS consists of an array of three full and one backup (excluding the IR imager) cloud tracking systems and was designed and fabricated at the request of Space Launch Operations, Systems Engineering Directorate, at The Aerospace Corporation. Each full tracking system consists of coaligned, visible and infrared (IR) (8–12 μm) imagers, mounted on an azimuth- and elevation-encoding tripod, with an associated data acquisition and display console. The combination of visible and IR imagers permits cloud tracking in both daylight and darkness. The unique capabilities built into the VCR hardware include digital insertion of imager azimuth (Az), elevation (El), time, and GPS location. The system electronics are integrated in a single package, which has been ruggedized for field use. Prewiring of this package makes deployment of these imager systems straightforward, usually requiring less than 45 min for instrumentation at a site to become fully operational.

For the Titan IV #K16 mission, the operators at each site set the FOV of the visible imager to its maximum (i.e., $24_V° \times 32_h°$) using its 10 to 110 mm electronic zoom lens. Each operator continuously adjusted the iris setting to maximize contrast for detection of the edge of the ground cloud.

All three imaging systems deployed for the Titan IV #K16 mission were capable of total autonomy. Differential-ready GPS receivers documented each imager's position with moderate spatial resolution. Typically, 35 m is the precision in the horizontal plane, and 100 m is the precision in the vertical plane. Gasoline-powered AC generators (Honda Ex1000) are insurance against loss of fixed power. The Stirling cooler option for the AGEMA 900 series IR imagers was chosen so that liquid nitrogen would not be required at the sites. Each unit is transportable in a standard utility wagon (e.g., Ford Explorer).

The Az/El angle encoder for all imager systems was calibrated using reference objects (e.g., SLC-41) within the field of view of the imagers. When reference objects are not part of the geodetic survey database, the GPS location uncertainty is the dominant term in the positional accuracy. Imager pixelation and operator error in edge detection contribute as well to the error in defining the cloud boundary. The 0.07° step-size in the tripod angle encoders is a third source of error. The analysis accuracy is determined either by the availability of optimal references for Az/El calibration or by the step size for the tripod angle encoder. Typically the VIRIS system provides 0.1° accuracy in both elevation and azimuth.

2.4 Processing of Imagery Data

The processing of the imagery data requires several transformations that are performed upon return to The Aerospace Corporation:

1. Digitizing frames of the visible imagery.

2. Measuring the pixel locations of the reference sites within each image (i.e., FOV and angular calibration).

3. Measuring the pixel locations of cloud features in digitized images.

4. Converting pixel locations to azimuth and elevation readings.

5. Calculating cloud characteristics (i.e., position in Cartesian coordinates relative to the launch pad).

The processing requires the use of specialized hardware and software. Visible images of the cloud are digitized at precise times, beginning with time intervals of 15 s, then 30 s, then 1 min as the cloud evolves. When infrared imagery is used, the AGEMA 900 imagers produce digital images every 15 s in the field. A set of digitized images is selected for specific times following the launch and from each of the available imagery sites. Time, Az, and El are tabulated for each set. A setup file is created for each of these sets, containing all relevant information necessary to compute the cloud geometry. The Aerospace program **PLMTRACK** is run to digitize the x, y, and z coordinates of cloud features. The x and y coordinates are reported relative to the launch pad while the z coordinate is reported as height above MSL.

PLMTRACK is a software program developed in the Environmental Monitoring and Technology Department (EMTD) of The Aerospace Corporation by Brian P. Kasper. It is designed to analyze pairs of cloud images synchronized in time. When using the **PLMTRACK Line Method**, the operator selects the location of a particular cloud feature in the images from the two imager sites by moving a screen pointer to the desired feature in each image and clicking a mouse button. **PLMTRACK** then calculates the point of nearest approach to the two rays defined by the selected points. The three-dimensional location of this feature is then written to a data file.

Another implementation of **PLMTRACK** is illustrated in Figure 1. When using the **PLMTRACK Box Method**, the operator draws a rectangle about a cloud feature in the images from the two imager sites by moving a screen pointer to the extreme corners of the rectangles and clicking a mouse button. **PLMTRACK** then calculates the closest approach for various rays, as illustrated in Figure 1 and described below. The top of the cloud is defined by rays determining T1 and T2 (i.e., T1 $\times$ T2); the bottom is determined by rays defining B1 and B2 (i.e., B1 $\times$ B2); and the middle is defined by the geometric mean of top and bottom (i.e., M1 $\times$ M2). To define the "faces" of the "box," the points of closest approach for ray M1 with L2 and R2 (the left and right tangents to the cloud from Imager 2) are defined (i.e., M1 $\times$ L2 and M1 $\times$ R2). A similar procedure is used to define the points of closest approach for M2 with L1 and R1, yielding M2 $\times$ R1 and M2 $\times$ L1. In addition to the centers of the faces of the "box," the intersects of the left and right rays document the four vertices for the XY polygon. Thus, eleven points are defined for the six-faced "box" surrounding the cloud (a point in the center of each of the six faces, four vertices for the XY polygon, plus a middle point for the "box"). These eleven sets of x, y, and z coordinates are written to a file.

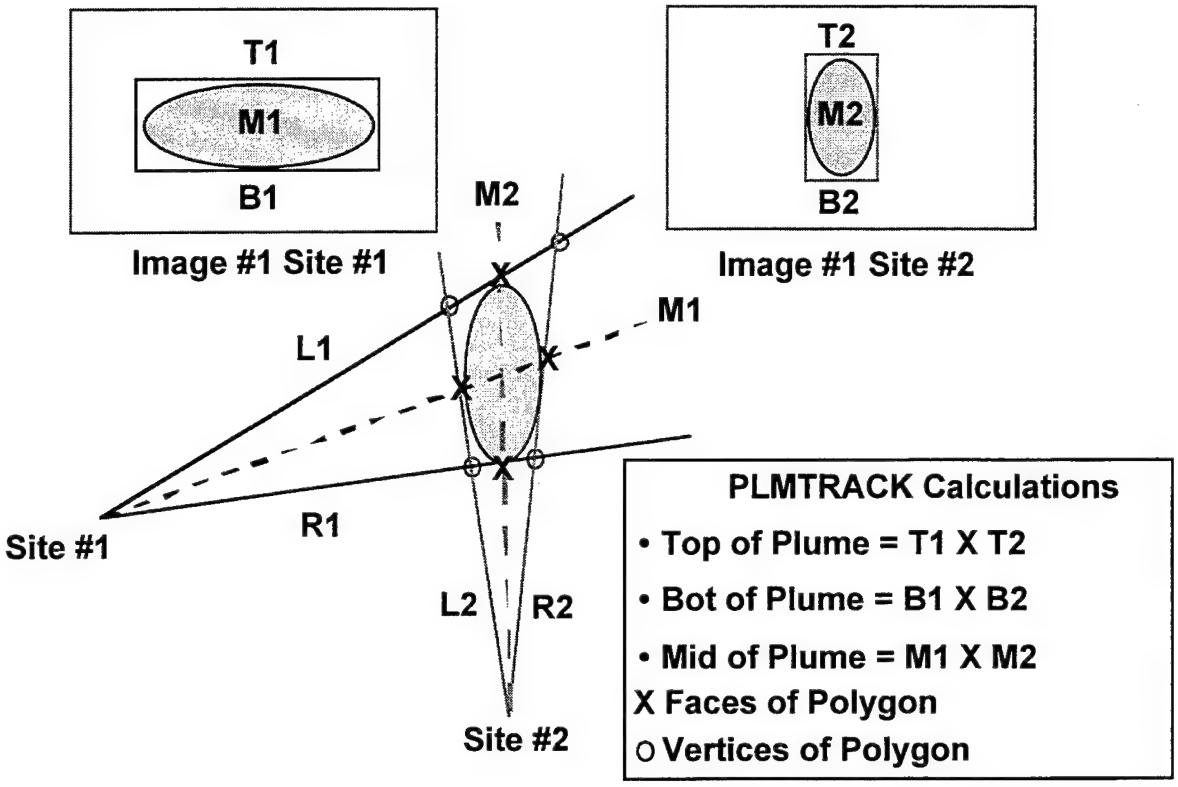

Figure 1. Implementation of the "box" method with two imagers.

When two imagers are viewing the cloud simultaneously, a four-sided polygon method (documented in Figure 2) has been employed as a way to document the maximum extent of the cloud (i.e., a ground-plane projection) for each set of images. With three imagers, there is a triply redundant determination of the top, middle, and bottom of the cloud by **PLMTRACK**, and a six-sided polygon can be used to determine the cloud's extent for each set of three images. The horizontal extent of the cloud is determined by defining the rays from each imager that are tangential to the widest part of the cloud as seen from that site. Projection of these extreme rays for each imager on the x-y ground plane forms a polygon that bounds all material in the cloud at all altitudes, as shown in Figure 2. Thus, one expects to see aircraft HCl sampling "hits" fall within this polygon, regardless of the sampling altitude. When the polygon area is combined with the mean cloud height (i.e., the difference between the top and the bottom of the cloud), one can obtain an upper bound for cloud volume. As illustrated in Figure 2 (a ground projection of the cloud's extent), the shaded area within the polygon typically overestimates the extent of the cloud (i.e., the smaller shape drawn within the polygon) when only two imagery sites are used.

The utility of the polygon method has been documented in a previous report for the #K23 mission. In that report, the polygons from imagery were correlated with the aircraft's HCl measurements of cloud dimensions and average HCl concentrations for the Titan IV #K23 launch cloud. After correcting for Geomet time response, the #K23 data set established that HCl concentrations detectable by an aircraft-based Geomet total HCl detector were mostly contained by the six-sided polygon areas for the first 20 min after launch. The #K23 data established that the imagery-derived position of the visible cloud correlates with the measurable HCl concentrations. A similar treatment is possible with the #K16 imagery and aircraft data. However, the extent of the cloud would have been more accurately mapped if the third camera site had correctly functioned during the #K16 mission.

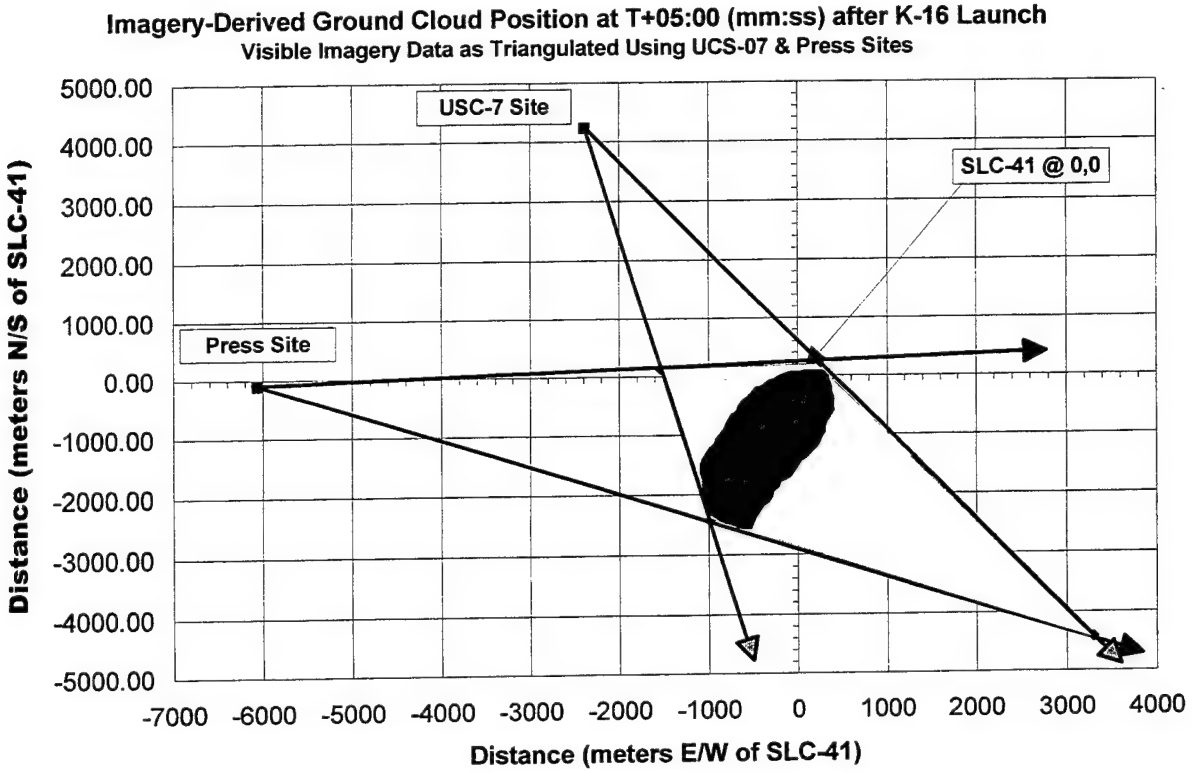

Figure 2. Implementation of the polygon method for two imagers. The imager positions and rays are actual #K16 data for T + 05:00 (mm:ss) after launch. The cloud's shape was synthesized for heuristic purposes to illustrate that the shaded polygon can overestimate the clouds extent.

2.5 Results and Discussion

2.5.1 Correlation of Ground Cloud Trajectory with Wind Direction

Figure 3 presents the imagery-derived and the T–0.7 hour REEDM-predicted ground cloud trajectories as arrows drawn on a map. Figure 3 also documents the rawinsonde wind directions at the imagery-derived top, middle, and bottom of the stabilized ground cloud. Lastly, Figure 3 documents the locations of the rawinsonde release site and of the three imager sites (UCS-7, Press Site, and SLC-34) used by The Aerospace Corporation while imaging the #K16 cloud. All directions are reported in rawinsonde convention (defined fully in Subsection 2.5.4). Briefly, the arrows indicate the direction the cloud would move for a wind coming from the indicated angle (clockwise from north).

As illustrated in Figure 3, the visible imagery revealed that the wind shear moved the bottom of the ground cloud along a 5° trajectory (i.e., wind from north-northeast pushing the cloud to the south-southwest). In contrast, the imagery documented that the top of the ground cloud remained almost stationary over the launch pad during the first 6 min after launch. The operators continued to pan the rapidly stretching ground cloud for 55 min after launch. They

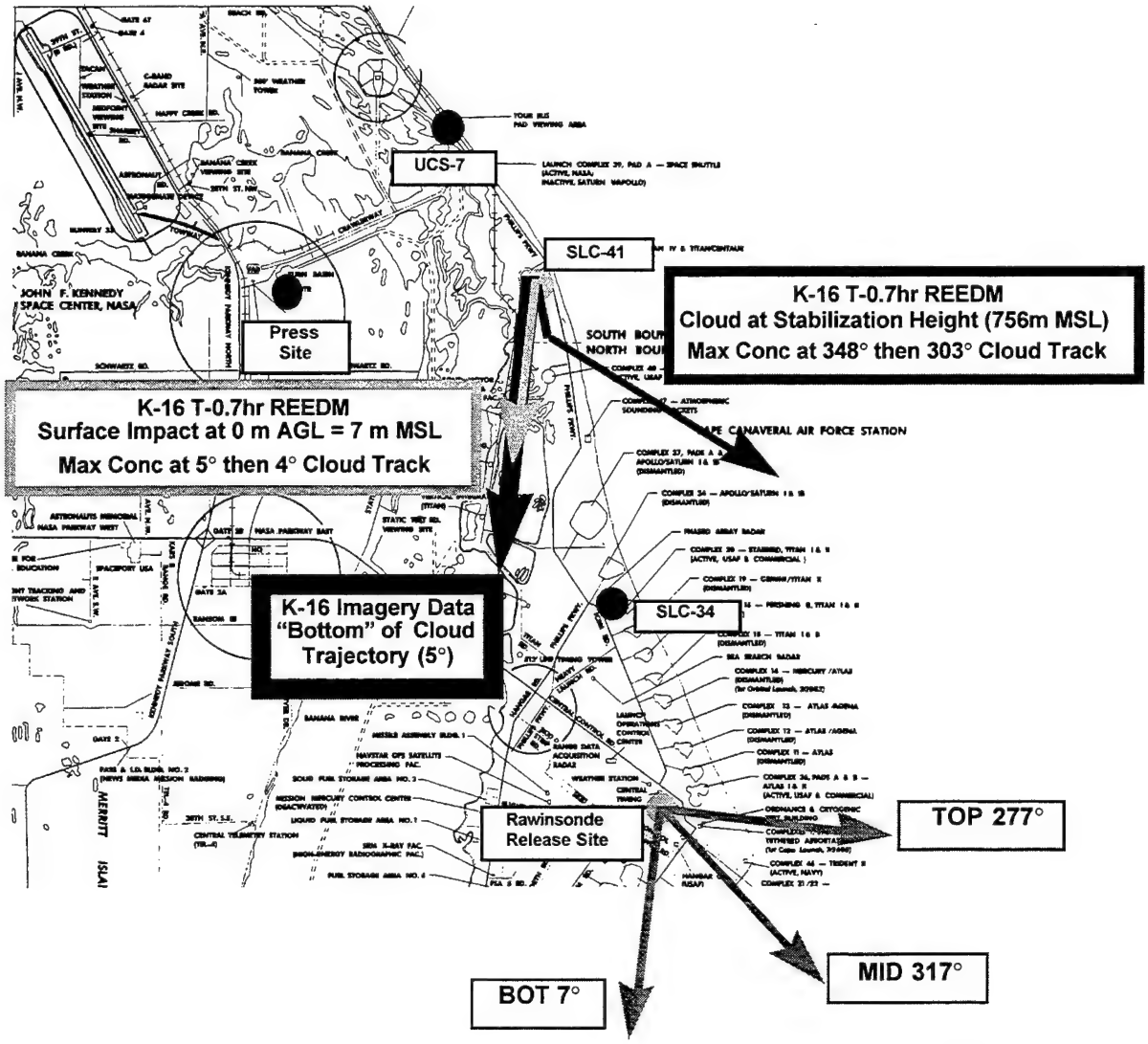

Figure 3. A map documenting the imagery sites, the rawinsonde release site, the #K16 ground cloud's track derived from visible imagery, the T–0.7 hour REEDM stabilized cloud track, and the 22:55 GMT (T–0.7 hour) rawinsonde wind vectors at the measured cloud stabilization heights.

observed the continued movement of the bottom of the ground cloud in a southwesterly direction throughout this period.

According to the T–0.7 hour REEDM prediction, the maximum cloud concentration at the predicted stabilization height of 756 m MSL should be along a heading of 348° (i.e., winds from north-northwest pushing the cloud to the south-southeast) at early times after launch. After stabilization, REEDM predicted a cloud bearing of 303 (i.e., winds from the west-northwest pushing the cloud to the east-southeast). This wind direction is the average wind for the second transition layer (674–1815 m AGL). REEDM used an altitude range of 206.7 to 1815 m AGL in computing the layer averages. REEDM predicted 214 m MSL (206.7 m AGL + 7 m) as the height of the bottom of the stabilized cloud. It is noteworthy that the imagery-derived bottom of the cloud (219 m MSL) is within the first mixing layer (0–674 m AGL according to the T–0.7 hour REEDM run). The imagery-derived ground cloud trajectory (5) is not consistent with

REEDM's T–0.7 hour prediction of 303 for the stabilization height, but instead is closer to the 4 prediction for the impact at ground level.

Appendix A includes not only the T–0.7 hour REEDM predictions (presented in Figure 3) but also the T–0.5 hour and T–0.2 hour predictions. The cloud headings were roughly southerly (i.e., winds from 4°, 340°, and 13°) at ground level and east southeasterly (i.e., winds from 303°, 297°, and 289°) at the predicted stabilization heights. The cloud trajectories (listed parenthetically in the previous sentence) are for the T–0.7, T–0.5, and T–0.2 hour predictions, respectively.

Figure 3 also presents the rawinsonde-derived wind directions associated with the bottom (7° wind at 202 m AGL), middle (317° wind at 1060 m AGL), and top (277° wind at 1815 m AGL) of the stabilized ground cloud. These winds are from the T–0.7 hour rawinsonde data and at the indicated sounding heights, which are close to the imagery-derived heights of 219 m MSL, 1023 m MSL, and 1877 m MSL for the bottom, middle, and top of the ground cloud, respectively. Since SLC-41 is at 7 m MSL, 7 m must be added to height AGL to convert it to height MSL. It is evident from examination of Figure 3 that there was a huge angular shear in wind direction at the altitudes occupied by the stabilized ground cloud. This wind shear is responsible for stretching the ground cloud, as observed by the imagery. The imagery documented that the high-altitude launch column moved out to sea (i.e., consistent with the 277° wind direction at the top of the cloud), while the lower portion of the ground cloud moved to the south southwest (i.e., consistent with 7° wind direction at the bottom of the cloud). The imagery documented that the upper portion of the ground cloud remained almost stationary above the pad. This seems inconsistent with the wind speed and direction reported at that altitude.

Appendix B includes not only the T–0.7 hour rawinsonde data (presented in Figure 3) but also the T–0.5 hour and T–0.2 hour rawinsonde data. The wind vectors were similar in all three soundings. These soundings documented a strong shear in wind direction at altitudes corresponding to the imagery-derived bottom (i.e., winds out of 7°,12°, and 14°), middle (i.e., winds out of 317°, 301°, and 313°), and top (i.e., winds out of 277°, 279°, and 277°) of the cloud. The winds (listed parenthetically for each cloud altitude) are for the T–0.7, T–0.5, and T–0.2 hour soundings, respectively.

Figures 4 through 7 are selected visible images of the Titan IV #K16 launch cloud as seen from the Press site and UCS-7 at the specified times after launch. It is immediately obvious that the cloud is not spherically symmetric in any of these images and that the geometry of the cloud changes rapidly in the first few minutes after launch.

Figure 4 parts (a) Press Site and (b) UCS-7 Site document simultaneous imagery from the two camera sites at 30 s (T + 00:30) after ignition. Press Site is to the west while UCS-7 is to the north-northwest of SLC-41, as illustrated in Figure 3. In these early images, SLC-41 pad is directly below the center of the ground cloud. In Figures 4 through 7, the bearing to SLC-41 is easily identified by a bush that stands above the tree line in the "a" (Press Site) images and by a white sphere in the "b" (UCS-7 Site) images. It is apparent from Figure 4 that the exhaust duct produces an asymmetry in the ground cloud by ejecting exhaust predominantly to the east (i.e., to the left in Figure 4b) of the pad while the prevailing wind rotated the eastern end to the south (i.e., to the right in Figure 4a) of the pad. The analyst used the top of the exhaust duct cloud as a marker for the top of the ground cloud during the first several minutes after launch.

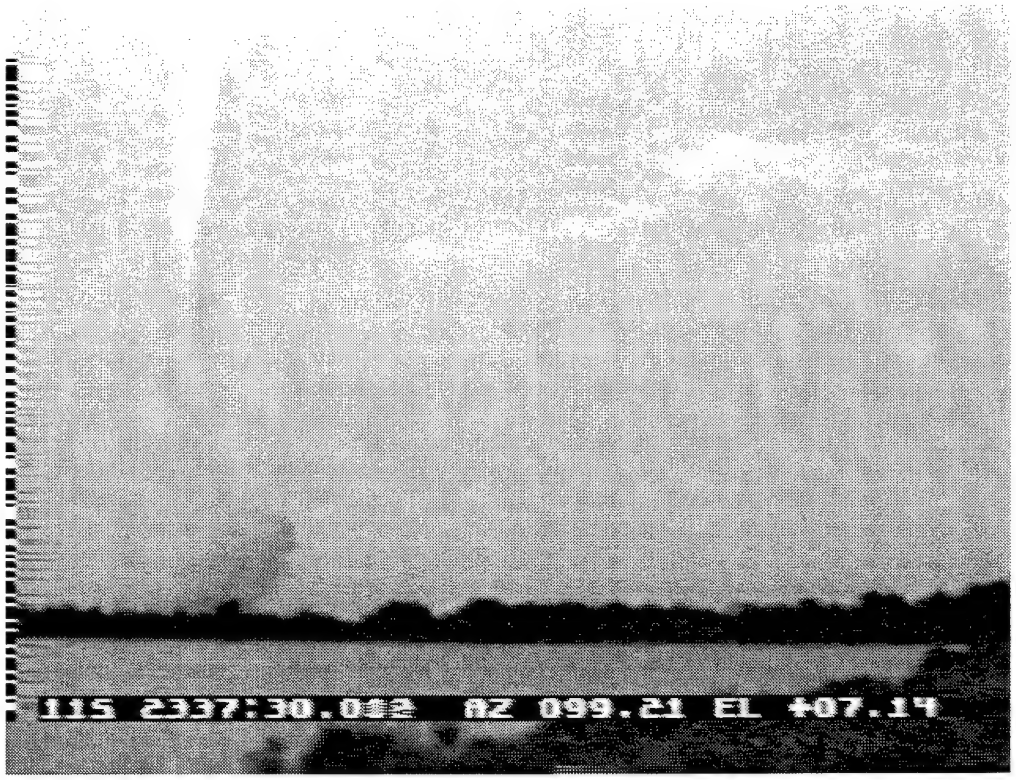

(a)

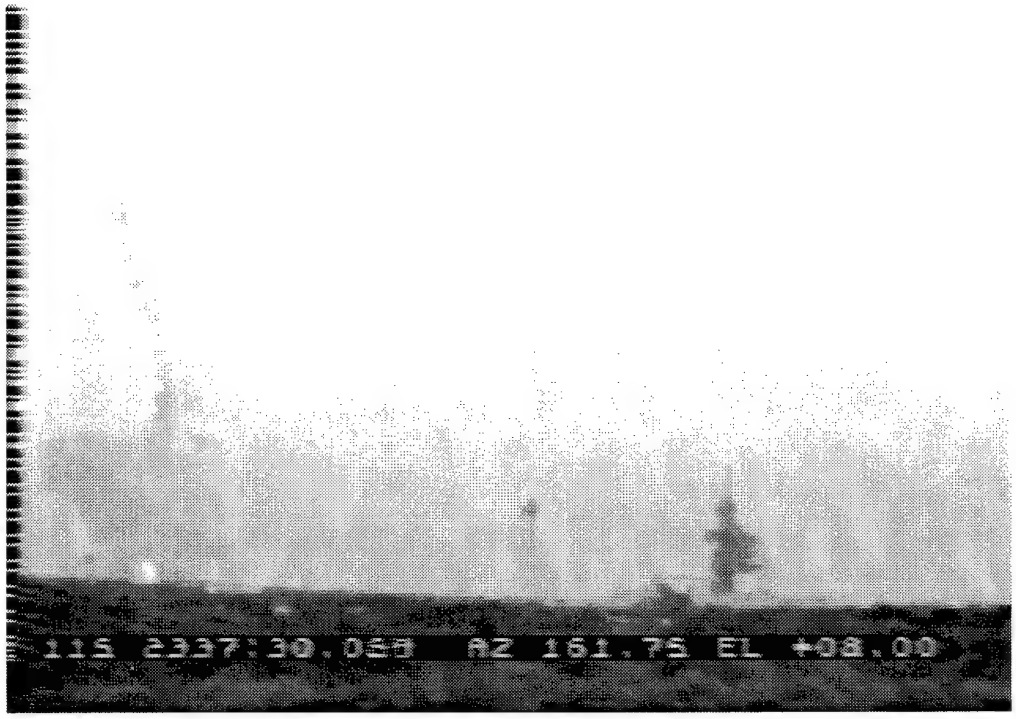

(b)

Figure 4. #K16 launch cloud viewed using visible imagery at T + 00:30 (mm:ss after launch) from (a) press site and (b) UCS-7 site.

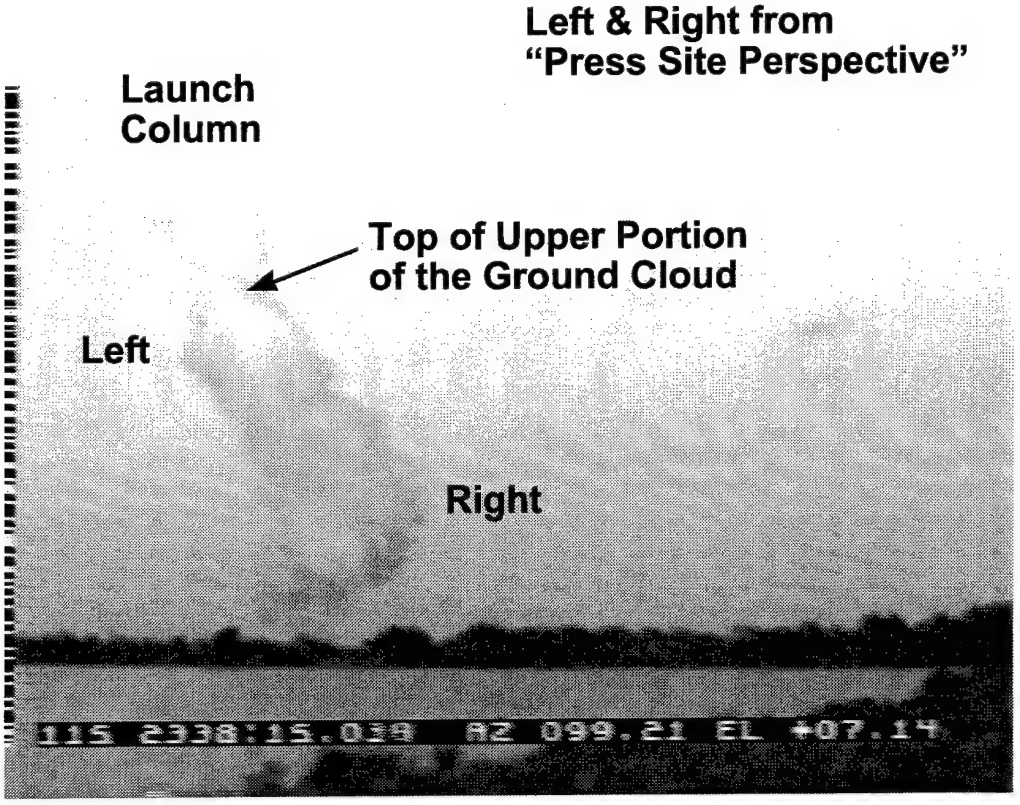

(a)

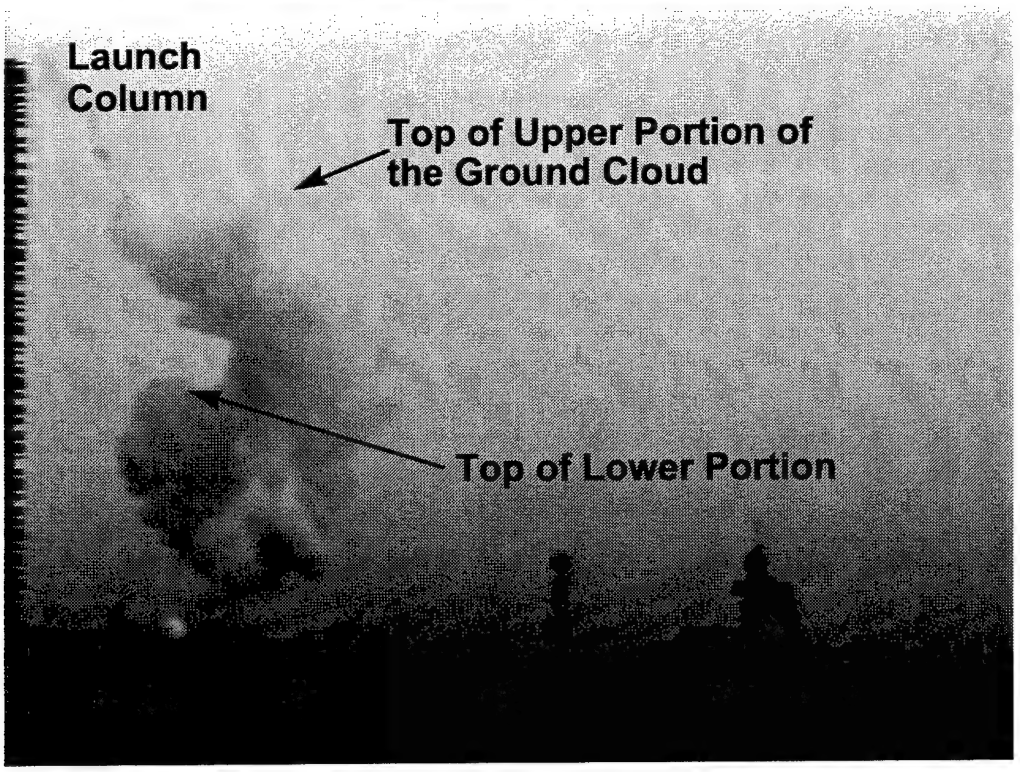

(b)

Figure 5. #K16 launch cloud viewed using visible imagery at T + 01:15 (mm:ss after launch) from (a) Press Site and (b) UCS-7 Site.

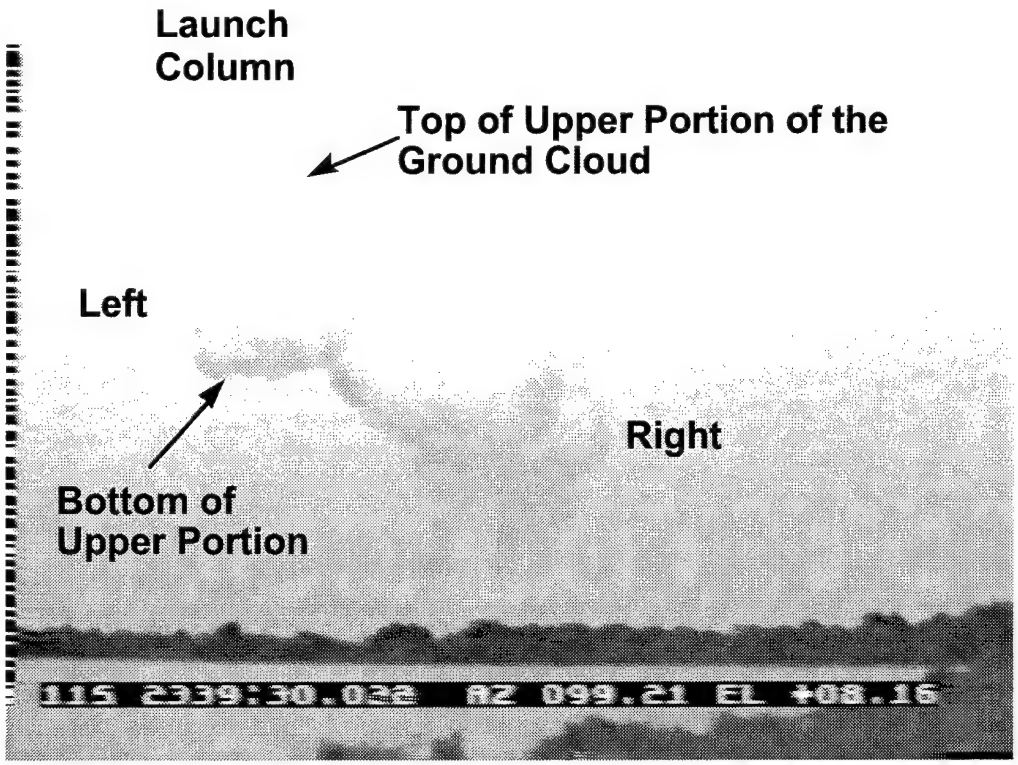

(a)

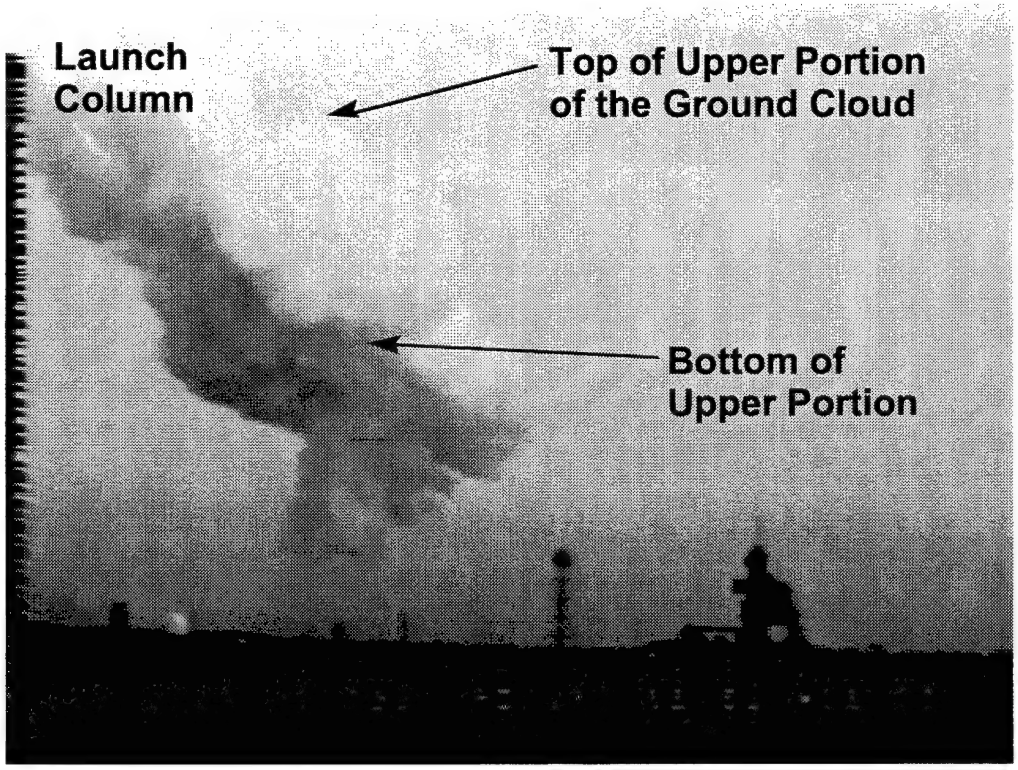

(b)

Figure 6. #K16 launch cloud viewed using visible imagery at T +02:30 (mm:ss after launch) from (a) Press Site and (b) UCS-7 Site.

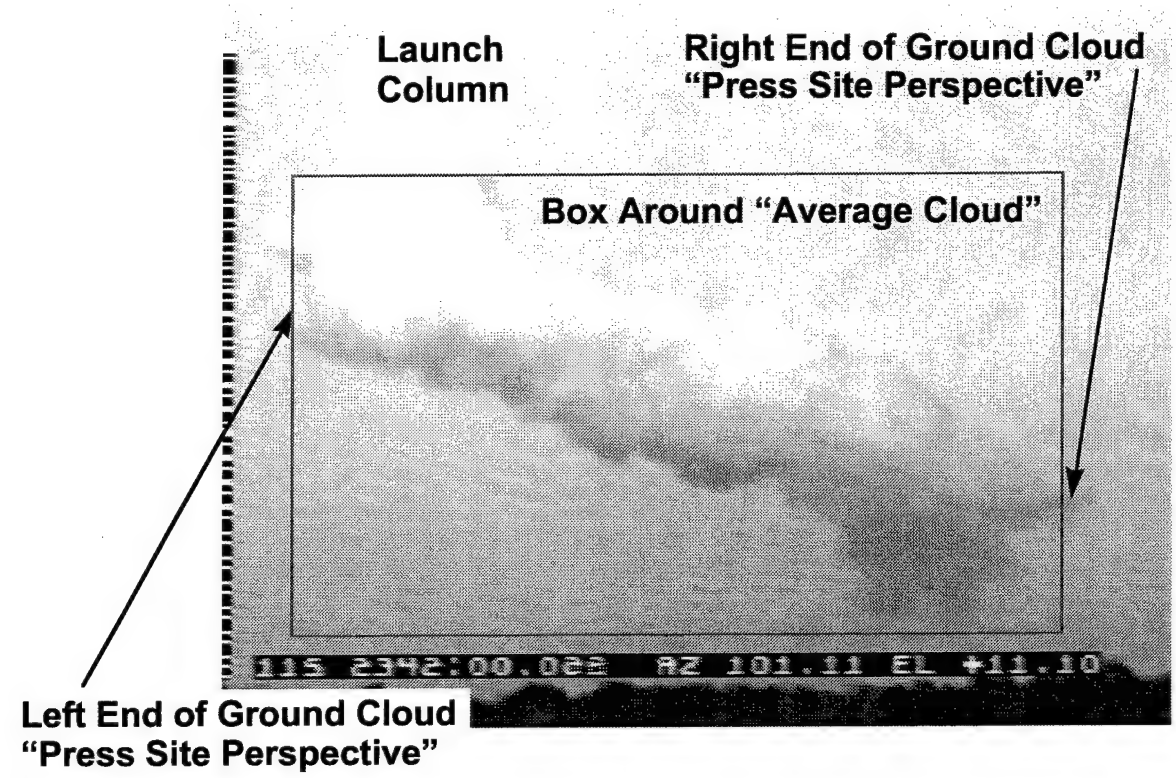

(a)

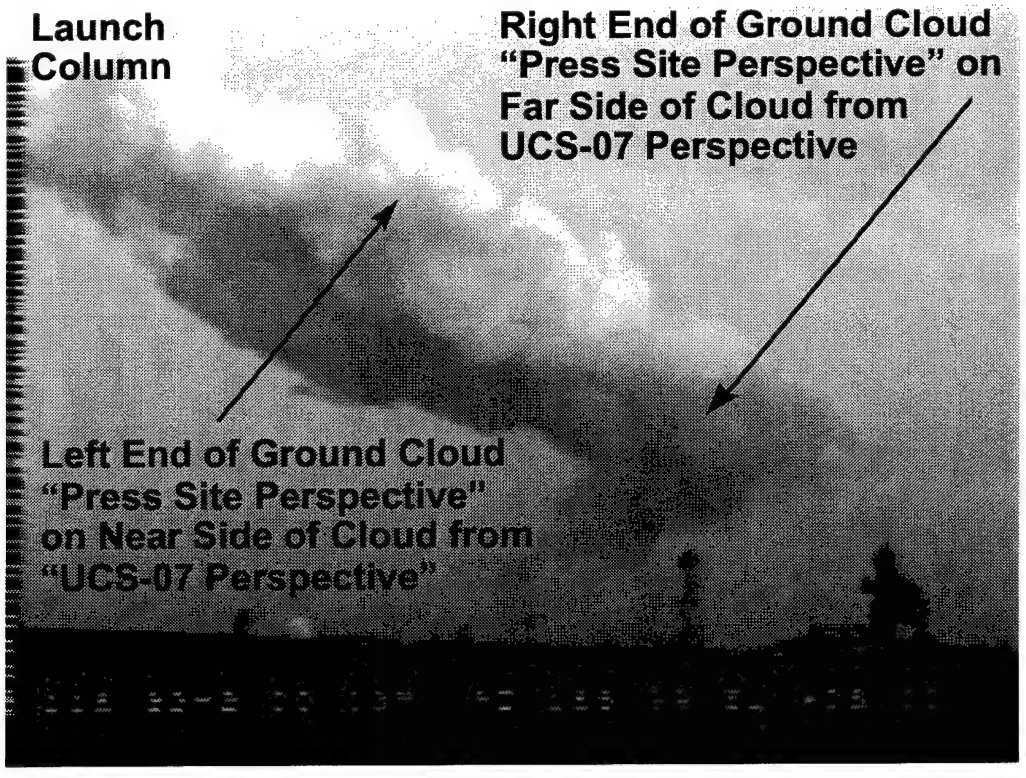

(b)

Figure 7. #K16 launch cloud viewed using visible imagery at T + 05:00 (mm:ss after launch) from (a) Press Site and (b) UCS-7 Site.

Figure 5 parts (a) Press Site and (b) UCS-7 Site document simultaneous imagery from the two camera sites at T + 01:15 (mm:ss) after ignition. It is difficult to see in the hardcopy, but the analyst identified the top of the ground cloud as the position of the wind shear that blows the launch column out to sea (i.e., to the left in Figure 5b) while leaving the top of the ground cloud almost stationary over SLC-41 (i.e., the bush in Figure 5a and the white sphere in Figure 5b). Figure 5 documents the movement of the bottom of the ground cloud to the south (i.e., to the right in Figure 5a) and to the west (i.e., to the right in Figure 5b). This trend continues as documented in Figures 6 (T + 02:30) and 7 (T + 05:00). The top of the ground cloud remains almost stationary over the launch pad (i.e., the bush in "a" and the white sphere in "b") while the bottom of the ground cloud moves to the south-southwest (i.e., to the right in "a" is to the south and to the right in "b" is to the west). By five minutes after launch (i.e., Figure 7), the top and bottom of the cloud have spread significantly, as illustrated by the ground cloud occupying almost the entire 32° horizontal field of view of the visible imagers.

The imagery data were subjected to an iterative analysis to ensure that only cloud features contributing to the stabilized ground cloud (as documented by the entire 6 min of imagery) were included in the **PLMTRACK** "boxes." In spite of the late hour (i.e., the sunset) and the hazy background, the visible imagery provided excellent contrast for detecting the edges of the cloud at all altitudes well after the cloud overfilled the field of view of the cameras. Hence, the operators continued to pan the extent of the ground cloud for 55 min after the launch. This VCR imagery includes Az/El encoding for the tripod's pointing angles. However, it is not possible to use the **PLMTRACK Box Method** once the cloud becomes larger than the field of view of the imagers. This quantitative imagery could be processed further using other methods. σ

2.5.2 Cloud Rise Times and Stabilization Heights

Figures 8 through 10 present the time-dependent altitude of the "bottom," the "middle," and the "top" of the ground cloud as determined by quantitative visible imagery using the **PLMTRACK Box Method**. The rise and stabilization height data are plotted against time after launch separately for the bottom (Figure 8), the middle (Figure 9), and the top (Figure 10). For clarity, all plots include a polynomial fit to the data, the average stabilization height, and the ±3 error bars for the stabilization height.

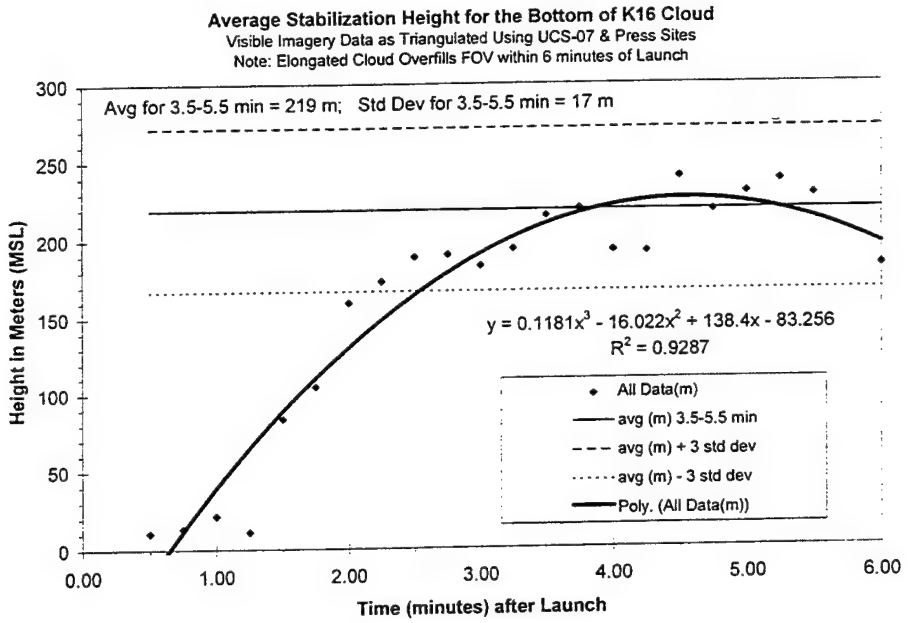

Figure 8. Cloud rise plot for the bottom of the #K16 cloud as determined using the PLMTRACK Box Method on visible imagery from Press and UCS-7 sites. The third-order polynomial fit to the data is plotted as H(t) vs t (in minutes) along with the average stabilization height and the 3σ error bands for the stabilization height. The variance (R^2) of 0.9287 indicates the high quality of the fit.

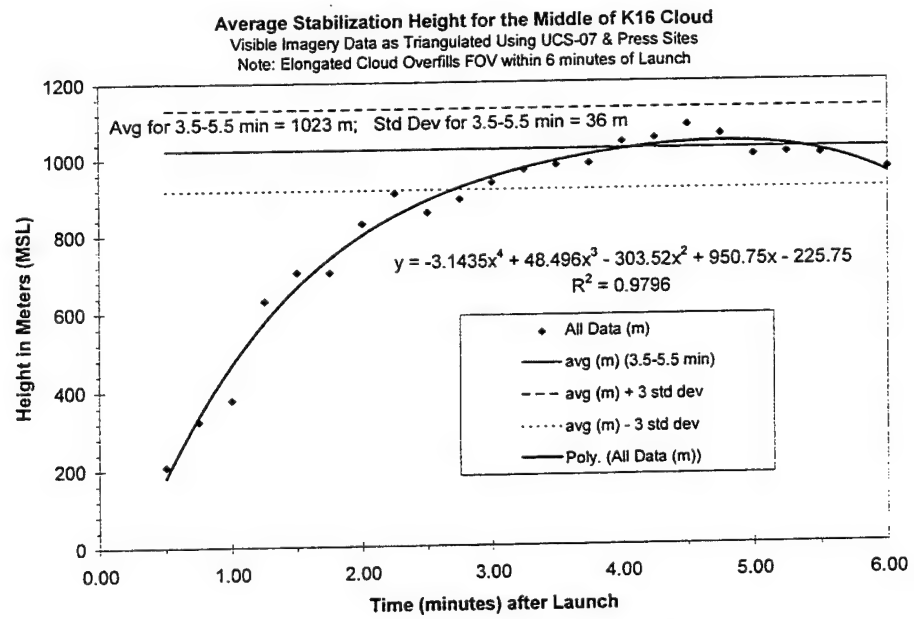

Figure 9. Cloud rise plot for the middle of the #K16 cloud as determined using the PLMTRACK Box Method on visible imagery from Press and UCS-7 sites. The fourth-order polynomial fit to the data is plotted as H(t) vs t (in minutes) along with the average stabilization height and the 3σ error bands for the stabilization height. The variance (R^2) of 0.9796 indicates the high quality of the fit.

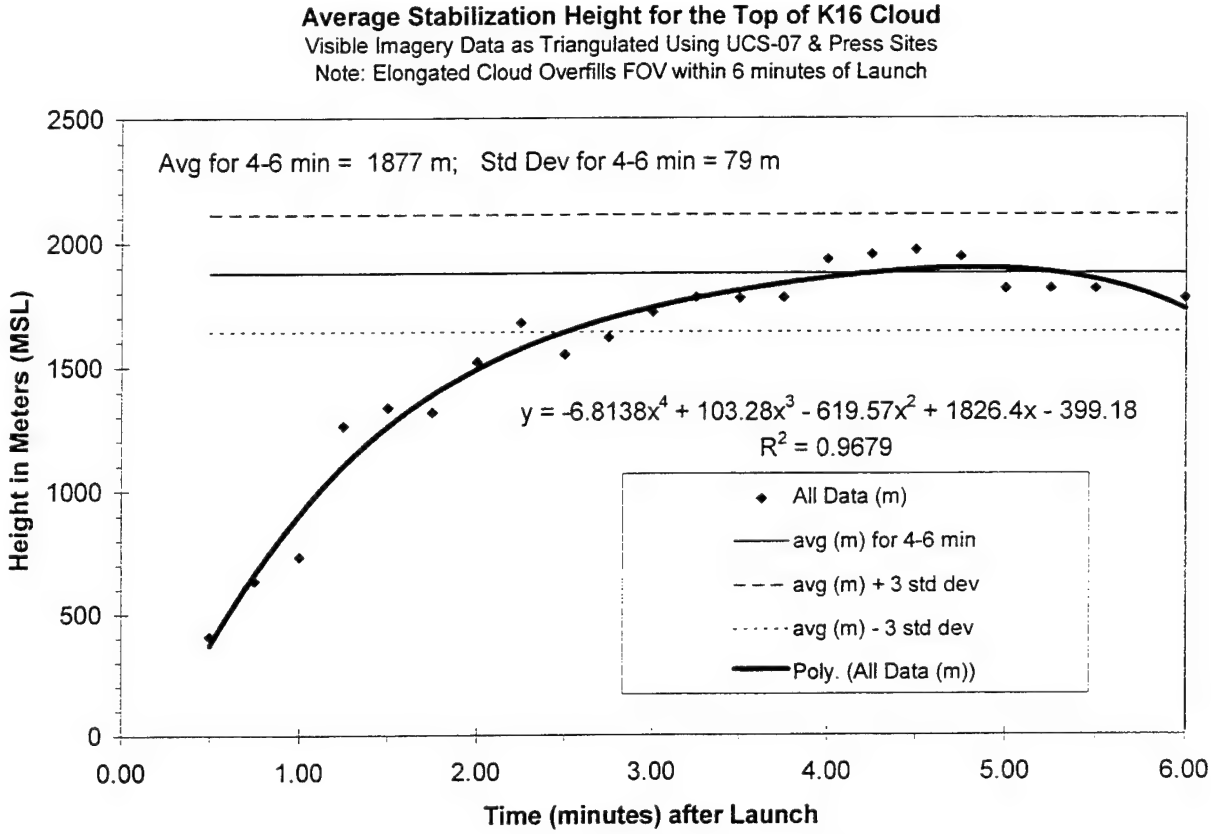

Figure 10. Cloud rise plot for the top of the #K16 cloud as determined using the PLMTRACK Box Method on visible imagery from Press and UCS-7 sites. The fourth-order polynomial fit to the data is plotted as H(t) vs t (in minutes) along with the average stabilization height and the 3σ error bands for the stabilization height. The variance (R^2) of 0.9679 indicates the high quality of the fit.

2.5.3 Comparison of REEDM Prediction to Imagery Data—Stabilization Height

Figure 11 presents the imagery-derived heights for the ground cloud's top, middle, and bottom plotted as a function of time following the launch. It can be seen that the measured stabilization height of the middle of the ground cloud (1023 ±36 m) is 35% higher than predicted (756 m MSL) by the T–0.7 hour REEDM modeling run (Appendix A). The time required to reach the stabilization height (approximately 3.5 min documented by visible imagery) is 20% faster than the 4.4 min predicted by the T–0.7 hour REEDM modeling run. For comparison, the T–0.5 and T–0.2 hour predictions are 764 m and 734 m MSL for the stabilization height and 4.4 and 4.2 min for the stabilization times. Appendix A provides complete REEDM output as well as tabular comparisons of imagery, rawinsonde, and REEDM data.

The variances (R^2) of the polynomial fits to the data (i.e., Figures 8–10) indicate that the fits are very good. A polynomial fit was used in those figures as a convenient method to permit the representation of cloud overshoot and subsequent damped oscillation around the stabilization height. To be consistent with REEDM, stabilization time and height refer to the first maximum in these fits. REEDM predicts that the cloud goes through damped oscillatory motion with a period of

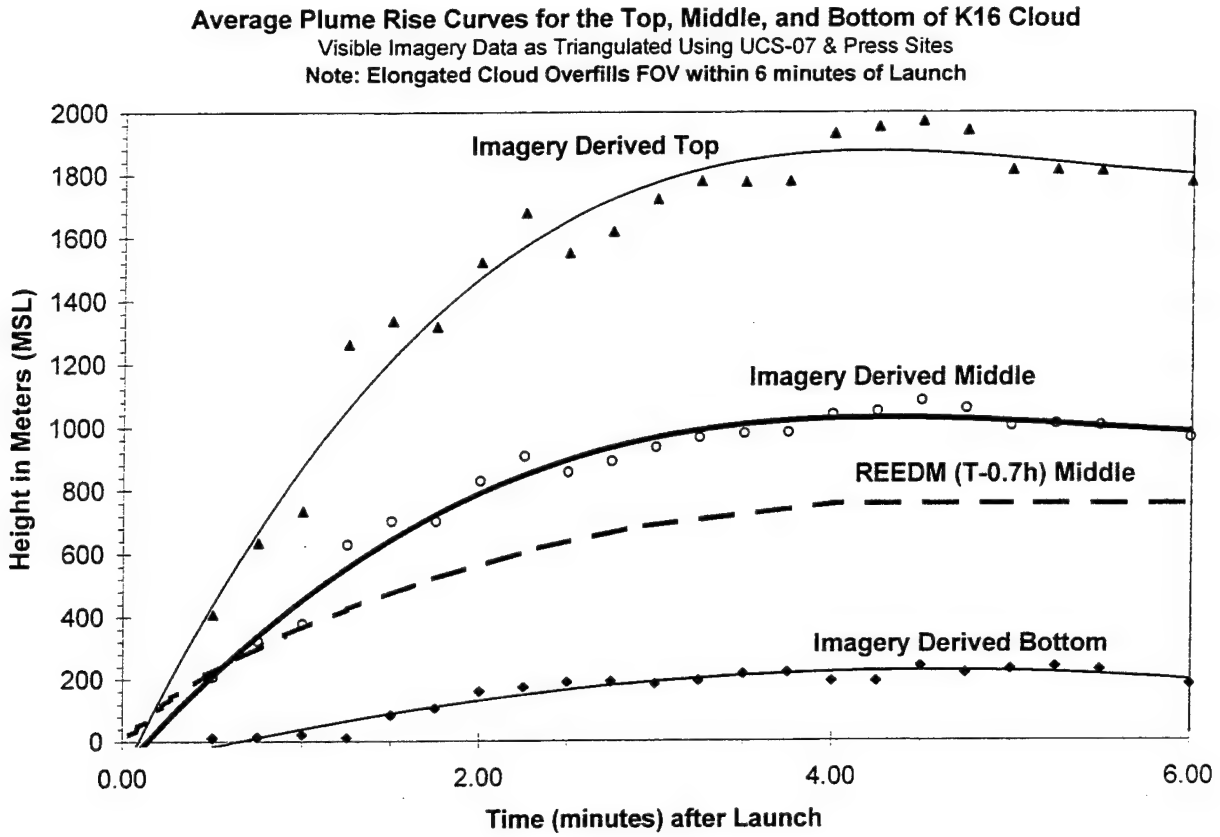

Figure 11. Imagery derived stabilization heights compared to T–0.7 hour REEDM predictions. The visible imagery data for the top, middle, and bottom of the ground cloud are plotted as H(t) vs t. The T–0.7 hour REEDM modeling run predictions for the cloud middle are presented for comparison. The predicted stabilization height was 756, 764, and 734 m MSL for the T–0.7, T–0.5, and T–0.2 hour runs, while the imagery-derived stabilization height was 1023 ±36 m MSL.

$2\pi/S^{1/2}$, where S is the static stability parameter [Ref. 1, Eq. (7)].[1] Sensitivity of REEDM predictions to input parameters has been examined by Womack.[2] Careful imaging of launch ground clouds under a variety of meteorological conditions is a vital element in REEDM evaluation.

2.5.4 Comparison of REEDM Prediction to Imagery Data—Trajectory and Speed

Figures 12 and 13 document the imagery-derived trajectory and speed for various ground cloud features. The "box" method of analysis for the imagery data does not yield independent values of the cloud track for the top, middle, and bottom of the cloud. Typically, we have chosen to present data for the middle of the cloud as defined by the **PLMTRACK Box Method**. However, the #K16 ground cloud represents a special case where the track and speed for the "middle" of the cloud represent the average of two extremes. Therefore, we plotted the data for the extremes and discuss the averages.

---

[1] J. R. Bjorklund, User's Manual for the REEDM Version 7 (Rocket Exhaust Effluent Diffusion Model) Computer Program, Vol. I, TR-90-157-01, AF Systems Command, Patrick AFB, FL (April 1990).

[2] J. M. Womack, Rocket Exhaust Effluent Diffusion Model Sensitivity Study, TOR-95(5448)-3, The Aerospace Corporation, El Segundo, CA (May 1995).

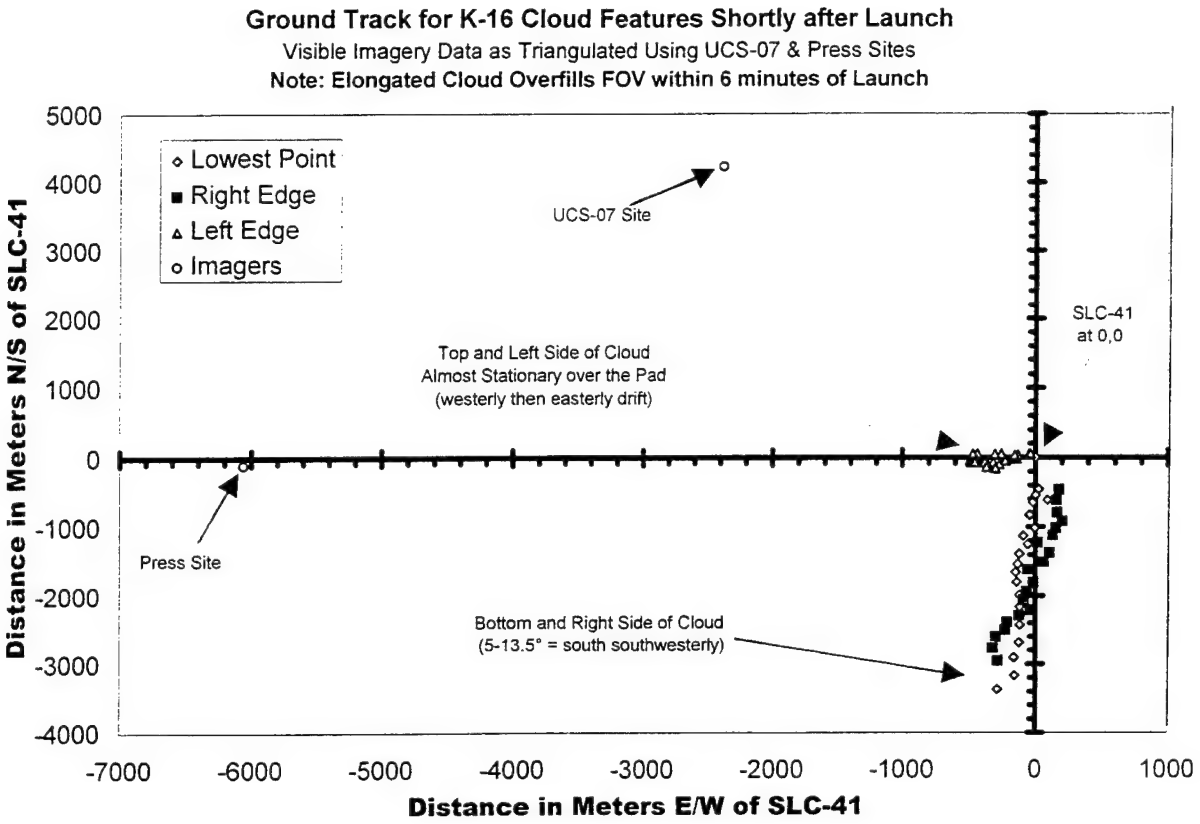

Figure 12. Trajectory for various features of the #K16 launch cloud as determined by visible imagery using the PLMTRACK Line Method. From the Press Site perspective, the "left" and "right" edges of the #K16 launch cloud correspond to the middle altitude of the "upper" and "lower" ends of the cloud, respectively. The "bottom" is the "lowest point" of the ground cloud observable from both UCS-7 and Press Sites. It is apparent from this plot that the "lower" end and the "bottom" of the cloud headed south-southwest (i.e., winds from 13.5° and 5°, respectively) while the "upper" portion drifted slightly to the west before returning to a position directly over the pad. As evidenced by the imagery, the top of the ground cloud remained almost stationary over the pad while the bottom of the ground cloud moved to the southwest. We have not bothered to plot the PLMTRACK Box Method data since it is a wandering southerly trajectory consistent with averaging the wandering position of the "upper" portion of the ground cloud with the south-southwesterly track of the "lower" portion of the ground cloud.

In this report, the angles conform to the convention of rawinsonde wind vectors (the angle from which the wind originates that would push the cloud into its imaged position). Thus, the angles are related by

$$\vartheta = 180 + \Phi\,, \tag{2}$$

where ϑ is the equivalent rawinsonde wind angle, and Φ is the measured polar angle of the cloud relative to SLC-41 and clockwise of true north. For example, when the cloud is due east of SLC-41, Φ is 90° and ϑ is 270°. Figure 3 showed the mean cloud track vectors documented in Figure 12 along with the wind vectors (T–0.7 hour rawinsonde) at the measured stabilization heights superimposed on the map of CCAS/KSC.

To be precise, the cloud data in Figure 12 represent the ground-plane projection of the trajectory of the various cloud features as a function of time. We used the **PLMTRACK Line Method** to triangulate the position for the various features of the #K16 launch cloud using pairs of visible imagery from UCS-7 and Press Sites. From the Press Site perspective, the "left" and "right" edges of the #K16 launch cloud correspond to the middle altitude of the "upper" and "lower" ends of the cloud, respectively. The "bottom" is the "lowest point" of the ground cloud observable from both UCS-7 and Press Sites. It is apparent from Figure 12 that the "lower" end and the "bottom" of the cloud headed south-southwest (i.e., winds from 13.5° and 5°, respectively) while the "upper" portion drifted slightly to the west before returning to a position directly over the pad. This conclusion is consistent with our earlier discussion of the imagery. We have not bothered to plot the track obtained using the **PLMTRACK Box Method** since it is a wandering southerly trajectory consistent with averaging the wandering position of the "upper" portion of the ground cloud with the south-southwesterly track of the "lower" portion of the ground cloud.

Figure 13 presents imagery-derived data for various ground cloud features as a plot of distance from the launch pad versus time. The analyst used the **PLMTRACK Line Method** to triangulate the position of the various cloud features as a function of time. The ground-plane distance of the cloud feature from SLC-41 increases linearly with time for the "lower" portion and "bottom" of the cloud. A linear regressive fit to these data provides the velocity of the lower portion of the ground cloud. The imagery-derived 8.5 m/s cloud velocity obtained for both the "lower" portion and "bottom" of the ground cloud is over a factor of 2 higher than the 3.6 m/s velocity obtained using the **PLMTRACK Box Method** for the middle of the cloud. This is consistent with the data plotted in Figure 13, which document a zero velocity for the "upper" portion of the ground cloud. Therefore, the "middle" of the cloud moves at the average speed for the "lower" and "upper" portions (3.6 m/s by Box Method ~ (8.5 – 0)/2 = 4.25 m/s by Line Method).

The imagery-derived cloud velocity for the "lower" portion of the ground cloud is of the same order of magnitude as the rawinsonde wind speeds (7.3, 7.2, and 6.7 m/s for the T–0.7, T–0.5, and T–0.2 hour soundings) at 207 m AGL (i.e., the rawinsonde level closest to the imagery-derived bottom of the cloud). For comparison REEDM predicts an average wind speed of 4.5 to 7.0 m/s for transition layer 1 for the various runs.

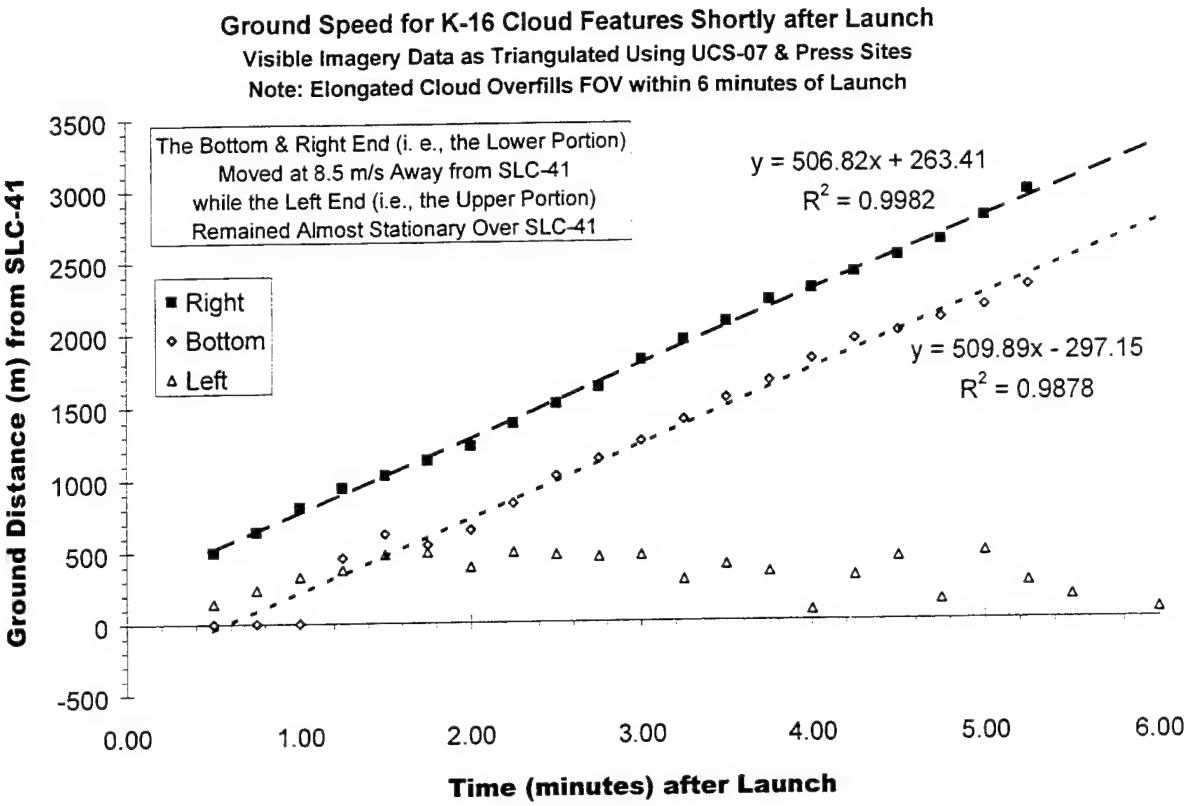

Figure 13. The distances from SLC-41 were derived using the PLMTRACK Line Method for various #K16 cloud features and are plotted against time in this figure. From the Press Site perspective, the "left" and "right" edges of the #K16 launch cloud correspond to the middle altitude of the "upper" and "lower" ends of the cloud, respectively. The "bottom" is the lowest part of the ground cloud observable from both UCS-7 and Press Sites. The variances (R^2 = 0.9982 and 0.9878) of the linear fits to the data indicate the quality of the fits. The average cloud speed of 3.6 m/s derived from the PLMTRACK Box Method is substantially lower than the 8.5 m/s speed for the "lower" and "bottom" of the cloud and substantially higher than the 0 m/s for the "upper". It seems reasonable that the middle of the cloud would move at the average speed of the "lower" (8.5 m/s) and the "upper" (0 m/s) portions of the cloud.

2.5.5 Comparison of REEDM Prediction to Imagery Data—Summary Table

Table 1 summarizes the imagery-derived, T–0.7 hour rawinsonde measured, and T–0.7 hour REEDM-predicted data for the #K16 launch cloud. Several conclusions can be derived from review of the contents of this table and the previous discussions in this section:

- the imagery-derived stabilization height (1023 m MSL) is 35% higher than the T–0.7 hour REEDM predicted stabilization height (756 m MSL);

- the imagery-derived stabilization time (3.5 min) is 20% faster than the T–0.7 hour REEDM predicted stabilization time (4.4 min);

- the imagery-derived direction and speed of the "middle" of the cloud (as determined by the **PLMTRACK Box Method**) are roughly the average of the results obtained using the **PLMTRACK Line Method** to track the speedy southerly moving "lower" portion and the almost stationary "upper" portion;

Table 1. Summary for #K16 Launch Cloud Data Derived from Visible Imagery, T–0.7 hour Rawinsonde Sounding Data and T-0.7 hour REEDM Predictions

Attribute	Feature	Visible Imagery	Rawinsonde (T–0.7 h)	REEDM 7.07 (T–0.7 h) (Max Conc @ H(m))	REEDM 7.07 (T–0.7 h) (Long Range Tracks @ H(m))
Height (m MSL)	Top	1877	#N/A	#N/A	#N/A
Stabilization	Middle	1023	#N/A	756	756
(SLC-41 = 7 m MSL	Bottom	219	#N/A	#N/A	#N/A
Time (min)	Top	4.0	#N/A	#N/A	#N/A
Stabilization	Middle	3.5	#N/A	4.4	4.4
	Bottom	3.5	#N/A	#N/A	#N/A
Bearing (deg)	Top	None	277	#N/A	#N/A
(Rawinsonde convention)	Middle	~N-NW (Box)	317	348° (Max @ 756 m MSL)	303° (Cloud @ 756 m MSL)
	Bottom	5° to 14° (Line)	7	5° (Max @ 0 m AGL)	4° (Cloud @ 0 m AGL)
Speed (m/s)	Top	~0	7.7	#N/A	#N/A
	Middle	3.6 (Box)	6.2	#N/A	5.8° (Cloud @ 756 m MSL
	Bottom	8.5 (Line)	7.3	#N/A	7.0° (Cloud @ 0 m AGL)

- the imagery-derived track and speed for the "lower portion" and "bottom" of the cloud (5 to 13.5° at 8.5 m/s at altitudes between 276 and 917m MSL) is fairly close to the T–0.7 hour REEDM prediction for the first transition layer (8.1° at 7.0 m/s at altitudes between 0 and 674m AGL)

- the imagery-derived track and speed for the "upper" portion of the cloud (i.e., practically stationary) does not seem consistent with the T–0.7 hour winds nor REEDM predictions.

Appendix A contains T–0.7, T–0.5, and T–0.2 hour REEDM predictions and additional summary tables for T–0.5 and T–0.2 hour runs. The imagery-derived stabilization height (1023 m MSL) is significantly higher than predicted by any of these REEDM predictions (i.e., stabilization heights of 756 m, 764 m, and 734 m MSL for the T–0.7, T–0.5, and T–0.2 hour REEDM runs, respectively). The imagery-derived trajectory for the "lower portion" of the ground cloud is closer to REEDM's surface impact predictions (i.e., southwesterly to southeasterly ground impact track) than to REEDM's stabilized cloud predictions (i.e., east southeasterly cloud trajectory). All of these REEDM runs used REEDM version 7.07 defaults for a normal launch as documented in Appendix A.

2.6 Summary and Conclusions

The Titan IV #K16 mission was launched successfully from the Eastern Range (SLC-41) at 19:37 EDT (23:37 GMT) on 24 April 1996. Personnel from The Aerospace Corporation deployed three VIRIS platforms (using only visible imagery) to monitor the event and to track the time evolution and the trajectory of the solid rocket motor exhaust cloud. The three chosen sites (UCS-7, SLC 34, and the Press Site) were located to the north-northwest, south-southeast, and west relative to launch complex SLC-41. Although the ground cloud filled the field of view of the imagers within 6 min of the launch, the operators continued to pan the extent of the ground cloud for 55 min after the launch. When combined with the Az/El readings and the IRIG-B time data, the quantitative visible imagery from UCS-7 and Press sites were used to quantify the rise, stabilization, and movement of the cloud for 6 min after the launch. The imagery documented a

rapid stretching of the ground cloud due to a wind shear between the top and bottom of the ground cloud. In addition, this data set is unusual because portions of the ground cloud were contained in both the first and second atmospheric transition layers according to the T–0.7 hour REEDM run. Therefore, the quantitative imagery of the #K16 ground cloud will be extremely useful for tuning current and future dispersion models.

The definition of the #K16 exhaust cloud's geometric features is complicated by its unusual three-dimensional shape (far from spherical). However, the imagery successfully documented this complex shape as the cloud evolved (i.e., asymmetric ejection from the exhaust duct, rapid rise of the hot ground cloud, shear between the high-altitude launch column and the top of the ground cloud, and shear between the top and bottom of the ground cloud). The analyst included only the portions of the exhaust cloud that became incorporated into the stabilized ground cloud.

The analyst used the **PLMTRACK Box Method** to characterize the average behavior of the cloud (i.e., its stabilization time, stabilization height, track, and speed). However, due to the dramatic differences in the track and speed of the "lower" and "upper" portions of the cloud, the analyst used the **PLMTRACK Line Method** to triangulate these portions of the cloud separately. The Box Method documents a track and speed that is close to the average of the extremes documented by the Line Method for the speedy southerly moving "lower portion" and for the almost stationary "upper portion" of the ground cloud.

Analysis of the imagery data presented in this report has focused on determining parameters that are directly comparable to REEDM predictions. The most accurately determined quantities by imagery are the cloud rise time, its stabilization height, its trajectory, and its speed. For Titan IV #K16, T–0.7 hour REEDM predictions were substantially different from those measured by imagery. According to the quantitative visible imagery from UCS-7 and Press sites, the cloud took 3.5 min to stabilize (20% faster than predicted), stabilized at 1023 m in altitude (35% higher than predicted), moved in a south southwesterly direction (versus the east southeasterly prediction), and moved at an average speed of 3.6 m/s (38% slower than predicted).

Seven other Titan IV launches have been imaged in a similar manner by The Aerospace Corporation as part of the Model Validation Program. All of the available Titan IV imagery documents that REEDM consistently underestimates the stabilization height of the ground cloud. Such overly conservative REEDM predictions can result in unnecessary launch holds at a considerable cost to the Air Force. Therefore, additional Titan IV exhaust cloud data are needed to validate and to tune current and future dispersion models for both ranges (V AFB and CCAS) and for various meteorological conditions.

3. Aircraft Elevated HCl Measurements

[The material in this section was contributed by Dr. R. N. Abernathy and Karen L. Foster of the Environmental Monitoring and Technology Department of The Aerospace Corporation's Space and Environment Technology Center.]

3.1 Background

On 24 April 1996, the Titan IV #K16 mission was successfully launched from CCAS at 19:37 EDT (23:37 GMT). This section describes the HCl concentration data collected by an aircraft that sampled the dispersing ground cloud at altitudes ranging from ground level to 1500 m MSL. The aircraft used a modified Geomet total hydrochloric acid (HCl) detector to measure the HCl concentrations within the exhaust cloud for 88 min subsequent to the launch. This aircraft sampling campaign involved Air Force, NASA, NOAA, and contractor (I-NET and SRS) organizations. The Aerospace Corporation analyzed the aircraft's HCl concentration data as described in this section. Based upon sampling at altitudes below 1500 m, the aircraft's HCl concentration data documented the movement of the "lower portion" of the ground cloud to the south-southwest immediately following the launch, the mixing of HCl to altitudes as low as ground level (at the Melbourne airport), and the movement of the "upper portion" of the exhaust cloud to the southeast and to the east. The aircraft's altitude was measured using a global positioning system (GPS) receiver with differential service (±35 m in latitude and in longitude and ±70 m in altitude).

The aircraft's Geomet data (i.e., total HCl concentration measurements) are reported here in several graphical formats to facilitate comparison with REEDM predictions (Appendix A), rawinsonde sounding data (Appendix B), and imagery data (Section 2). The aircraft setup is described in Appendix C. For clarity, this section includes some data from other sections in its figures, tables, and text. It is apparent from review of this section that these data will be useful for validating current and future dispersion models. In fact, we documented an error in the REEDM output of cloud height relative to mean sea level.

The purpose of this report was to document the quality and quantity of the aircraft data available for validating dispersion models. However, it is difficult to extract the data for a single pass through the cloud from summary plots that contain 36 passes through the cloud. Therefore, in order to facilitate the comparison of these data to individual dispersion model runs, two subsequent reports will provide: (1) a detailed correlation between imagery and aircraft data for the first six minutes after launch and (2) a detailed graphical analysis of the aircraft's HCl concentration profiles using polar and Cartesian coordinates for each 10-min time window throughout the 88-min flight time. These subsequent detailed analyses will provide the data in a format that will allow direct comparison to model runs for specific times, altitudes, and distances from the release site. The aircraft data are also available as comma-separated-variable files providing time, latitude, longitude, altitude, Geomet response, and HCl concentration.

3.2 Introduction

I-NET, a NASA contractor, modified a Geomet for mounting in the nose of a Piper (PA-44-180) Seminole (a twin-engine, four-seat aircraft) (see Appendix C). The Geomet is a total HCl monitor that produces a response proportional to the combined HCl present in both the vapor or the aerosol phases. It reports the HCl concentration as parts-per-million (ppm) by volume (i.e., $V_{HCl}\ 10^6/\ V_{total}$). This instrument sampled the air through a horizontal four-foot-long ceramic inlet wetted with a bromate/bromide-containing reagent. The HCl diffuses to the wetted walls of the ceramic tube and produces bromine vapor through reactions with the reagent. The bromine vapor is swept into a buffered hydrogen peroxide/Luminol solution resulting in photoluminescence detected by a filtered photometric detector. I-NET disabled the Geomet's autoranging electronics so that a single range produced a millivolt response that was proportional to the combined HCl vapor and aerosol concentration entering the inlet. I-NET calibrated the Geomet against HCl vapor before and after the #K16 mission as discussed in this section.

SRS Technologies Inc., a contractor, provided an interface between the I-NET laboratory and the Florida Institute of Technology (FIT) flight crew. NASA, NOAA/Air Resources Laboratory/Field Research Division, I-NET, SRS, and FIT cooperated in the integration of the NOAA data system, the FIT aircraft, and the Air Force Geomet into an airborne sampling and data logging system. FIT personnel piloted the aircraft during the #K16 mission, while 45th AMDS/SGPB personnel operated the NOAA data system and the Geomet detector. The NOAA data system logged GPS time and position as well as Geomet response every 0.25 s during the flight. NOAA provided a comma-separated-variable (csv) data file to The Aerospace Corporation.

The Aerospace Corporation imaged the rise, movement, and growth of the ground cloud for 55 min subsequent to the #K16 launch, as documented in Section 2. This quantitative imagery documented the stabilization height (above mean sea level, MSL) and the trajectory (relative to SLC-41) of the ground cloud. Rudimentary knowledge of the rawinsonde wind data (Appendix B), REEDM predictions (Appendix A), and the imagery data (Section 2) was required for the interpretation of the aircraft's HCl sampling data as reported in this section.

When comparing the aircraft's GPS-derived altitude to the imagery, rawinsonde, and REEDM data, it is essential to use the same frame of reference for measuring the height. REEDM reports the predicted height of the exhaust cloud relative to MSL and relative to ground level, but incorrectly assumes that the height of the rawinsonde release site is the same as the height of the launch pad. This is almost true for Cape Canaveral, but is far from the case for VAFB and can result in a significant error in REEDM's output. We assert that REEDM's predicted height above ground level (AGL) was intended to be height above origin, which for a launch is height above the launch pad not above the rawinsonde release site. Therefore, in Section 2, the observed height of the imaged cloud and the predicted (i.e., by REEDM) height of the stabilized cloud were reported in meters MSL. For this conversion, we assumed the height AGL reported by REEDM was the same as the height above SLC-41. Since SLC-41 is 7.0 m (23 ft) above MSL, height relative to SLC-41 is converted to height MSL by adding 7 m (23 ft). REEDM incorrectly uses the height of the rawinsonde release site (16 ft, 4.9 m) rather than the height of the launch pad (23 ft, 7.0 m) for its conversion of height AGL to height MSL. Therefore, the height MSL reported by REEDM in Appendix A is low by 2.1 m (7 ft). Although this is a negligible error for CCAS, the error is 40 m (133 ft) for VAFB. Table 2 provides the imaged and the predicted (i.e., by REEDM) heights

relative to MSL and to SLC-41 (AGL) by correctly using the launch pad as the origin for the launch.

Table 2. Imagery-Derived Stabilization Heights and REEDM's T–0.7 hour Prediction Expressed Relative to MSL (comparable to the aircraft's GPS data) and Relative to SLC-41 (i.e., AGL, which is reported by REEDM). Note that SLC-41 is 7 m (23 ft) above mean sea level (MSL).

Stabilized Exhaust Cloud Characteristic	H (m MSL) (comparable to the aircraft's GPS data) (7+ H (m AGL))	H (ft MSL) (23 + H (ft AGL)	H (m AGL) (as reported by REEDM)	H (ft AGL) (unit conversion from H (m AGL)
Imaged Bottom	1877	6158	1870	6135
Imaged Middle	1023	3356	1016	3333
Imaged Top	219	719	212	696
REEDM's Middle	756	2480	749	2457

3.3 Results and Discussion

The aircraft's data are most easily interpreted in light of rudimentary knowledge of the rawinsonde and imagery results. Figure 14 plots various wind and cloud bearings using the rawin sonde convention [defined fully in Subsection 3.3.2]. Briefly, the arrows indicate the direction the cloud would move for a wind coming from the indicated angle (clockwise from north). The cloud trajectories are anchored to SLC-41 on the map. The heaviest arrows (i.e., thickest linewidth) are used for the 5° and 14° bearings derived from the #K16 imagery data and apply to the "bottom" and "lower portion" of the cloud, respectively. As discussed in Section 2, these cloud headings were measured during the first 6 min after launch (i.e., during the rise and stabilization of the ground cloud). Four additional cloud trajectories are included in Figure 14 and document the T–0.7 hour REEDM predictions. The REEDM cloud trajectories depicted in Figure 14 include the following: (1) the 5° bearing to the maximum concentration at ground level (i.e., 0 m AGL = 7 m MSL = SLC-41 height); (2) the 4° bearing for the surface impact of the ground cloud at later times; (3) the 348° bearing to the maximum concentration at 756 m MSL (or 749 m AGL, which was REEDM's T–0.7 hour prediction for the stabilization height); and (4) the 303° average wind bearing for the second mixing layer (i.e., this dominates the trajectory at the stabilization height for the cloud at later times). Therefore, REEDM's cloud trajectories could be interpreted as a 348° bearing during rise and a 303° bearing after stabilization at the stabilization height. In contrast, REEDM's surface impact predictions could be interpreted as a 5° bearing to maximum ground-level concentration and a 4° bearing for surface impact at greater distances. Figure 14 also documents three rawinsonde-derived wind directions associated with the imagery-derived heights for the bottom (7°), middle (317°), and top (277°) of the ground cloud. These rawinsonde-derived wind directions are anchored to the rawinsonde release site and document a dramatic shear in wind direction over the altitudes occupied by the stabilized ground cloud. Lastly Figure 14 documents the locations of the three imagery sites chosen by The Aerospace Corporation for the #K16 imagery.

It is evident from examination of Figure 14 and from the discussion in the preceding paragraphs that REEDM predicts a southeasterly to easterly trajectory for the ground cloud (at its predicted stabilization height) in contrast to the imagery-derived southwesterly trajectory. Indeed, the

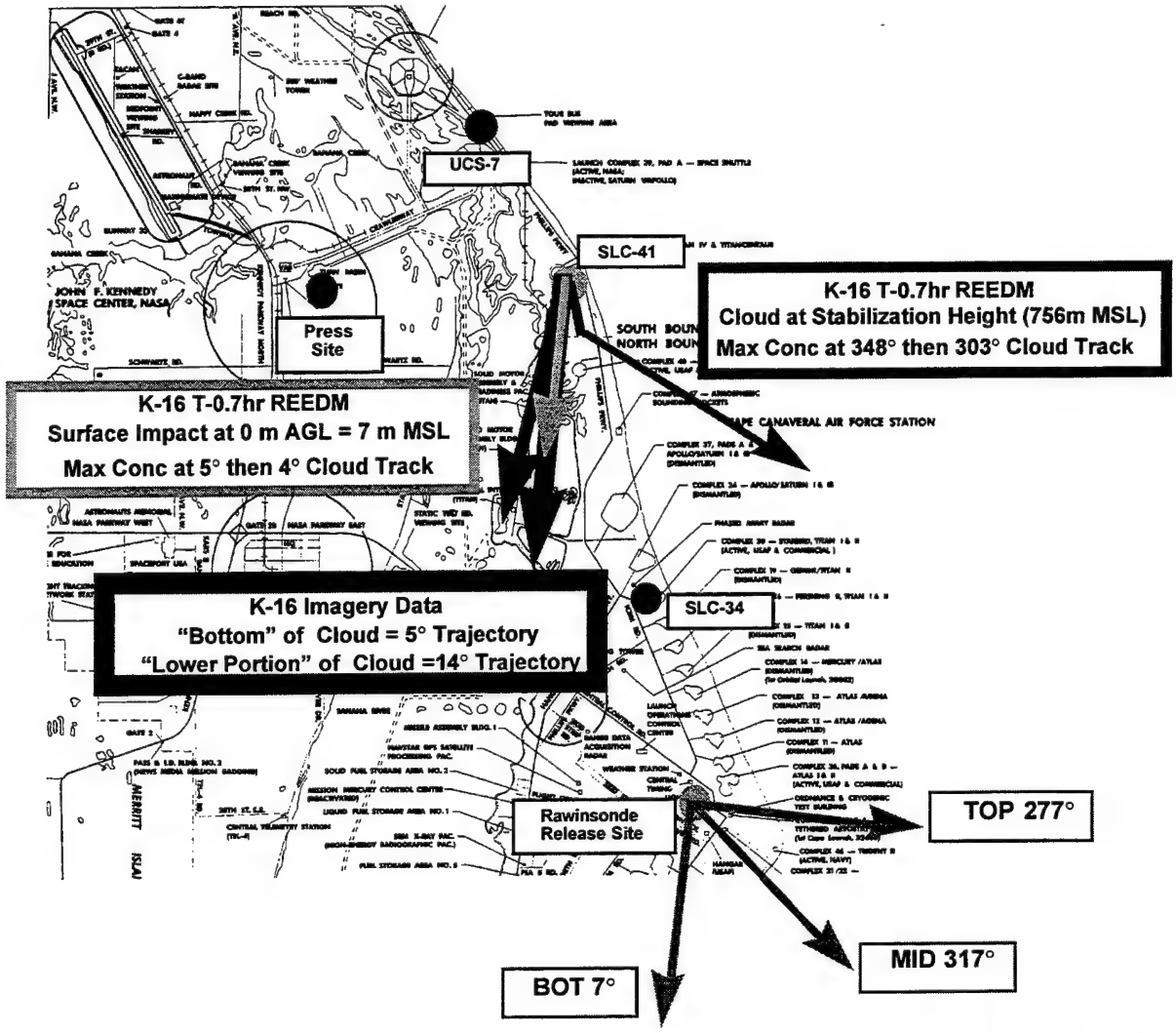

Figure 14. Partial map of CCAS documenting the locations of the three imagery sites and the rawinsonde release site as well as the available ground cloud and wind data. The exhaust cloud data includes the imagery-derived #K16 ground cloud tracks (5° to 14° for the "bottom" and "lower portion" of the ground cloud), the REEDM surface impact (5° to maximum then 4° bearing along surface), the REEDM stabilization height predictions (348° to maximum concentration at stabilization height and 303° bearing after stabilization), and the rawinsonde-derived wind directions at the imagery-derived heights for the top (277°), middle (317°), and bottom (7°) of the ground cloud. The rawinsonde sounding was at 22:55 GMT (T–0.7 hour). The cloud track trajectories are anchored to SLC-41 pad.

imagery-derived cloud trajectory (14°) for the "lower portion" (ranging from 276 to 917 m MSL) of the ground cloud is closer to the REEDM's ground-level predictions (4° to 5°) than to its ground-cloud predictions (i.e., 348° to 303° at the predicted stabilization height). Since the imagery revealed that the top of the cloud remained almost stationary above the pad, the ground cloud's trajectory is dominated by the movement of the lower portion to the south-southwest. Hence, it is not surprising and is evident from examination of Figure 14 that the imagery-derived south-southwesterly cloud direction (5° to 14°) is closer to the rawinsonde-derived wind direction

measured at the bottom (7°) than at the middle (317°) of the stabilized ground cloud. In addition, one must remember that the imagery only followed the cloud for the first 6 min after launch, whereas REEDM predictions typically are used for longer times and greater distances. REEDM predicted the dispersion of the cloud using a single rawinsonde sounding from a site that is remote from the launch pad. One can imagine that the winds can vary with time and terrain. The REEDM predictions in Figure 14 are extracted from the REEDM output (T–0.7 hour) in Appendix A. The T–0.7 hour rawinsonde data in Figure 14 are extracted from rawinsonde sounding data in Appendix B.

The following will review the aircraft's HCl concentration measurements and compare them to rawinsonde-derived wind directions, imagery-derived cloud characteristics, and REEDM predictions. The early aircraft data documented an initial south southwesterly cloud trajectory (18°) at lower altitudes that is similar to the imagery-derived track (14°) for the "lower portion" of the ground cloud. Likewise the aircraft data documented an east-southeasterly trajectory for the "upper portion" of the ground cloud, which is consistent with the rawinsonde-derived winds coming from the west-northwest at higher altitudes. The aircraft's HCl concentration profiles are consistent with REEDM's predicted movement of the "upper portion" of the ground cloud (i.e., the cloud at its predicted stabilization height) to the east-southeast while the surface impact remained along a southwesterly track for two out of three runs (Appendix A) based upon the three rawinsonde soundings (Appendix B).

3.3.1 Overview of Aircraft Sampling Data

3.3.1.1 Raw Aircraft Data

Table 3 presents a sample of the aircraft's data as delivered to The Aerospace Corporation with added headings. The headings are as follows: Log (mission log number assigned by NOAA); yr (year); d (Julian day of the year); hm (local time by inaccurate data logger clock in hour and minutes, two digits each); s (seconds); ppm (raw HCl concentration based upon single-point calibration and mV response from the Geomet); rng (range of the Geomet, disabled function); mV (Geomet response in millivolts); tGPS (GPS receiver GM time in hhmmss [documenting hours minutes seconds as six digits without separation]); lat (latitude, ddmm.mmmm, in degrees and decimal minutes); N/S (label for latitude, North/South); lon (longitude, ddmm.mmmm, in degrees and decimal minutes); E/W (label for longitude, East/West); diff (differential, 2, or normal, 1, GPS mode); # Sat (number of GPS Satellites); HDOP (horizontal dilution of precision [measure of GPS accuracy]); alt (altitude reported from GPS receiver); and units (M, meters for alt). The hm column is local and inaccurate computer time. Therefore, tGPS was used to interpret the aircraft data (using the "s" column to bin data reproducibly into fractions of a second). The hm data were only used to interpolate between valid tGPS entries when the GPS failed to increment time. Personnel from The Aerospace Corporation have reviewed these data in 10-min increments, applied baseline corrections to eliminate negative HCl concentrations, and removed obviously bad GPS entries (i.e., aircraft stationary while flying). Personnel from The Aerospace Corporation have also performed the conversions necessary to report distance, polar angles, and Cartesian position in meters relative to SLC-41.

Table 3. Portion of the Aircraft's Data File Provided to The Aerospace Corporation by NOAA. These data include the first aircraft encounter with the Titan IV #K16 exhaust cloud. Note that the "hm" column does not agree with the "tGPS" column. The Aerospace Corporation registered all data to the GPS time using the fractional seconds from the "s" column. When "tGPS" was not available, the computer time ("hm" column) was used to interpolate between valid "tGPS" entries.

Log	yr	d	hm	s	ppm	rng	mV	tGPS	lat N/S	lon E/W	diff	# Sat	HDOP	alt units
113	1996	115	1940	23	-0.001	195.7	-27.63	234027	2834.4583N	8035.5792W	1	7	1.1	618 M
113	1996	115	1940	23.25	-0.002	195.7	-56.59	234027	2834.4583N	8035.5792W	1	7	1.1	618 M
113	1996	115	1940	23.5	-0.003	195.7	-70.2	234028	2834.4412N	8035.5528W	1	7	1.1	619 M
113	1996	115	1940	23.75	-0.002	195.7	-58.92	234028	2834.4412N	8035.5528W	1	7	1.1	619 M
113	1996	115	1940	24	0.772	1803	19.31	234028	2834.4412N	8035.5528W	1	7	1.1	619 M
113	1996	115	1940	24.25	1.766	1375	441.4	234028	2834.4412N	8035.5528W	1	7	1.1	619 M
113	1996	115	1940	24.5	4.502	1375	1125	234029	2834.4239N	8035.5264W	1	7	1.1	621 M
113	1996	115	1940	24.75	5.422	1375	1356	234029	2834.4239N	8035.5264W	1	7	1.1	621 M
113	1996	115	1940	25	5.71	1375	1427	234029	2834.4239N	8035.5264W	1	7	1.1	621 M
113	1996	115	1940	25.25	5.437	1375	1359	234029	2834.4239N	8035.5264W	1	7	1.1	621 M
113	1996	115	1940	25.5	5.438	1375	1359	234030	2834.4064N	8035.5002W	1	7	1.1	623 M
113	1996	115	1940	25.75	6.023	1375	1506	234030	2834.4064N	8035.5002W	1	7	1.1	623 M
113	1996	115	1940	26	5.274	1375	1319	234030	2834.4064N	8035.5002W	1	7	1.1	623 M
113	1996	115	1940	26.25	4.296	1375	1074	234030	2834.4064N	8035.5002W	1	7	1.1	623 M
113	1996	115	1940	26.5	3.517	1375	879	234031	2834.3886N	8035.4742W	1	7	1.1	625 M
113	1996	115	1940	26.75	2.728	1375	682.1	234031	2834.3886N	8035.4742W	1	7	1.1	625 M
113	1996	115	1940	27	2.108	1375	527	234031	2834.3886N	8035.4742W	1	7	1.1	625 M
113	1996	115	1940	27.25	1.62	1375	405.1	234031	2834.3886N	8035.4742W	1	7	1.1	625 M
113	1996	115	1940	27.5	1.217	1375	304.3	234032	2834.3702N	8035.4486W	1	7	1.1	627 M
113	1996	115	1940	27.75	0.951	1375	237.7	234032	2834.3702N	8035.4486W	1	7	1.1	627 M
113	1996	115	1940	28	0.785	827	1963	234032	2834.3702N	8035.4486W	1	7	1.1	627 M
113	1996	115	1940	28.25	0.646	828	1615	234032	2834.3702N	8035.4486W	1	7	1.1	627 M
113	1996	115	1940	28.5	0.555	828	1388	234033	2834.3513N	8035.4234W	1	7	1.1	628 M
113	1996	115	1940	28.75	0.49	827	1226	234033	2834.3513N	8035.4234W	1	7	1.1	628 M
113	1996	115	1940	29	0.424	828	1060	234033	2834.3513N	8035.4234W	1	7	1.1	628 M
113	1996	115	1940	29.25	0.362	828	905	234033	2834.3513N	8035.4234W	1	7	1.1	628 M
113	1996	115	1940	29.5	0.336	828	839	234034	2834.332N	8035.3986W	1	7	1.1	630 M
113	1996	115	1940	29.75	0.319	828	799	234034	2834.332N	8035.3986W	1	7	1.1	630 M

3.3.1.2 Cartesian Plot of Aircraft Data Relative to SLC-41

Figure 15 plots the spatial extent of aircraft's sampling during the 88 min following the launch of #K16. It represents conversion of the latitude and the longitude of the aircraft's position to Cartesian coordinates centered on the SLC-41 launch complex. The aircraft's position is labeled with HCl concentration at each sampling by using different plot symbols to bin concentration ranges. The HCl concentrations are based on calibrations performed by the NASA Toxic Vapor Detection/Contamination Monitoring Laboratory personnel and applied to the logged data files by NOAA personnel. Aerospace personnel applied a small constant baseline offset to eliminate negative HCl concentrations and filtered incorrect positional and time entries when GPS coverage was intermittent . As shown in Figure 15, the aircraft's flight pattern was largely confined to a 10 km × 25 km rectangle south of the launch complex. Time (0–88 min), polar angle (0–360°), distance (0–60000 m), and altitude (0–1600 m) are variables in the flight tracks presented in Figures 6 through 8. Thus, the HCl concentration hits noted in Figure 15 can be interpreted in light of these other critical variables. Briefly, the aircraft sampled the "lower portion" of the ground cloud only briefly at early times (first 8 min) and at late times (74 to 86 min). At all other times, the aircraft mapped the extent of the "upper portion" of the ground cloud, which moved out to sea (i.e., to the east southeast). The initial aircraft-derived trajectory (18°) for the "lower portion" of the ground cloud is very close to the imagery-derived trajectory (14°) measured during the first 6 min after launch.

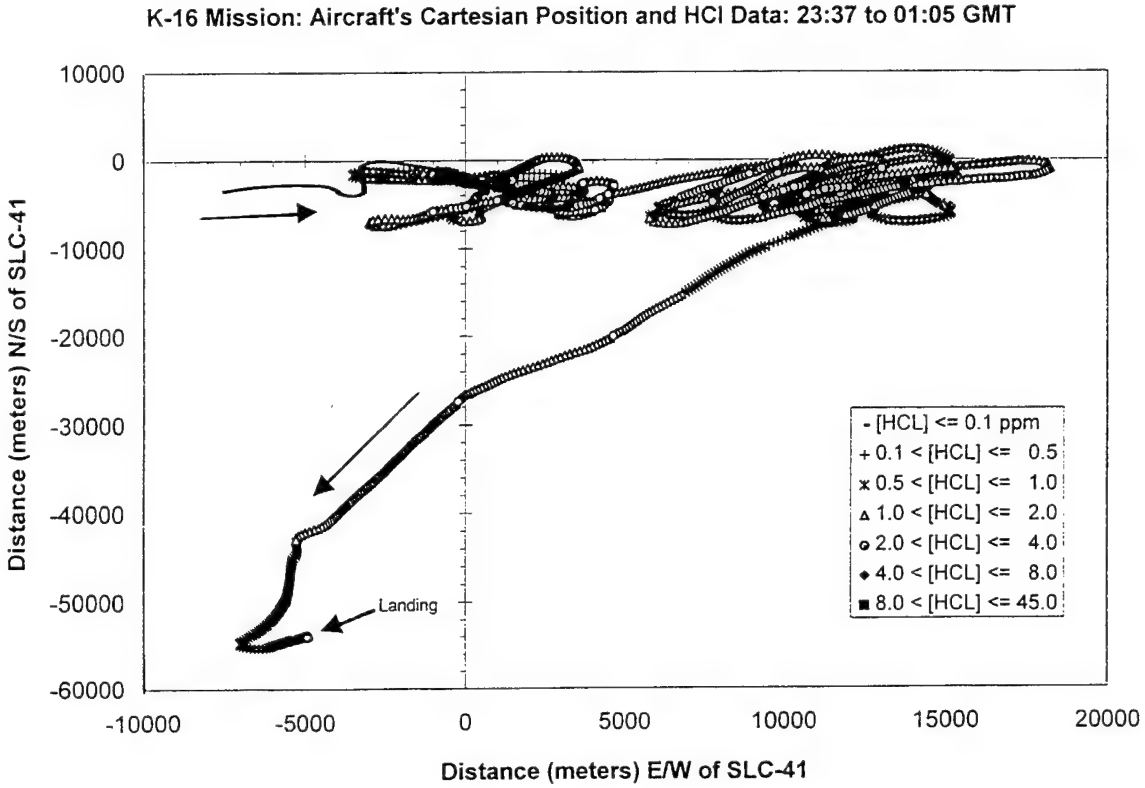

Figure 15. Cartesian plot documenting the aircraft's position relative to SLC-41 and the measured HCl concentration (based upon the Geomet detector) throughout the 88-min #K16 exhaust cloud sampling mission.

3.3.1.3 Geomet Detector Response to Calibration Gases

Figure 16 documents calibration gas response curves recorded using a data logger for the Geomet as deployed for the #K16 mission. The Geomet's configuration was equivalent for the #K23, #K15, K22, and #K16 missions. For the #K16 mission, the values for the plateaus in response to 1.8 ppm HCl vapor ranged from 1.8 ppm prior to launch (i.e., set by operator), to 1.6 ppm after launch (before recoating the inlet with reagent), and 1.7 ppm after recoating the inlet. Therefore, the Geomet's plateau in response to the calibration vapor degraded to 89% of its pre-flight value during the #K16 mission. Recoating the inlet with reagent recovered a few percent of the loss in response, yielding 94% of the pre-flight value. This behavior is documented by the #K16 response curves in Figure 16. Note that the response time changed more dramatically than the value of the plateau in response. The dramatic change in response time is consistent with depletion of the reagent from a portion of the inlet to the Geomet. As is evident in Figure 16, the time to 10% of the value of the plateau in response, following a sharp change in HCl concentration, is rapid for all calibration curves (i.e., even for the post-flight depleted inlet).

The data plotted in Figure 16 represent five challenges of the Geomet against a constant concentration of HCl vapor. For each challenge, the total exposure time can be calculated as the time between the start of the response to the calibration gas and the start of the fall at the end of the plateau. It is readily apparent that the exposure time was not a constant for these five calibrations.

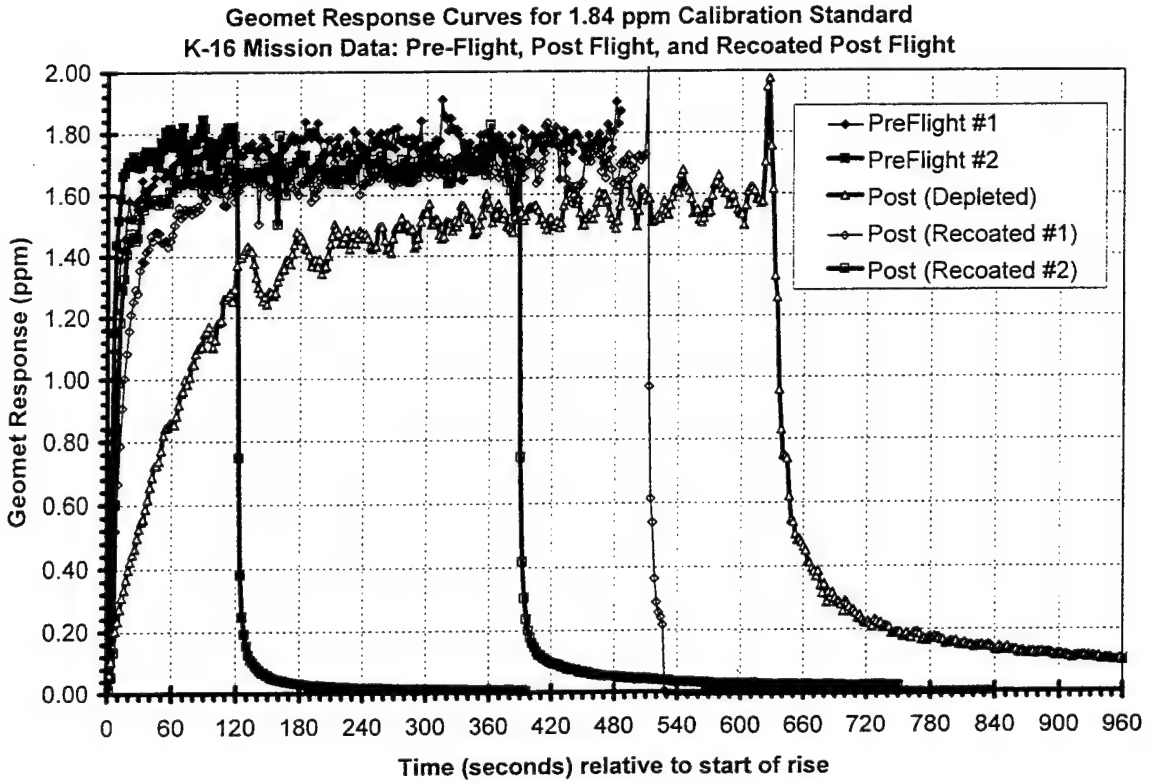

Figure 16. Geomet response curves illustrating rapid initial rise followed by rollover prior to reaching a plateau in response. These data are for the #K16 mission, which used a data logger to record the Geomet data. "Pre-Flight" #1 and #2 refer to the first and second exposure to the calibration gas after a single pre-flight coating of the inlet. Likewise "Post (Recoated" #1 & #2) refer to the first and second exposure to the calibration gas after washing and recoating the inlet after the flight (post-flight). "Post (Depleted)" refers to the exposure to the calibration gas after the flight (post-flight) but prior to washing and recoating of the inlet.

The inlet was coated with reagent prior to the first pre-flight calibration and after the post-flight challenge of the "reagent-depleted" inlet to the calibration gas. It is apparent from Figure 16 that the post-flight "reagent-depleted" inlet requires a longer time to reach a lower plateau in response than any of the other challenges.

The response characteristics of the Geomet detector are not perfectly matched to aircraft sampling. As configured for Titan IV missions (#K23, #K15, #K16, and #K22) and as illustrated by Figure 16 (#K16 data), the Geomet requires more than 15 s to reach 90% of its plateau in response as deployed for the Titan IV missions. Figure 16 also documents that the response time changes as a result of exposure to HCl vapor (i.e., the second exposures were faster than the first exposures after coating the inlet). This is consistent with passivation of active sites within the freshly coated inlet. Lastly, Figure 16 documents the fact that the magnitude of the plateau in response as well as the time to reach it can worsen when the exposure times are extremely long (as in the #K16 mission, which had an hour hold prior to extended sampling of the launch cloud). This is consistent with depletion of the reagent that coats the inlet. For all of the Titan IV mis-

sions, the Geomet's inlet was coated with reagent once prior to the flight. Therefore, one would expect some variation in response characteristics during each sampling mission.

Since the aircraft is moving at more than 70 m/s, and it takes 15 (or more) seconds for the Geomet to provide 90% response to the new HCl concentration, it is likely that the Geomet may underestimate the maximum HCl concentration for short encounters with the cloud. However, Figure 16 illustrates that the initial response to 10% of the plateau in response is extremely rapid. Thus, there should be little offset between the Geomet's first indication of change and the aircraft's encounter with the edge of the exhaust cloud. Therefore, we use the Geomet's HCl data to establish the position and relative strength of the exhaust cloud with the realization that the reported HCl concentration is an average value that depends upon the exposure history of the Geomet and the abruptness of HCl concentration changes.

In Figures 17 and 18, the Geomet's raw response and its integrated response are plotted against time for pre-flight and post-flight calibrations (data previously included in Figure 16). The integrated response is normalized in these figures to the total HCl dose (i.e., the total exposure time multiplied by the average value of the plateau in response). The total HCl dose is the area under the square calibration exposure function (i.e., the Geomet is exposed to a constant concentration for a given period of time). The integrated Geomet response is the area under the actual Geomet

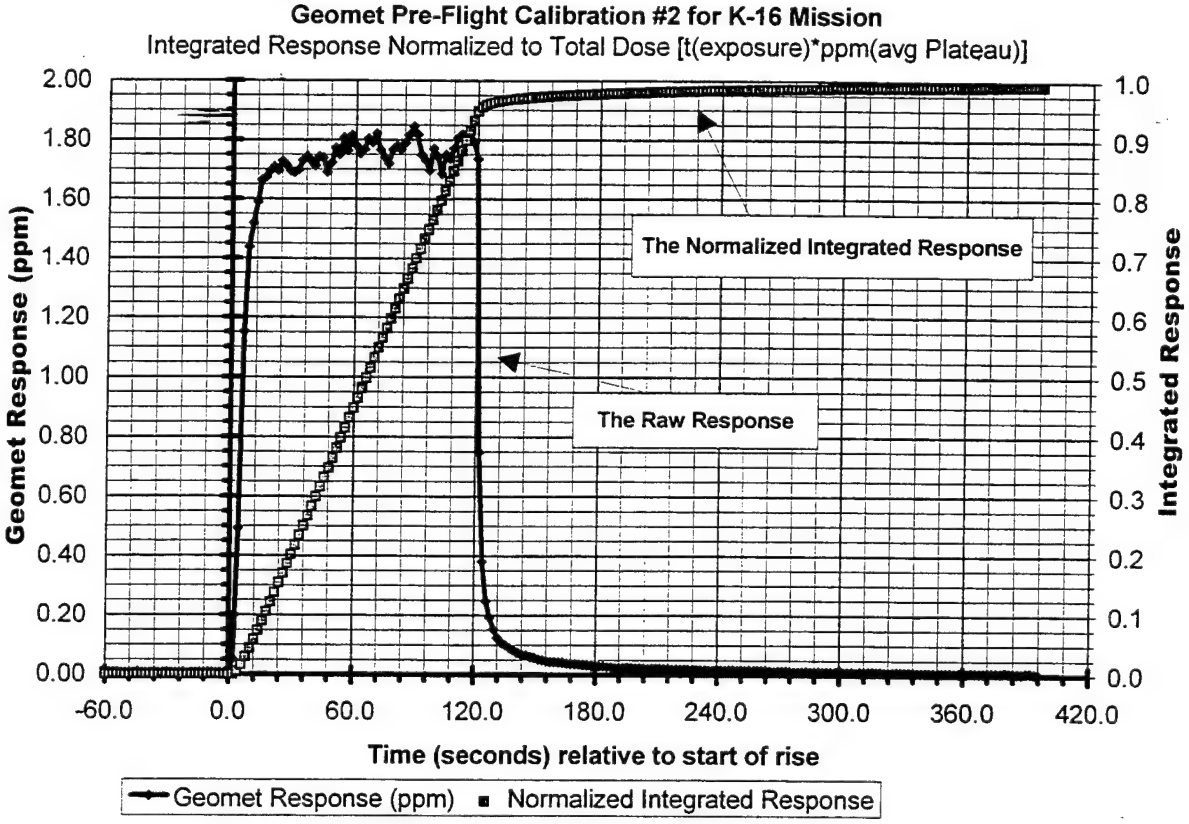

Figure 17. #K16 pre-flight raw and integrated response of the Geomet.

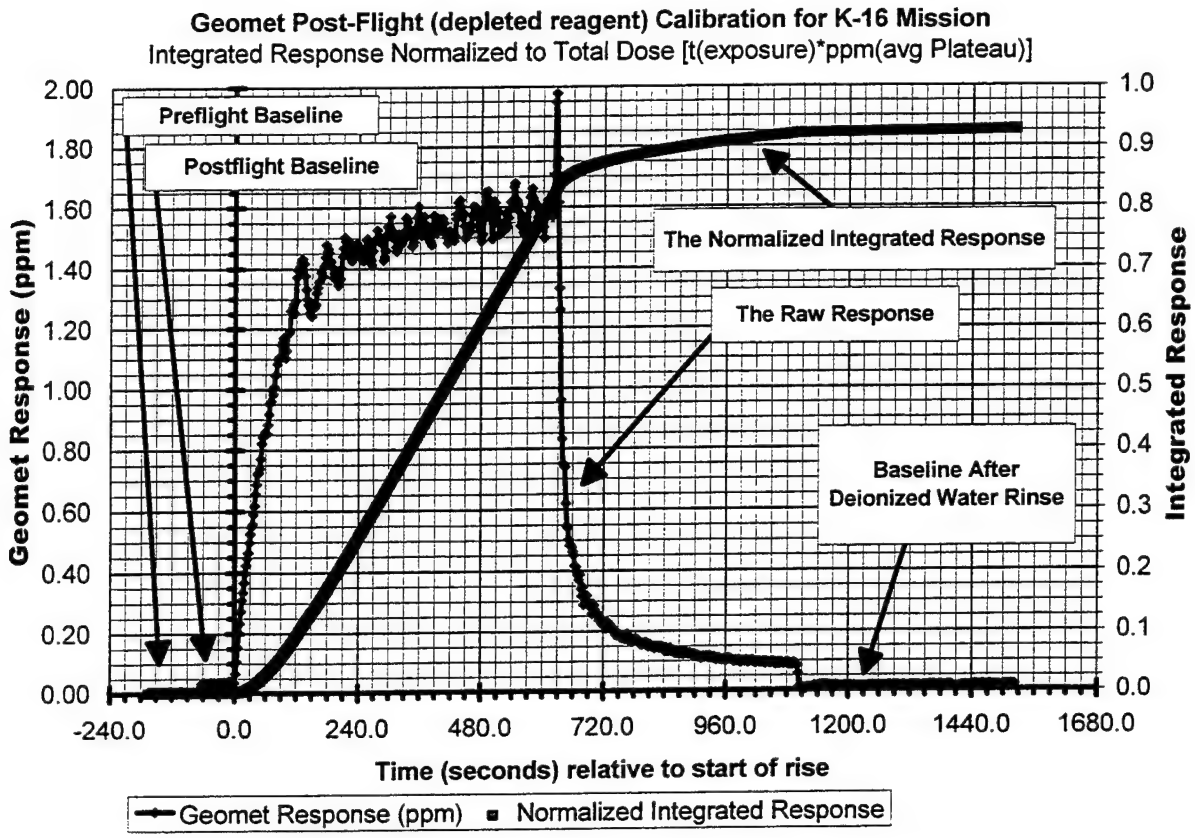

Figure18. #K16 post-flight raw and integrated response of the Geomet.

calibration response curve (which includes the sharp initial rise, the slower rollover to plateau, the plateau, the sharp falloff after the exposure is ended, and the slow recovery to baseline). The normalized integrated response (plotted in Figures 17 and 18) is the integrated response divided by the total HCl dose. These plots document that the Geomet accurately integrates the total HCl dose for these HCl vapor exposures. Unfortunately, I-NET did not record all of the "tail" of the Geomet's response to the post-flight calibration. Therefore, we can only say that the integrated response accounted for more than 92% of the total dose for the post-flight "depleted" inlet. On the other hand, there is quantitative behavior (i.e., more than 98% of total dose) for the pre-flight challenge.

The Geomet calibrations are HCl vapor challenges using constant concentration for long exposure times. These data illustrate that the Geomet has an almost instantaneous response to sudden large changes in HCl vapor concentration but requires a longer time to reach the plateau in response. Therefore, the Geomet should accurately map the extent but not necessarily the strength of the Titan IV exhaust cloud.

3.3.1.4 Geomet vs GFC Response to a Titan IV Exhaust Cloud

The temporal, relative, and absolute accuracy of the Geomet's response to a Titan IV exhaust cloud has been documented for the first few minutes after launch by comparison of the Geomet's cloud data to that of the Spectral Sciences gas filter correlation (GFC) spectrometer that flew on the same aircraft for the #K15 mission. The GFC spectrometer provided an instantaneous response to the exhaust cloud and was mounted beneath the aircraft. The inlet to the Geomet extended out of the front of the same aircraft. No GFC spectrometer was flown on the #K16 mission so we will reference the #K15 data in this discussion.

Spectral Sciences provided a description of the GFC spectrometer setup, its calibration, and their analysis of the #K15 exhaust cloud data in Section 4 of the #K15 report.[3] In that chapter, they documented that the GFC spectrometer's optics were irreversibly coated with exhaust cloud aerosols every pass through the cloud. This resulted in a dramatic decrease in signal-to-noise ratio with every encounter with a cloud. However, the GFC technique, as deployed for #K15, has an almost instantaneous response to HCl vapor since there was no inlet to their GFC cell (i.e., that is why it was directly exposed to the exhaust cloud).

In Section 3 of the #K15 report, we compared the GFC data to the Geomet data to establish the significance of the Geomet's response characteristics for actual aircraft sampling of Titan IV #K15 exhaust cloud. This comparison documented excellent temporal agreement between the GFC spectrometer and the Geomet detector for actual exhaust cloud encounters. Therefore, the start of response upon entering the edge of the cloud and initial fall upon exiting the cloud should accurately map the extent of the cloud. This is consistent with the Geomet's rapid initial response to sudden changes in HCl concentration (i.e., the calibration data). These same comparisons documented excellent positional accuracy for the maximum concentration reported by the Geomet relative to that recorded by the GFC technique. Therefore, the Geomet's fast initial response to significant changes seems to make it useful for mapping the position and shape of Titan IV launch clouds.

Section 3 of the #K15 report also investigated the effect of averaging time upon the comparison of GFC data to Geomet data. The analysis of that data is consistent with the Geomet's documented two-part response curve: (1) rapid initial response to a change in HCl concentration and (2) a slower rollover in response prior to reaching a plateau. The Geomet's fast component allows it to map the extent and position of the launch cloud as well as 3.85-s averaged GFC data. The GFC data had to be averaged with an 18-s period to equal the Geomet's maximum response, which is consistent with the longer times required for full Geomet response. Since the GFC technique only responds to vapor while the Geomet responds to total (aerosol and vapor) HCl, this treatment could not provide quantitative rise characteristics for the Geomet. In summary, the Geomet not only provides quantitative integrated HCl for each pass through the cloud but also accurately maps the extent and position of the cloud by virtue of the fast component of its complicated response function.

---

[3] Ground Cloud Dispersion Measurements During the Titan IV Mission #K15 (05 December, 1995) at Vandenberg Air Force Base, The Aerospace Corporation, submitted for publication

3.3.2 HCl Concentration Hits as a Function of Bearing from SLC-41

Figure 19 substantiates that the aircraft focused on a modest range of polar angles relative to the launch complex for the #K16 mission. In this report, the angles will conform to the convention of rawinsonde wind directions (the angle from which the wind originates that would push the cloud to the sampled position). Thus, the angles are related by

$$\vartheta = 180 + \Phi, \tag{1}$$

where ϑ is the equivalent rawinsonde wind angle, and Φ is the measured polar angle of the aircraft relative to SLC-41 and clockwise of true north. For example, when the aircraft is due east of SLC-41, Φ is 90°, and ϑ is 270°. As documented by Figure 14, the imagery-derived trajectory of the ground cloud was 14° while the T–0.7 hour rawinsonde wind directions at the bottom, middle, and top of the observable ground cloud were 7°, 317°, and 277°, respectively.

Referring to Figure 19, we will document that these aircraft data are consistent with the detection of the "lower portion" of the ground cloud to the south-southwest (i.e., polar angles between 0° and 40°) and the "upper portion" of the ground cloud to the east-southeast (i.e., polar angles between 270° and 360°) relative to SLC-41. Therefore, the aircraft's measurements are consistent with the measured rawinsonde wind shear.

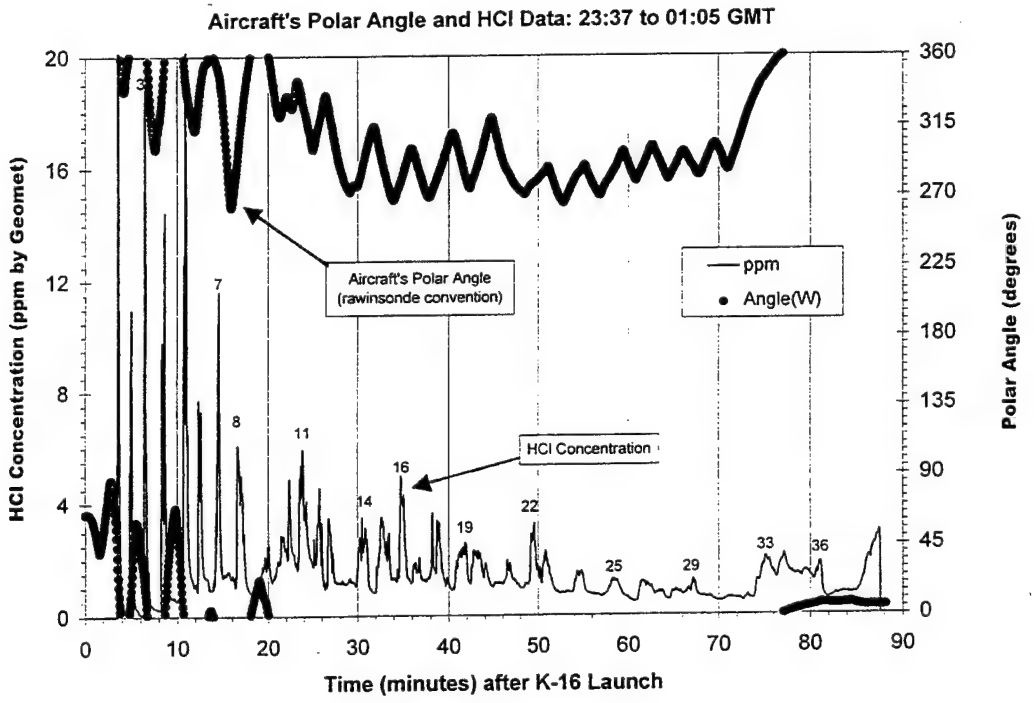

Figure 19. Summary of the aircraft's HCl concentration measurements and its polar angles (rawinsonde convention) plotted against time (min) after the Titan IV #K16 launch. These data are consistent with sampling of both the "lower" and "upper" portions of the ground cloud. The HCl peaks are numbered (1–36) to correlate cloud encounters in various figures.

3.3.3 HCl Concentration Hits as a Function of Radial Distance from SLC-41

Figure 20 is a plot of the HCl concentration and the aircraft's radial ground distance from SLC-41 against time after the #K16 launch. Figure 20 can be used to illustrate several conclusions regarding the aircraft's sampling campaign. The highest HCl concentrations were encountered at early times and in close proximity (<10 km) to the launch complex. As discussed previously, the HCl hits during the first 8 min can be assigned to the "lower portion" of the ground cloud based upon altitudes (less than 917 m MSL) and angles (0° to 40°). The other near-field hits are at altitudes and angles consistent with sampling the "upper portion" (southeasterly to easterly trajectory) of the ground cloud. Significant HCl concentrations (2–6 ppm) were observed at greater distances (i.e., 10 to 20 km from SLC-41) and were mainly confined to the altitudes and angles that apply to the "upper portion" of the ground cloud. All HCl hits were to the south of SLC-41, as discussed previously. While heading to the airport after sampling the "upper portion" of the ground cloud, the aircraft returned to lower altitudes, documenting several significant HCl hits at distances ranging from 20 to 54 km from SLC-41 along the length of the stretched and tilted ground cloud. The HCl detected at the airport required that portion of the cloud to move at a speed of 10.5 m/s, which is significantly greater than (1) the imagery-derived cloud speed (8.5 m/s) for the "lower portion" of the ground cloud during the first 6 min after launch, (2) the maximum rawinsonde-derived wind speed (7.5 m/s) at altitudes below the top of the ground cloud, and (3) the range of aircraft-derived cloud speeds (4–8 m/s) for the rest of the aircraft's HCl measurements.

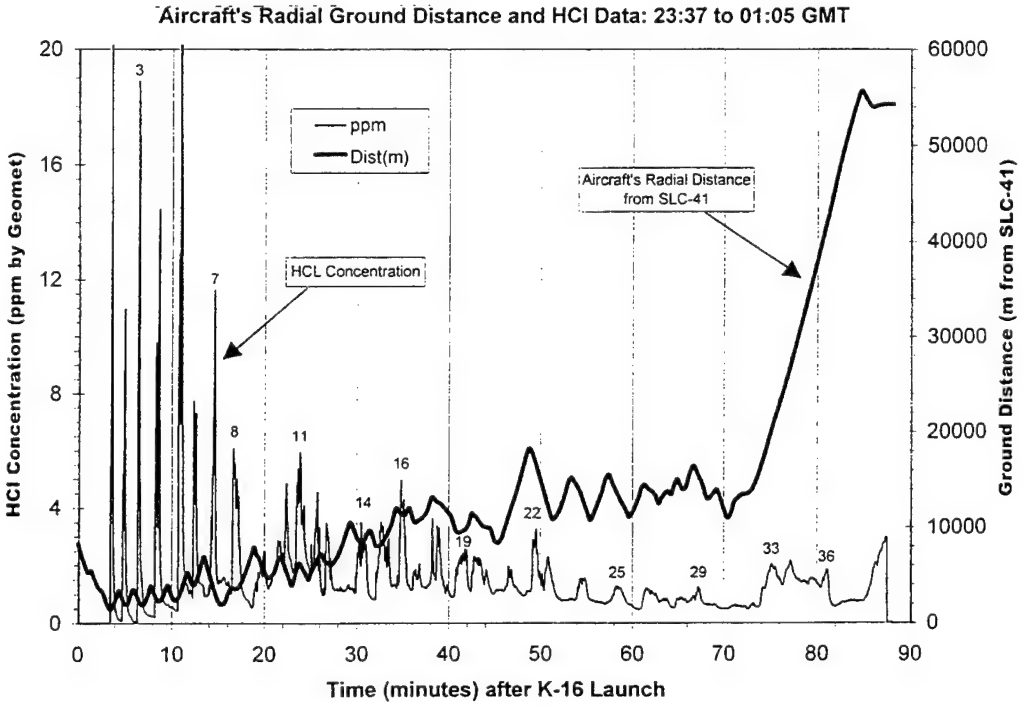

Figure 20. Summary of the aircraft's HCl concentration measurements and radial ground distance (m) from SLC-41 plotted against time (minutes) after the Titan IV #K16 launch. The "lower portion" of the ground cloud was sampled at early times (less than 8 min) and at late times (74 to 86 min). At other times, the aircraft sampled the "upper portion" of the ground cloud. The HCl peaks are numbered (1–36) to correlate cloud encounters in various figures.

3.3.4 HCl Concentration Hits as a Function of Altitude

Figure 21 is a plot of the aircraft's HCl measurements and of the aircraft's GPS altitude against time after launch. Figure 21 documents that at early times (i.e., first 8 min after launch), the HCl hits are at altitudes within the imagery-defined "lower portion" of the ground cloud (276 to 917 m MSL). The portions of the ground cloud as defined by imagery were discussed in a previous report (Section 2). The imagery revealed (1) that the top of the ground cloud stabilized within 3.5 min at an altitude of 1877 m MSL (±79 m) almost directly over SLC-41; (2) that the bottom of the cloud stabilized within 3.5 min at 219 m MSL (±17 m) with a south-southwesterly trajectory; and (3) that the launch column remained continuous with the top of the ground cloud but sheared to the east-southeast at higher altitudes. Given the altitude range, radial distance range, and polar angle range covered by the aircraft in the time period of 0–88 min, it is not surprising that so many HCl hits were observed. Examination of Figure 21 shows that the pilot concentrated on altitudes (~ 1000 to 1500 m by GPS) equivalent to the "middle" to "upper" portions of the ground cloud as defined by the imagery. The pilot followed the "upper portion" of the ground cloud out to sea rather than the "lower portion" of the ground cloud over the land. As noted in Figure 14, T–0.7 hour rawinsonde wind directions at the altitudes (219 to 1877 m MSL) ranged from 7 to 277°, respectively. These wind directions are consistent with the aircraft's HCl data that documented HCl hits to the east-southeast at high altitudes and HCl hits to the south-southwest at low altitudes.

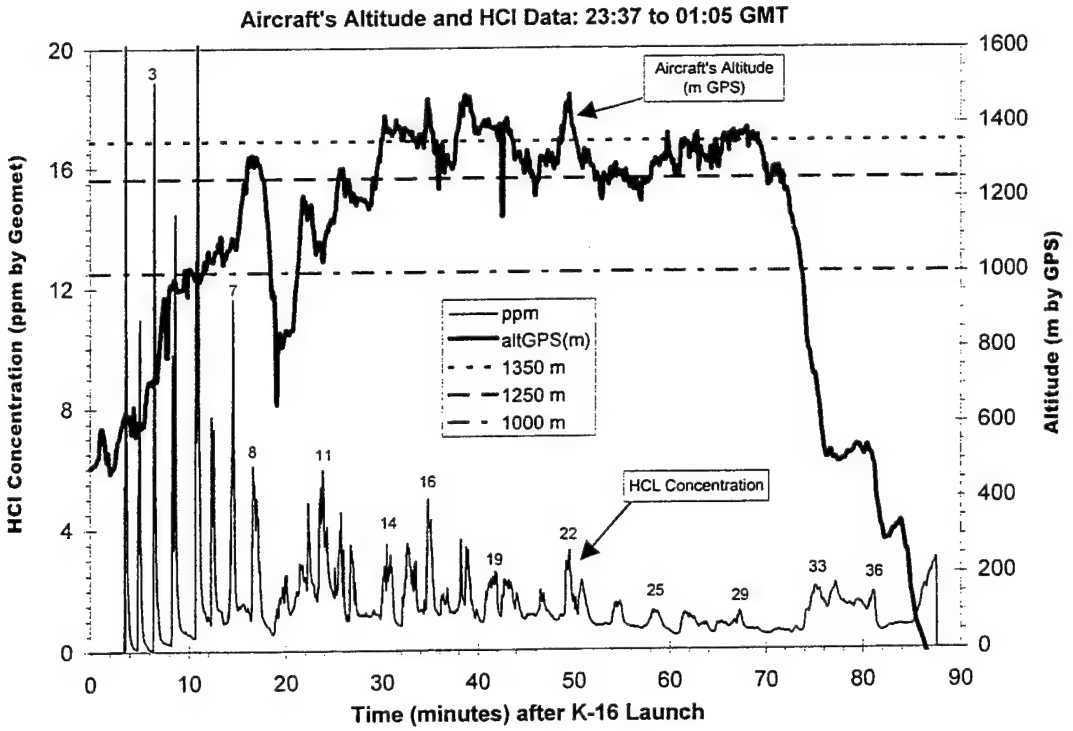

Figure 21. Summary of the aircraft's HCl concentration measurements and altitude (m) plotted against time (min) after the Titan IV #K16 launch. The "lower portion" of the ground cloud was sampled at altitudes below 917 m MSL as it headed to the south-southwest. At higher altitudes, the aircraft sampled the "upper portion" of the ground cloud as it moved out to sea. The HCl peaks are numbered (1–36) to correlate cloud encounters in various figures.

3.3.5 HCl Concentration Hits as a Function of Altitude and Aircraft Position

This section will provide substantiation for observations made in previous portions of this overview of the aircraft's sampling data. The figures referenced in this section are subsets of the data presented in the Cartesian plot in Figure 15.

3.3.5.1 HCl Hits at Altitudes Greater than 1350 m

Figure 22 is a Cartesian plot, centered at SLC-41, of the aircraft's sampling data collected at altitudes between 1350 and 1500 m by GPS. For these altitudes, the aircraft's HCl concentration profiles documented an southeasterly initial trajectory followed by an easterly trajectory at later times. There are no aircraft data at these altitudes that can be compared to the imagery data collected during the first 6 min after launch. However, the imagery documented (1) a south-southwesterly trajectory for the "lower portion" of the ground cloud; (2) an almost stationary "upper portion" of the ground cloud located above SLC-41; (3) an easterly bearing for the launch column; and (4) stabilization heights of 219, 1023, and 1877 m MSL for the bottom, middle, and the top, respectively, of the ground cloud. Therefore, the data in Figure 22 represent sampling of the "upper portion" of the ground cloud as defined by the imagery. The sampling angles are consistent with the rawinsonde winds at the middle and top of the ground cloud.

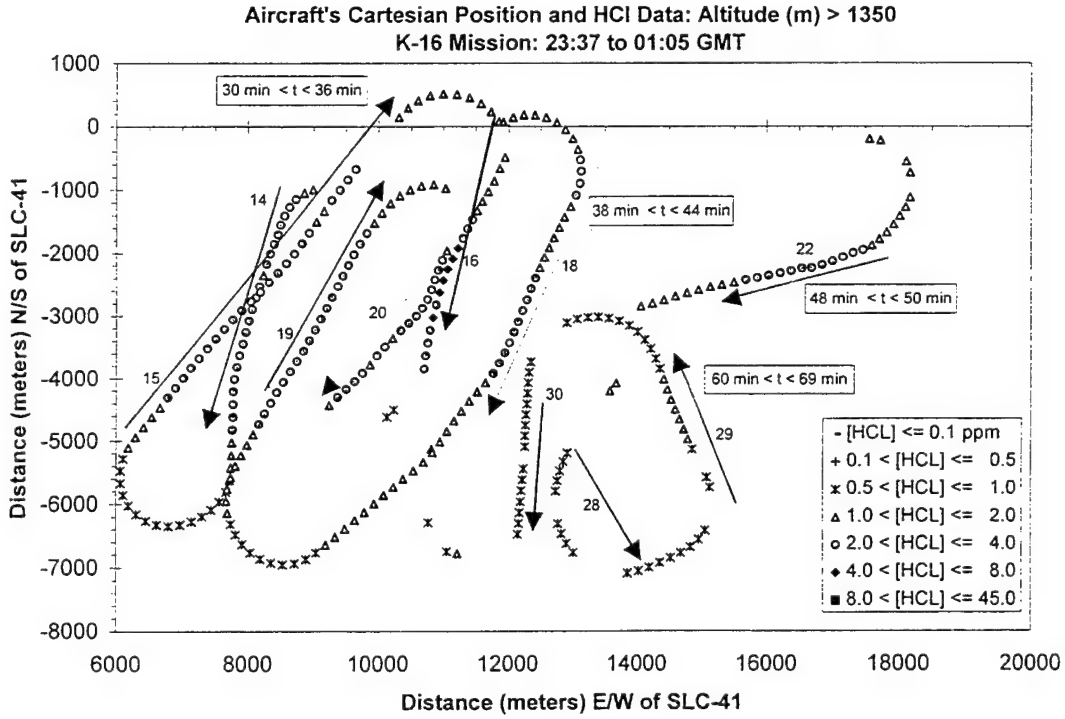

Figure 22. Summary Cartesian plot documenting the aircraft's position and measured HCl concentrations while sampling at altitudes between 1350 and 1500 m by GPS after the Titan IV #K16 launch. These data document an southeasterly initial cloud trajectory followed by an easterly trajectory at later times. These data represent sampling of the "upper portion" of the ground cloud as defined by imagery. The numbers (1–36) correlate cloud encounters in various figures.

3.3.5.2 HCl Hits at Altitudes Less than 1350 m and Greater than 1250 m

Figure 23 is a Cartesian plot, centered at SLC-41, of the aircraft's sampling data collected at altitudes between 1250 and 1350 m by GPS. For these altitudes, the aircraft's HCl concentration profiles documented an southeasterly initial trajectory followed by an easterly trajectory at later times. The data in Figure 23 represent sampling of the "upper portion" of the ground cloud as defined by the imagery. The sampling angles are consistent with the rawinsonde winds at the middle and top of the ground cloud. The extent and trajectory of the cloud at these altitudes is almost identical to the 1350 to 1500 m altitude data in Figure 22.

3.3.5.3 HCl Hits at Altitudes Less than 1250 m and Greater than 1000 m

Figure 24 is a Cartesian plot, centered at SLC-41, of the aircraft's sampling data collected at altitudes between 1000 and 1250 m by GPS. For these altitudes, the aircraft's HCl concentration profiles documented a southwesterly initial trajectory at the lowest altitudes, a southeasterly trajectory at slightly later times and greater altitudes, and an easterly trajectory at the latest times. The data in Figure 22 represent sampling of the "middle portion" of the ground cloud only at

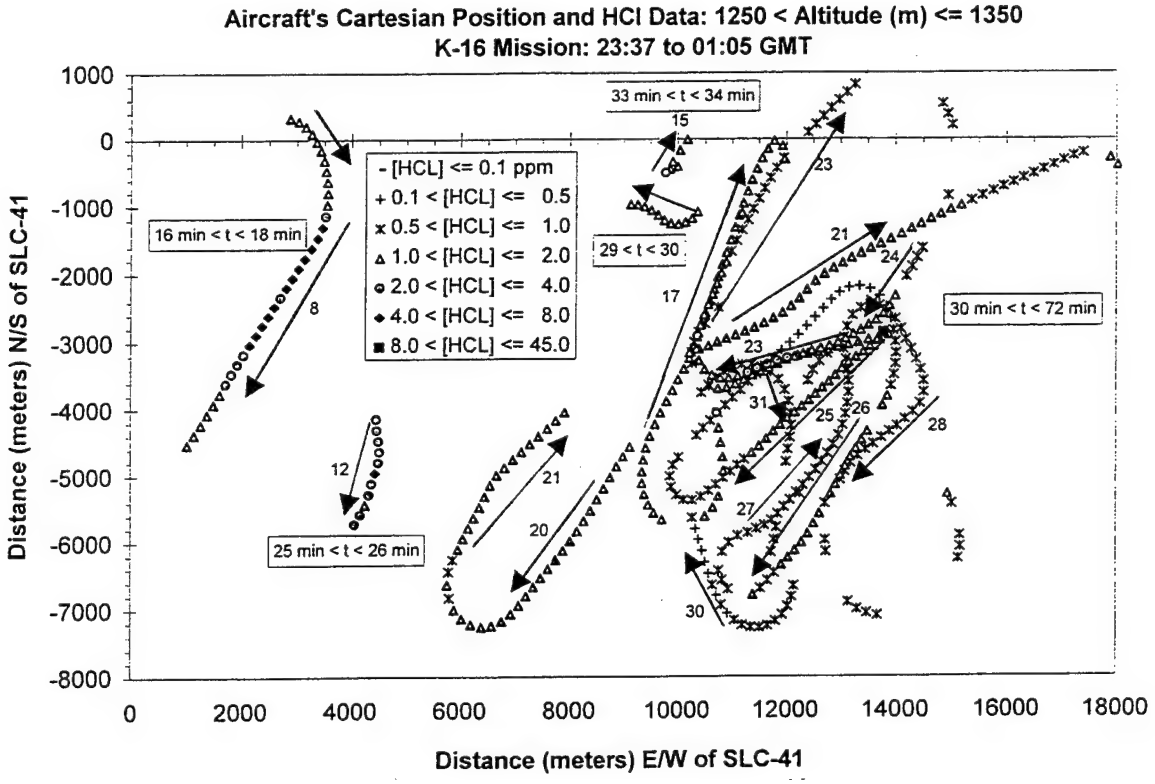

Figure 23. Summary Cartesian plot documenting the aircraft's position and measured HCl concentrations while sampling at altitudes between 1250 and 1350 m by GPS after the Titan IV #K16 launch. These data document an southeasterly initial cloud trajectory followed by an easterly trajectory at later times. These data represent sampling of the "upper portion" of the ground cloud as defined by imagery. The numbers (1–36) correlate cloud encounters in various figures.

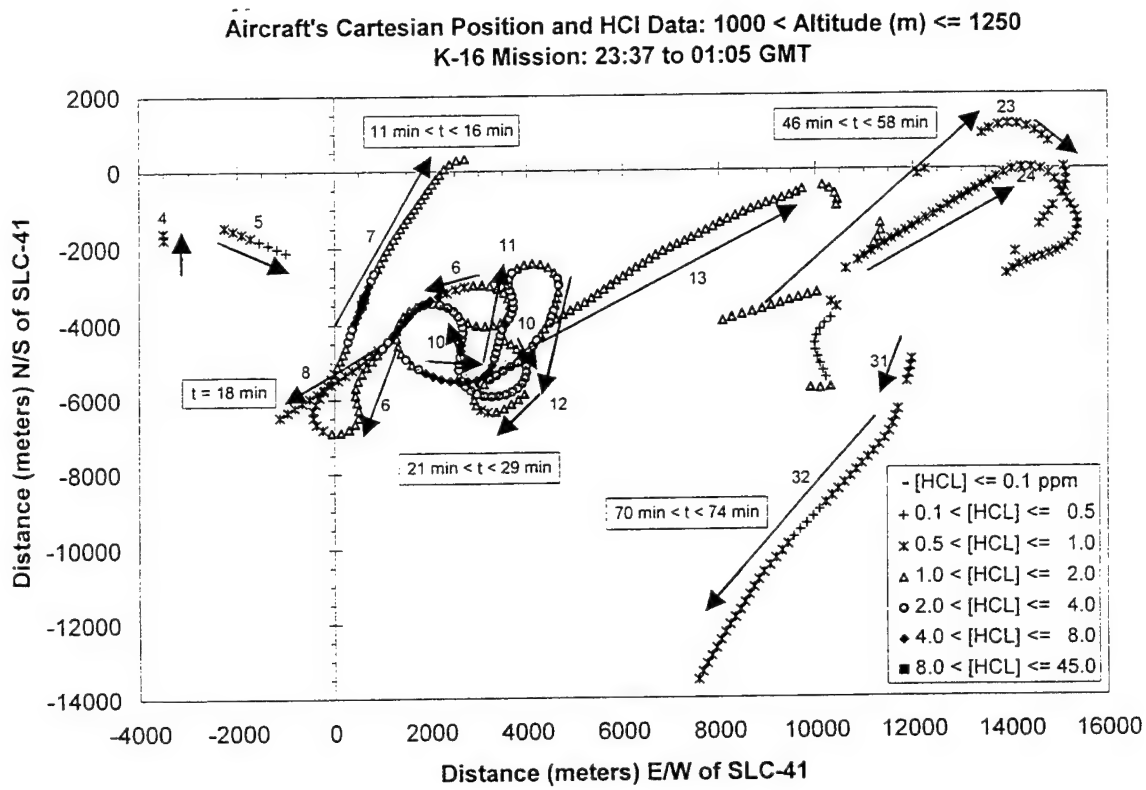

Figure 24. Summary Cartesian plot documenting the aircraft's position and measured HCl concentrations while sampling at altitudes between 1000 to 1250 m by GPS after the Titan IV #K16 launch. These data document a southwesterly initial cloud trajectory (at the lowest altitudes) shifting to the southeast at greater altitudes and ultimately to the east at the longest times. The numbers (1–36) correlate cloud encounters in various figures.

the earliest times and lowest altitudes within this altitude range. At later times, the data document the extent of the "upper portion" of the ground cloud. The extent and trajectory of the "upper portion" of the ground cloud at these altitudes is almost identical to the data in Figure 22 and Figure 23 for greater altitudes. These data are consistent with the wind shear documented by the rawinsonde sounding.

3.3.5.4 HCl Hits at Altitudes Less than 1000 m

Figure 25 is a Cartesian plot, centered at SLC-41, of the aircraft's sampling data collected at altitudes between 0 and 1000 m by GPS. At early times (less than 8 min), these data document the same south-southwesterly track that was observed by the imagery (0–6 min) for the "lower portion" of the ground cloud. At slightly later times (8–11 min), the data document a southeasterly trajectory consistent with sampling the "middle portion" of the ground cloud. At times later than 18 min after launch, the data document a southerly trajectory and mixing to the ground level at the airport. The south to southwesterly hits observed at the lowest altitudes is in sharp contrast to the trend observed at higher altitudes. Those data (i.e., Figure 22 through Figure 24) documented a southeasterly initial bearing shifting to an easterly bearing at later times. The

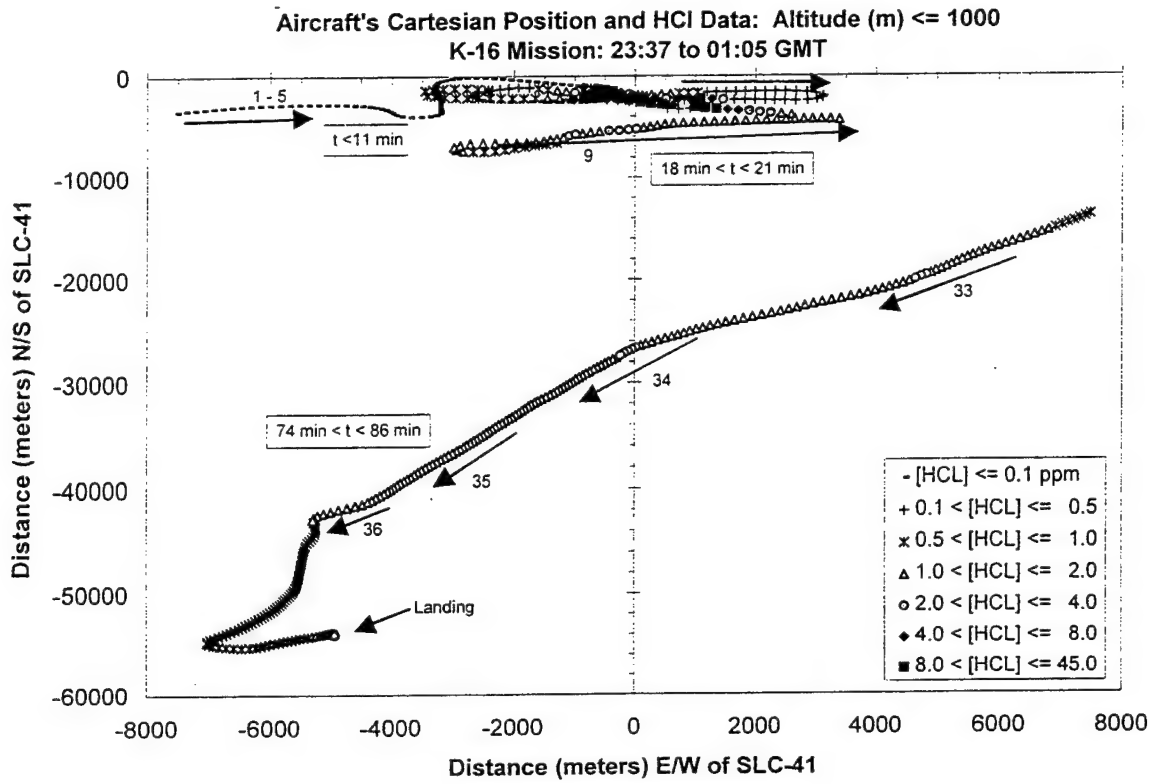

Figure 25. Summary Cartesian plot documenting the aircraft's position and measured HCl concentrations while sampling at altitudes between 0 to 1000 m by GPS after the Titan IV #K16 launch. The southerly cloud trajectory at altitudes less than 917 m is dramatically different from the southeasterly to easterly trajectories observed between 917 m and 1000m. Based upon both altitude and trajectory, most of these data represent sampling within the "lower portion" of the ground cloud. The numbers (1–36) correlate cloud encounters in various figures.

southerly trajectory documented by most of the data in Figure 25 and the low sampling altitudes suggest that most of these data apply to the "lower portion" of the ground cloud as defined by the imagery (i.e., altitudes less than 917 m). However, the strong hits in the southeastern quadrant are actually at altitudes between 917 m and 1000 m and represent sampling of the "middle portion" of the ground cloud. Therefore, the aircraft data are consistent with the shear documented by the rawinsonde-derived wind directions and observed by the imagery.

3.3.5.5 HCl Hits at Altitudes Less than 917 m and "Lower Portion" Trajectory

Figure 26 is a Cartesian plot, centered at SLC-41, of the aircraft's sampling data collected at altitudes between 0 and 917 m by GPS. Based upon quantitative imagery during the first 6 min after launch, the "lower portion" of the ground cloud ranged from 276 to 917 m MSL in altitude. Therefore, all of the data plotted in Figure 26 should represent sampling of this "lower portion" of the ground cloud or downward dispersion from the other portions of the ground cloud. The aircraft's HCl concentration profiles at these altitudes document an initial south-southwesterly

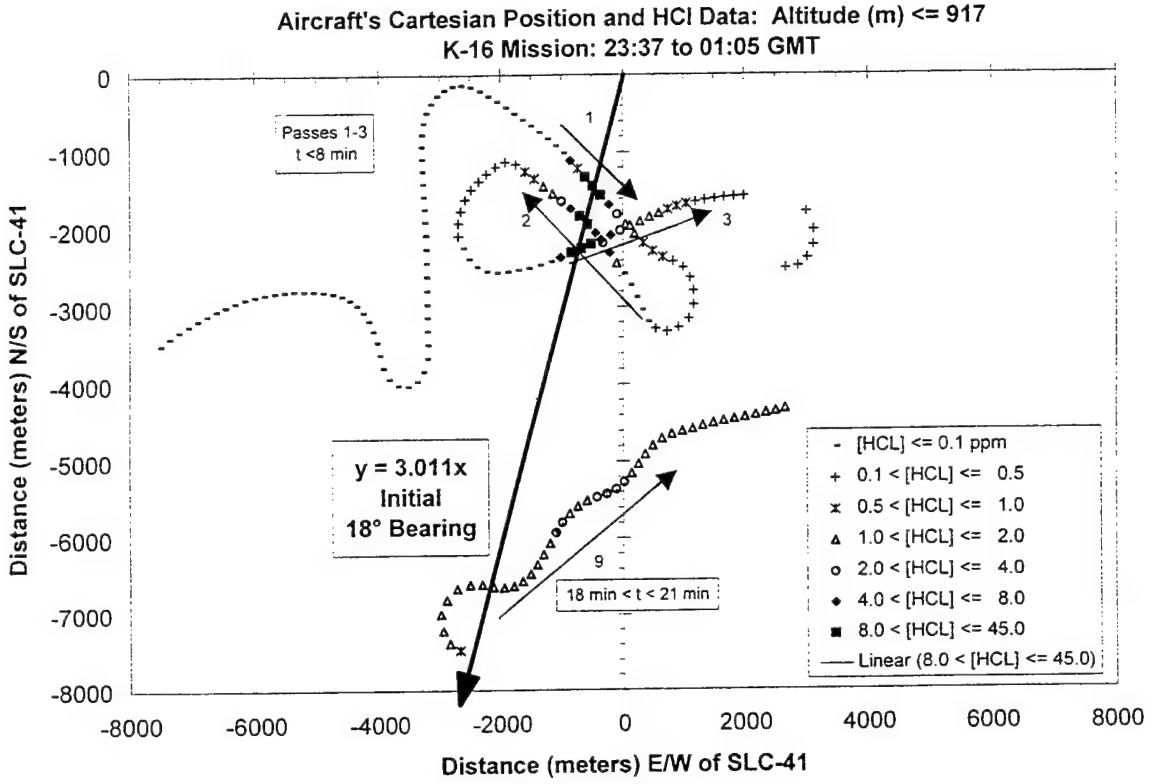

Figure 26. Summary Cartesian plot documenting the aircraft's position and measured HCl concentrations while sampling at altitudes below 917 m by GPS after the Titan IV #K16 launch. The south-southwesterly trajectory (18°) is comparable to the imagery-derived trajectory (14°) for the "lower portion" of the ground cloud. Likewise, the trajectory is comparable to the rawinsonde-derived wind direction (7°) at the bottom of the ground cloud. The numbers (1–36) correlate cloud encounters in various figures.

(18°) trajectory followed by a shift at later times to a more southerly trajectory. Within the accuracy of the measurements, this initial aircraft-derived trajectory is in good agreement with the imagery-derived trajectory (14°) for the "lower portion" of the ground cloud. Likewise, both of these measured trajectories are fairly close to the 7° rawinsonde-derived wind direction at the bottom of the ground cloud. Finally, REEDM's surface impact prediction (4°) is closer to the observed cloud trajectory for the "lower portion" of the ground cloud than REEDM's stabilization height prediction (348° to maximum shifting to 303° at later times).

3.4 Summary and Conclusions

The aircraft's Geomet total HCl detector monitored the ground cloud from the Titan IV #K16 launch and obtained a large quantity of HCl concentration data as a function of time and aircraft position. The aircraft's HCl concentration data documented a shear in trajectory for the ground cloud as a function of altitude and time. For the first 8 min after launch, the aircraft documented a southwesterly (18°) trajectory that is comparable with (1) the imagery-derived cloud track (14°)

for the "lower portion" of the ground cloud, (2) REEDM's surface impact prediction (4°), and (3) the rawinsonde wind direction (7°) at the bottom of the ground cloud. At higher altitudes and later times, the aircraft documented a southeasterly trajectory, shifting to an easterly trajectory that is comparable with the rawinsonde winds at the middle (317°) and the top (277°) of the ground cloud. During the last leg of the aircraft's flight, the HCl measurements documented a southeasterly and southerly trajectory at altitudes corresponding to the middle and bottom of the ground cloud. Again, these data are consistent with the rawinsonde wind directions at these altitudes. The aircraft remained below 1500 m throughout this mission. For comparison, the imagery-derived altitudes for the bottom, middle, and top of the stabilized ground cloud were 219, 1023, and 1877 m. Therefore, all of the aircraft's HCl measurements were at altitudes within or below the stabilized ground cloud (as defined by imagery during the first 6 min after launch).

The aircraft's data documented measurable levels of HCl to ground level at the Melbourne airport. The HCl detected at the airport would require a 10.5 m/s cloud velocity, which is significantly greater than (1) the imagery-derived cloud speed (8.5 m/s) for the "lower portion" of the ground cloud during the first 6 min after launch, (2) the maximum rawinsonde wind speed (7.5 m/s) at altitudes below the top of the ground cloud, and (3) the range of aircraft-derived cloud speeds (4–8 m/s) measured throughout the rest of the mission. However, we have no reason to doubt the accuracy of these Geomet readings, and the bearing to the airport is consistent with rawinsonde winds near the surface.

In a subsequent report, we will correlate the aircraft's HCl measurements with the imagery for the first 6 min after launch to document the dimensions and concentration distributions within the rising and the stabilized ground cloud. In a third report, we will provide a series of polar, Cartesian, and time plots for each 10-min increment in the aircraft's #K16 mission. In addition to average HCl concentrations for each transect, one can extract angular spreads and cloud dimensions for favorable transects. These subsequent detailed data reviews will provide the data in a format that will facilitate direct comparison to individual dispersion model runs (i.e., for a specific time after launch, altitude above the pad, and distance from the pad). The intent of this program is to document the results in sufficient detail to validate dispersion models.

As discussed in this report, the Geomet detector is useful for aircraft sampling of launch clouds. We provide data that illustrate quantitative integrated response as well as excellent temporal and spatial accuracy for mapping the extent and position of Titan IV clouds. We also establish that the concentration reported by any detector is a strong function of its response function (i.e., averaging time). The Geomet reports an HCl concentration that represents an average value for at least an 18-s period. In contrast, the temporal and spatial accuracy of the Geomet is consistent with an averaging time of only 3 to 4 seconds. We recommend use of caution when comparing measured HCl concentration to predicted HCl concentration since the averaging times associated with the detectors are not the same as those used in typical model runs.

Appendix A—REEDM T–0.7, T–0.5, and T–0.2 Hour Runs

[The material in this section was contributed by R. N. Abernathy of the Environmental Monitoring and Technology Department of The Aerospace Corporation's Space and Environment Technology Center.]

On 24 April 1996, the Titan IV #K16 mission was successfully launched from Space Launch Complex (SLC-41) at Cape Canaveral Air Station (CCAS) at 19:37 EDT (23:37 GMT). As part of the Model Validation Program (MVP), the resulting exhaust cloud was sampled by aircraft-based total HCl detectors and was imaged from three camera sites. The analysis of the quantitative imagery documented the rise time, stabilization height, and the trajectory of the ground cloud.

This appendix summarizes the Rocket Exhaust Effluent Diffusion Model (REEDM) predictions for the rise and dispersion of the exhaust cloud from the Titan IV #K16 launch. REEDM version 7.07 defaults were used in these normal launch runs. REEDM used the rawinsonde data from T–0.7, T–0.5, and T–0.2 hours prior to the launch. This appendix includes figures and tables that document the output of REEDM. The predictions are compared in tabular and graphical form to the imagery-derived cloud characteristics and to the rawinsonde wind data at the imagery-derived heights for the bottom, middle, and top of the stabilized launch cloud. In addition, the REEDM predictions for cloud trajectory are compared to the imagery-derived cloud trajectory (Section 2), the rawinsonde wind directions (Appendix B), and the aircraft's measurements of HCl concentration profiles (Section 3). These data are critical to the validation of current and future dispersion models.

In this appendix, all angles (cloud bearings and wind directions) are reported in the convention of rawinsonde wind vectors; the angle from which the wind originates. For example, when the cloud is due east of SLC-41, (i.e., the cloud is at 90° clockwise from north), we report the bearing to the cloud as 270° (i.e., the rawinsonde equivalent wind direction). This allows direct comparison of cloud data to rawinsonde data.

T-0.7 hour REEDM Version 7.07 Normal Launch Predictions

REEDM version 7.07 was run for a normal launch using its operational defaults and the T–0.7 hour rawinsonde data (Appendix B). This section of the appendix begins with a figure that graphically compares the imagery-derived cloud trajectory, the rawinsonde-measured wind directions, and the REEDM-predicted cloud trajectories. Next are the standard REEDM figures documenting the concentration isopleths at the surface and at the predicted stabilization height. A summary table quantifies the similarities and differences between the imagery-derived cloud characteristics, the rawinsonde-measured winds, and the REEDM-predicted cloud characteristics. Finally, all of these data are compared to the aircraft's measurements of HCl concentration profiles.

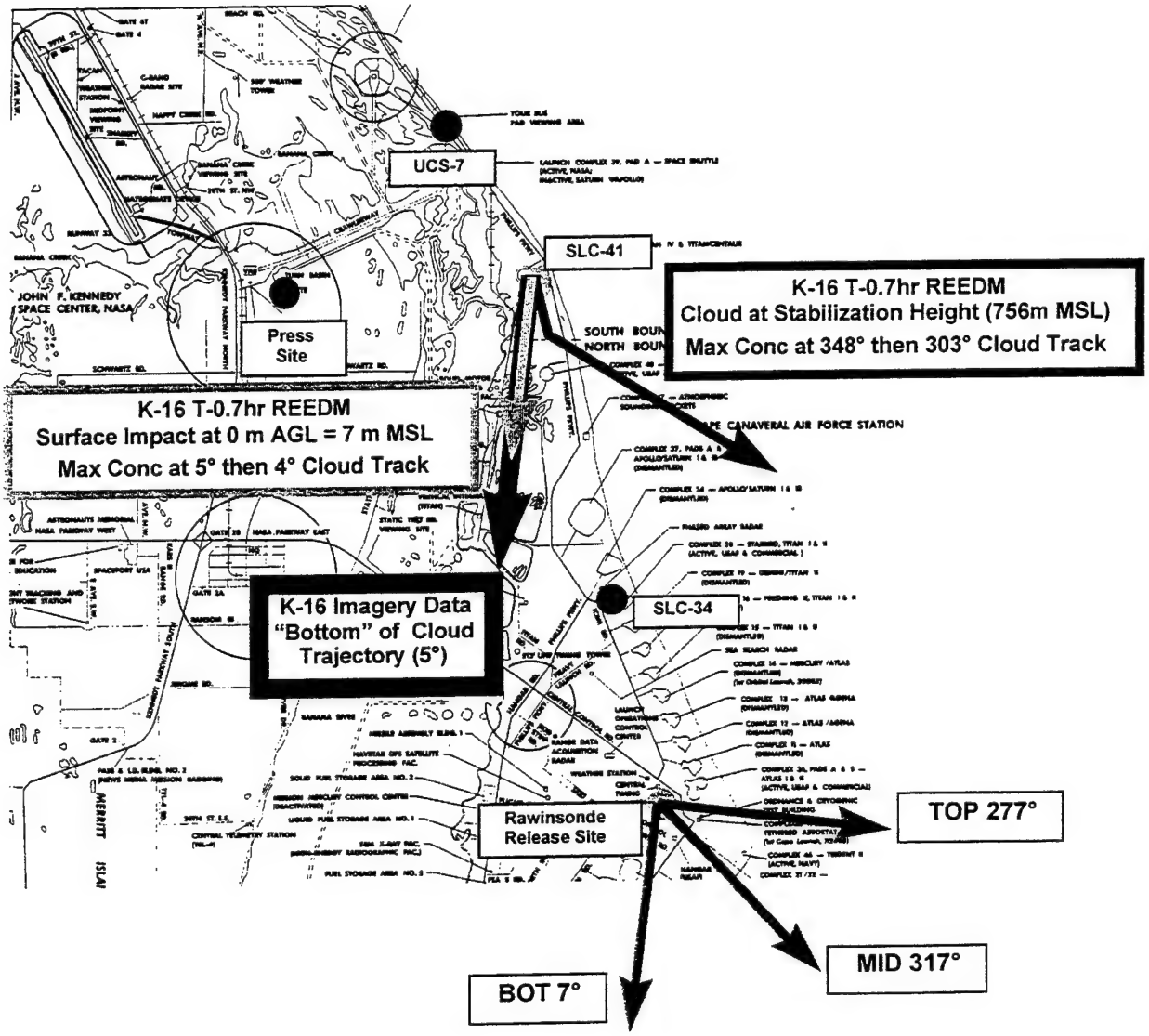

Figure A-1. Map documenting the imagery-derived ground cloud trajectory, the T-0.7 hour rawinsonde-measured winds, and the T-0.7 hour REEDM-predicted ground cloud tracks. The map also documents the positions of the three imagery sites and the rawinsonde release site.

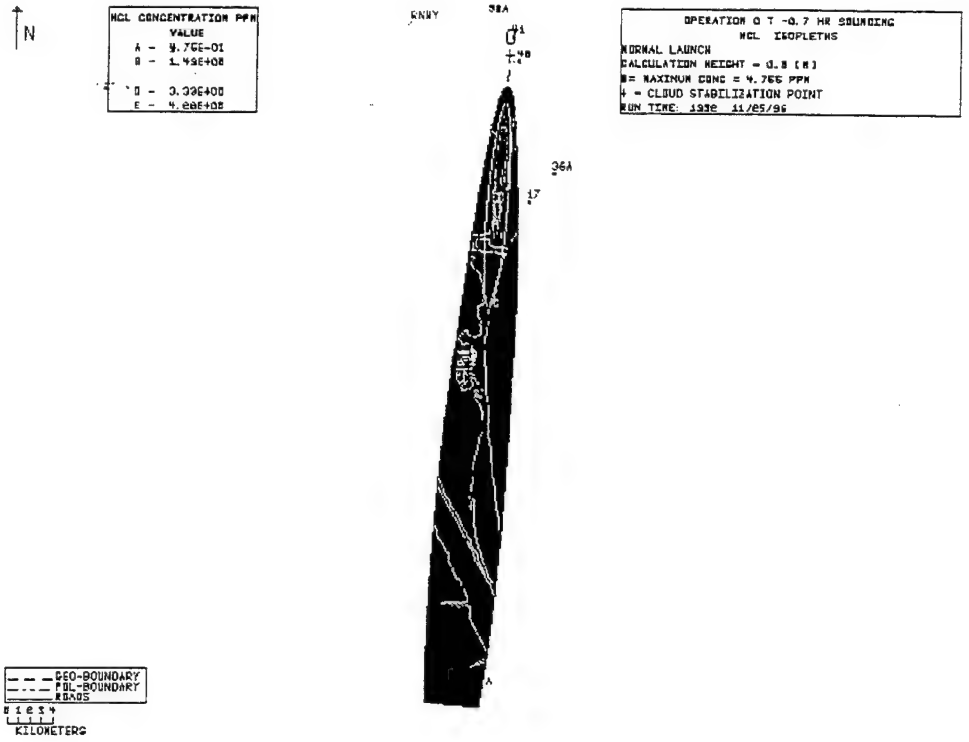

Figure A-2. T-0.7 hour REEDM prediction for surface impact

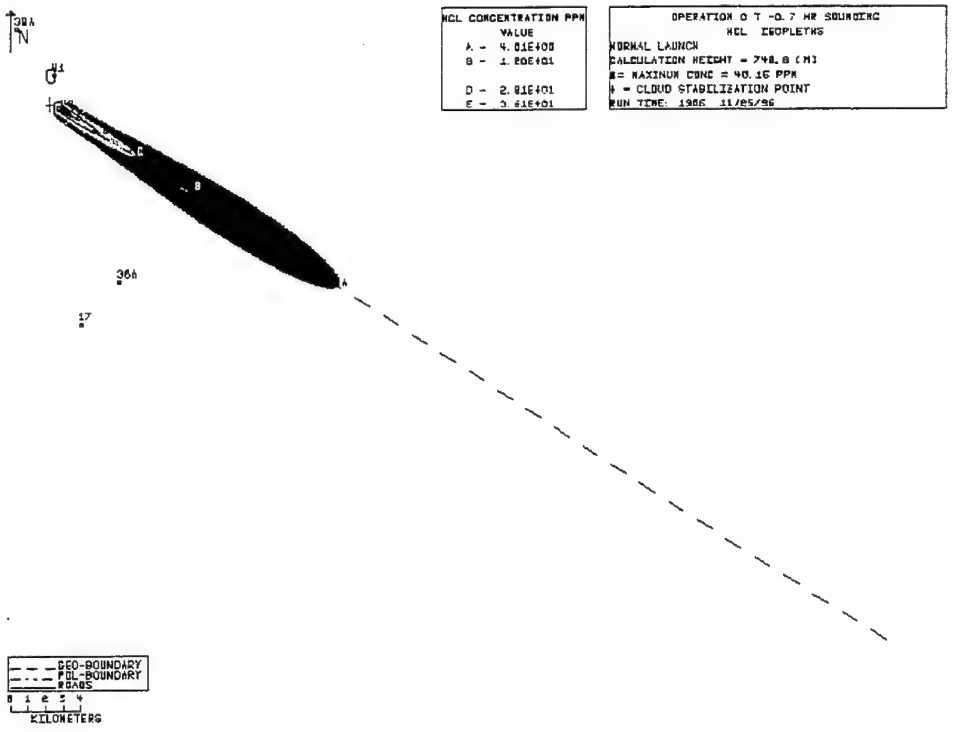

Figure A-3. T-0.7 hour REEDM prediction for stabilization height (749 m AGL = 756 m MSL).

Table A-1. Summary of Imagery-Derived, T–0.7 hour Rawinsonde Sound, and T-0.7 hour REEDM Data

Attribute	Feature	Visible Imagery	Rawinsonde (T–0.7 h)	REEDM 7.07 (T–0.7 h) (Max Conc @ H(m))	REEDM 7.07 (T–0.7 h) (Long Range Tracks @ H(m))
Height (m MSL)	Top	1877	#N/A	#N/A	#N/A
Stabilization	Middle	1023	#N/A	756	756
(SLC-41 = 7 m MSL	Bottom	219	#N/A	#N/A	#N/A
Time (min)	Top	4.0	#N/A	#N/A	#N/A
Stabilization	Middle	3.5	#N/A	4.4	4.4
	Bottom	3.5	#N/A	#N/A	#N/A
Bearing (deg)	Top	None	277	#N/A	#N/A
(Rawinsonde convention)	Middle	~N-NW (Box)	317	348° (Max @ 756 m MSL)	303° (Cloud @ 756 m MSL)
	Bottom	5° to 14° (Line)	7	5° (Max @ 0 m AGL)	4° (Cloud @ 0 m AGL)
Speed (m/s)	Top	~0	7.7	#N/A	#N/A
	Middle	3.6 (Box)	6.2	#N/A	5.8° (Cloud @ 756 m MSL
	Bottom	8.5 (Line)	7.3	#N/A	7.0° (Cloud @ 0 m AGL)

Review of Table A-1 reveals several interesting differences between the observed #K16 cloud behavior, the T–0.7 hour rawinsonde data, and the T–0.7 hour REEDM predictions for the exhaust cloud behavior. The observed stabilization height (1023 m MSL) was 35% higher than predicted (756 m MSL). The observed stabilization time (3.5 min) was 20% faster than predicted (4.4 min). The imagery documented that the "lower portion" of the ground cloud moved in a south-southwesterly direction (i.e., winds from 5 to 14° at 8.5 m/s). This was similar to the wind direction and speed measured by the rawinsonde sounding (i.e., wind from 7° at 7.3 m/s at the height of the bottom of the cloud). Likewise, the observed movement of the "lower portion" of the cloud was similar to REEDM's surface impact prediction (i.e., 4° at 7.0 m/s). In contrast, the imagery documented that the "upper portion" of the ground cloud remained almost stationary during the 6 min of tracking. This resulted in the observed average bearing of south-southwesterly (i.e., winds from the north-northwest) for the ground cloud. This is dramatically different from the rawinsonde data that document winds from 277° at 7.7 m/s at the height of the top of the cloud and winds from 317° at 6.2 m/s at the height of the middle of the cloud. These winds should have pushed the top and middle of the cloud to the east and to the southeast, respectively. Likewise, REEDM predicted a south-southeasterly bearing (348°) to the maximum concentration at the predicted stabilization height and a southeasterly bearing (303° at 7.0 m/s) for the ground cloud after it stabilized. The aircraft's HCl measurements tie all of the above together since the aircraft's data documented a south-southwesterly trajectory for the "lower portion" of the ground cloud and a southeasterly to easterly trajectory for the "upper portion" of the ground cloud.

T-0.5 hour REEDM Version 7.07 Normal Launch Predictions

REEDM version 7.07 was run for a normal launch using its operational defaults and the T–0.5 hour rawinsonde data (Appendix A). This section of the appendix begins with a figure that graphically compares the imagery-derived cloud trajectory, the rawinsonde-measured wind directions, and the REEDM-predicted cloud trajectories. Next are the standard REEDM figures documenting the concentration isopleths at the surface and at the predicted stabilization height.

A summary table quantifies the similarities and differences between the imagery-derived cloud characteristics, the rawinsonde-measured winds, and the REEDM-predicted cloud characteristics. Finally, all of these data are compared to the aircraft's measurements of HCl concentration profiles.

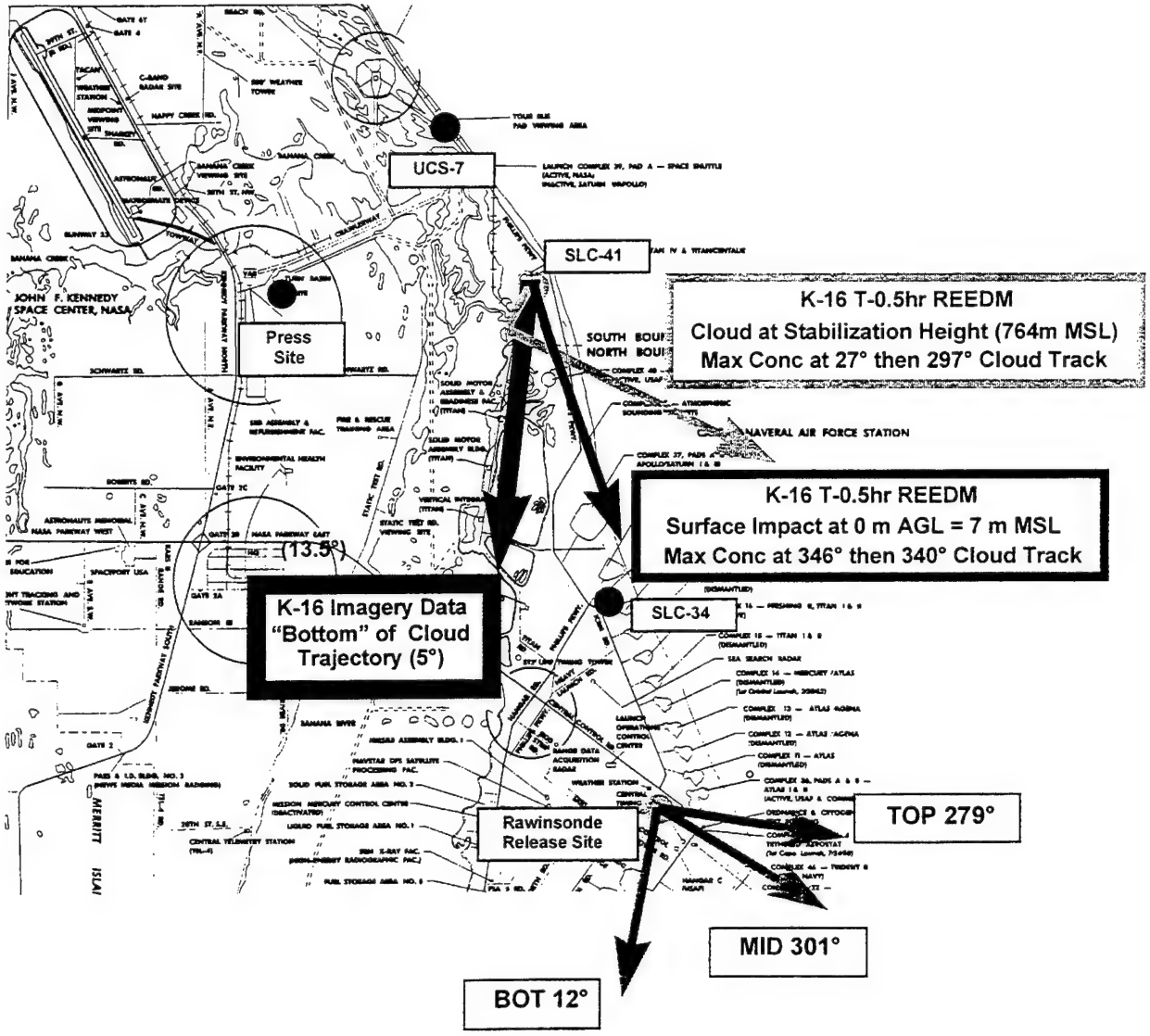

Figure 4. Map documenting the imagery-derived ground cloud trajectory, the T-0.5 hour rawinsonde-measured winds, and the T-0.5 hour REEDM-predicted ground cloud tracks. The map also documents the positions of the three imagery sites and the rawinsonde release site.

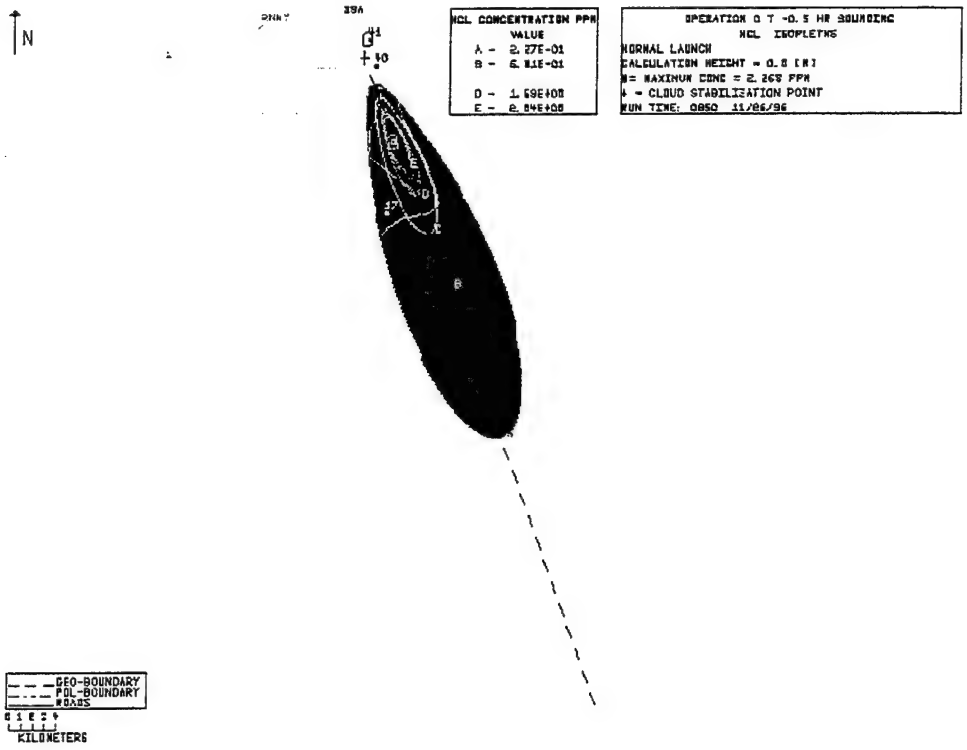

Figure 5. T-0.5 hour REEDM prediction for surface impact.

Table A-2. Summary of Imagery-Derived, T–0.5 hour Rawinsonde Sound, and T-0.5 hour REEDM Data

Attribute	Feature	Visible Imagery	Rawinsonde (T–0.5 h)	REEDM 7.07 (T–0.5 h) (Max Conc @ H(m))	REEDM 7.07 (T–0.5 h) (Long Range Tracks @ H(m))
Height (m MSL)	Top	1877	#N/A	#N/A	#N/A
Stabilization	Middle	1023	#N/A	764	764
(SLC-41 = 7 m MSL	Bottom	219	#N/A	#N/A	#N/A
Time (min)	Top	4.0	#N/A	#N/A	#N/A
Stabilization	Middle	3.5	#N/A	4.4	4.4
	Bottom	3.5	#N/A	#N/A	#N/A
Bearing (deg)	Top	None	279°	#N/A	#N/A
(Rawinsonde convention)	Middle	~N-NW (Box)	301°	27° (Max @ 764 m MSL)	297° (Cloud @ 764 m MSL)
	Bottom	5° to 14° (Line)	12°	346° (Max @ 0 m AGL)	340° (Cloud @ 0 m AGL)
Speed (m/s)	Top	~0	8.1	#N/A	#N/A
	Middle	3.6 (Box)	4.6	#N/A	5.8° (Cloud @ 756 m MSL
	Bottom	8.5 (Line)	7.2	#N/A	7.0° (Cloud @ 0 m AGL)

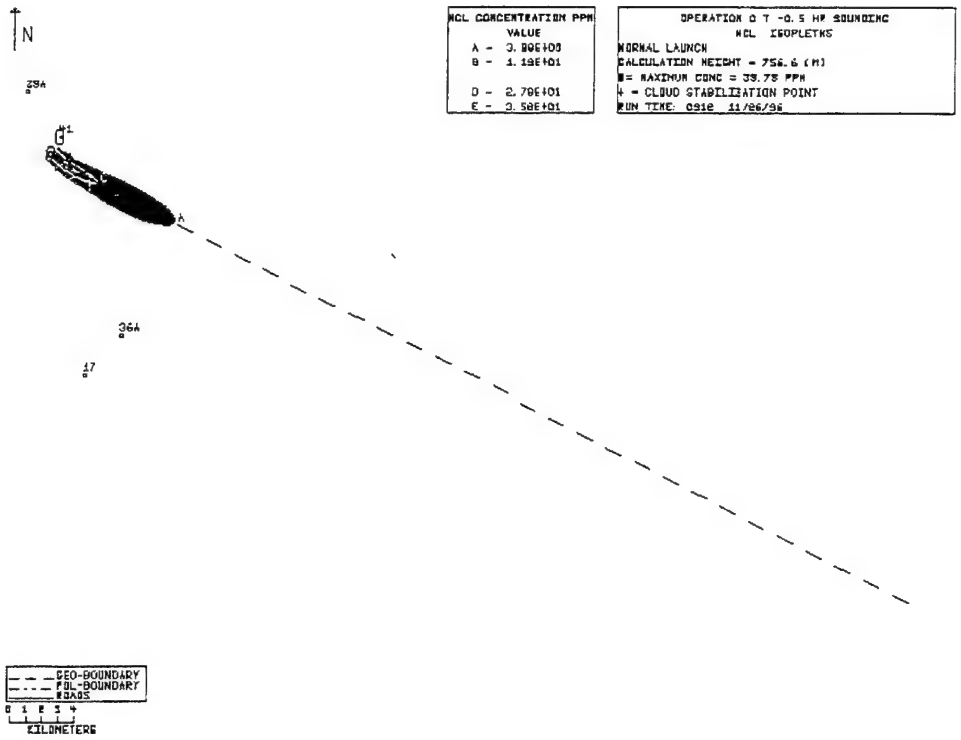

Figure 6. T-0.5 hour REEDM prediction for stabilization height (757 m AGL = 764 m MSL).

Review of Table 2 reveals several interesting differences between the observed #K16 cloud behavior, the T–0.5 hour rawinsonde data, and the T–0.5 hour REEDM predictions for the exhaust cloud behavior. The observed stabilization height (1023 m MSL) was 34% higher than predicted (764 m MSL). The observed stabilization time (3.5 min) was 20% faster than predicted (4.4 min). The imagery documented that the "lower portion" of the cloud moved in a south-southwesterly direction (i.e., winds from 5 to 14° at 8.5 m/s). This was similar to the wind direction and speed measured by the rawinsonde sounding (i.e., wind from 12° at 7.2 m/s at the height of the bottom of the cloud). In contrast, the observed movement of the "lower portion" of the cloud did not agree with REEDM's south-southeasterly prediction (i.e., 340° at 4.6 m/s at the surface). The imagery documented that the "upper portion" of the ground cloud remained almost stationary during the 6 min of tracking. This resulted in the observed average bearing of south-southwesterly (i.e., winds from the north-northwest) for the ground cloud. This is dramatically different from the rawinsonde data that document winds from 279° at 8.1 m/s at the height of the top of the cloud and winds from 301° at 4.6 m/s at the height of the middle of the cloud. These winds should have pushed the top and the middle of the cloud to the east and to the southeast, respectively. Likewise, REEDM predicted a south-southwesterly bearing (27°) to the maximum concentration at the predicted stabilization height but a east-southeasterly bearing (297° at 6.2 m/s) for the ground cloud after it stabilized. The aircraft's HCl measurements can be used to referee the above discrepancies since the aircraft's data documented a south-southwesterly trajectory for the "lower portion" of the ground cloud (agreeing with imagery but not with REEDM's prediction) and a southeasterly to easterly trajectory for the "upper portion" of the ground cloud (consistent with rawinsonde data and REEDM predictions).

T-0.2 hour REEDM Version 7.07 Normal Launch Predictions

REEDM version 7.07 was run for a normal launch using its operational defaults and the T–0.2 hour rawinsonde data (Appendix A). This section of the appendix begins with a figure that graphically compares the imagery-derived cloud trajectory, the rawinsonde-measured wind directions, and the REEDM-predicted cloud trajectories. Next are the standard REEDM figures documenting the concentration isopleths at the surface and at the predicted stabilization height. A summary table quantifies the similarities and differences between the imagery-derived cloud characteristics, the rawinsonde-measured winds, and the REEDM-predicted cloud characteristics. Finally, all of these data are compared to the aircraft's measurements of HCl concentration profiles.

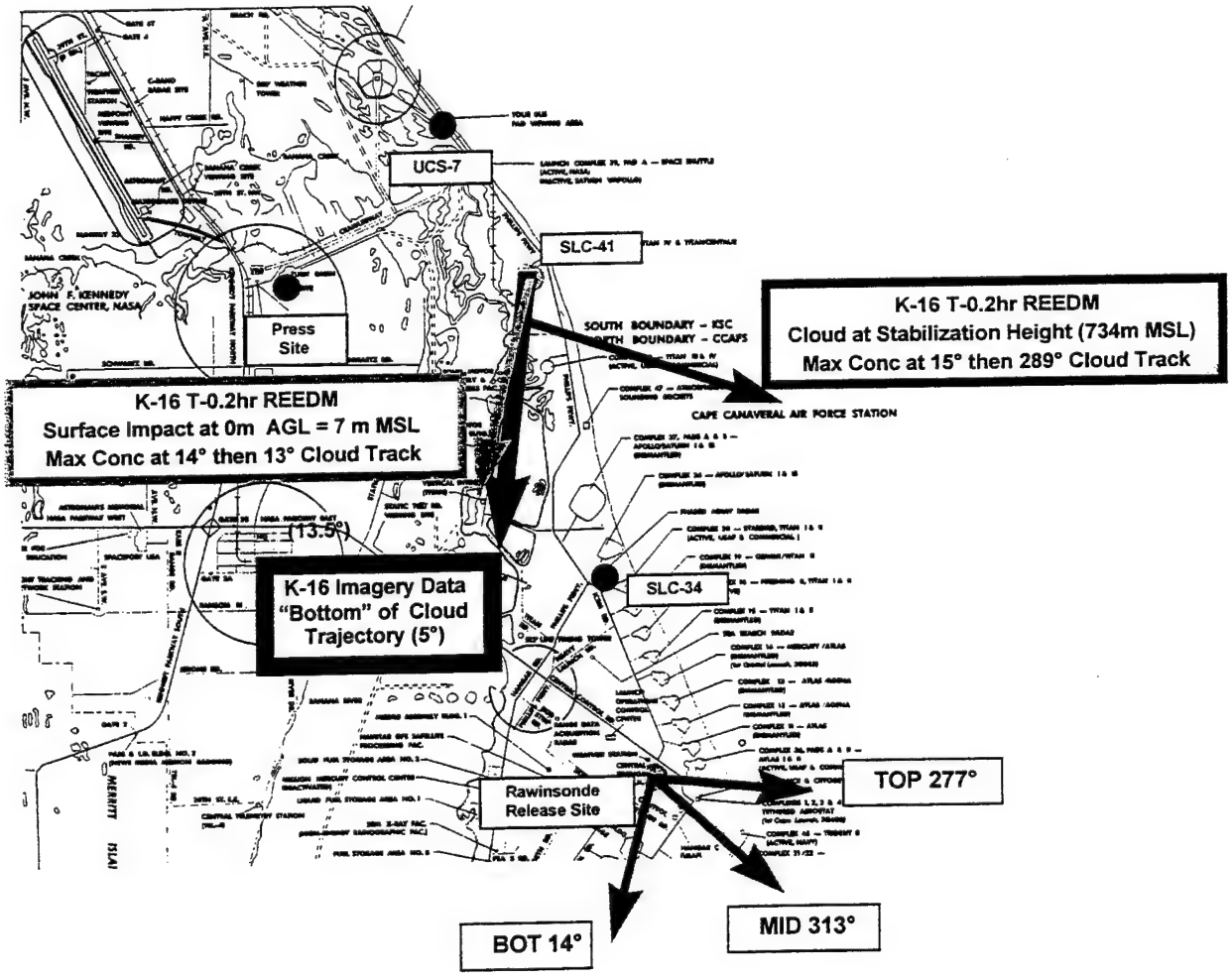

Figure 7. Map documenting the imagery-derived ground cloud trajectory, the T–0.2 hour rawinsonde-measured winds, and the T-0.2 hour REEDM-predicted ground cloud tracks. The map also documents the positions of the three imagery sites and the rawinsonde release site.

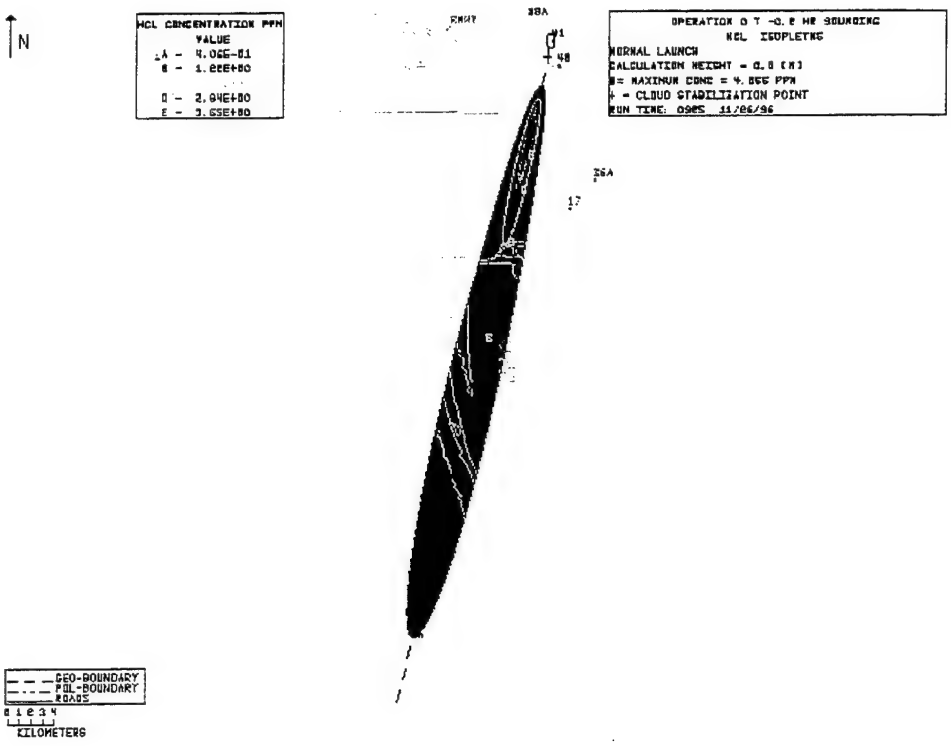

Figure 8. T-0.2 hour REEDM prediction for surface impact.

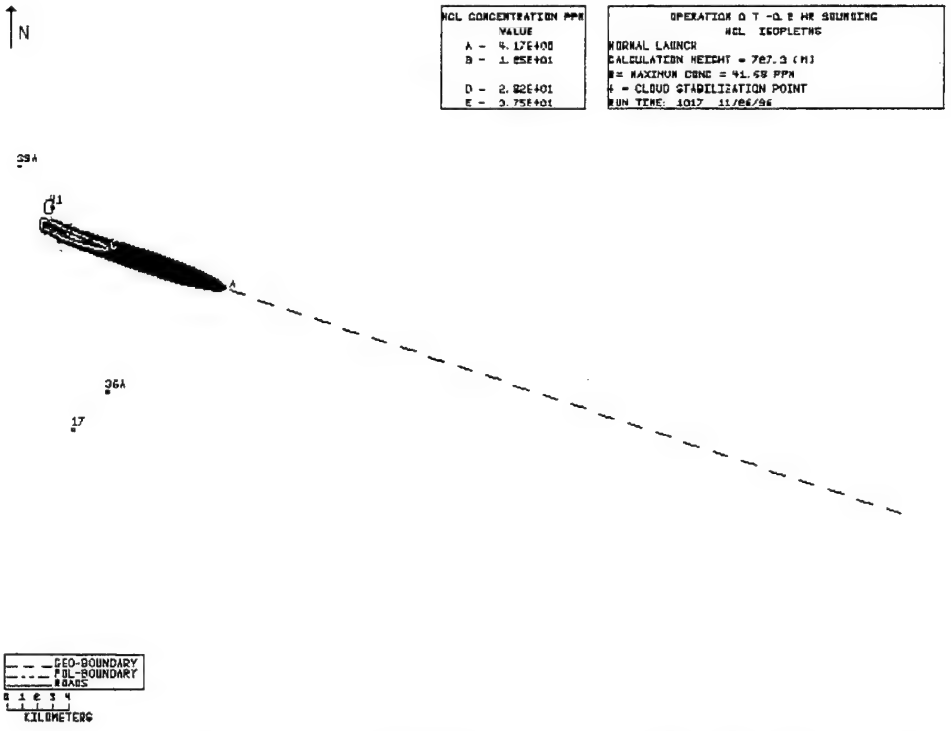

Figure 9. T-0.2 hour REEDM prediction for stabilization height (727 m AGL = 734 m MSL).

Table A-3. Summary of Imagery-Derived, T–0.2 hour Rawinsonde Sound, and T-0.2 hour REEDM Data

Attribute	Feature	Visible Imagery	Rawinsonde (T–0.2 h)	REEDM 7.07 (T–0.2 h) (Max Conc @ H(m))	REEDM 7.07 (T–0.2 h) (Long Range Tracks @ H(m))
Height (m MSL)	Top	1877	#N/A	#N/A	#N/A
Stabilization	Middle	1023	#N/A	734	734
(SLC-41 = 7 m MSL	Bottom	219	#N/A	#N/A	#N/A
Time (min)	Top	4.0	#N/A	#N/A	#N/A
Stabilization	Middle	3.5	#N/A	4.2	4.2
	Bottom	3.5	#N/A	#N/A	#N/A
Bearing (deg)	Top	None	277°	#N/A	#N/A
(Rawinsonde convention)	Middle	~N-NW (Box)	313°	15° (Max @ 734 m MSL)	289° (Cloud @ 734 m MSL)
	Bottom	5° to 14° (Line)	14°	14° (Max @ 0 m AGL)	13° (Cloud @ 0 m AGL)
Speed (m/s)	Top	~0	8.2	#N/A	#N/A
	Middle	3.6 (Box)	4.1	#N/A	6.6° (Cloud @ 734 m MSL
	Bottom	8.5 (Line)	6.7	#N/A	6.6° (Cloud @ 0 m AGL)

Review of Table A-3 reveals several interesting differences between the observed #K16 cloud behavior, the T–0.2 hour rawinsonde data, and the T–0.2 hour REEDM predictions for the exhaust cloud behavior. The observed stabilization height (1023 m MSL) was 39% higher than predicted (734 m MSL). The observed stabilization time (3.5 min) was 16% faster than predicted (4.2 min). The imagery documented that the "lower portion" of the cloud moved in a south-southwesterly direction (i.e., winds from 5 to 14° at 8.5 m/s). This was similar to the wind direction and speed measured by the rawinsonde sounding (i.e., wind from 14° at 6.7 m/s at the height of the bottom of the cloud). Likewise, the observed movement of the "lower portion" of the cloud was similar to REEDM's surface impact prediction (i.e., 13° at 6.6 m/s). In contrast, the imagery documented that the "upper portion" of the ground cloud remained almost stationary during the 6 min of tracking. This resulted in the observed average bearing of south-southwesterly (i.e., winds from the north-northwest) for the ground cloud. This is dramatically different from the rawinsonde data that document winds from 277° at 8.2 m/s at the height of the top of the cloud and winds from 313° at 4.1 m/s at the height of the middle of the cloud. These winds should have pushed the top and middle of the cloud to the east and to the southeast, respectively. Likewise, REEDM predicted a south-southwesterly bearing (15°) to the maximum concentration at the predicted stabilization height but a east-southeasterly bearing (289° at 6.6 m/s) for the ground cloud after stabilization. The aircraft's HCl measurements tie all of the above together since the aircraft's data documented a south-southwesterly trajectory for the "lower portion" of the ground cloud and a southeasterly to easterly trajectory for the "upper portion" of the ground cloud.

REEDM Stabilization Height Report for T-0.7 hour

The following 11 pages contain the detailed REEDM report for the T–0.7 hour calculations relevant to the predicted stabilization height. The analyst accepted the default settings for all parameters including the heights for the first and second mixing layers. The first page of the REEDM output contains trouble shooting error codes that are beyond the scope of this report, and, therefore, that page is not included in this appendix. The REEDM report is presented in a different font so that the column headings align with the columns.

REEDM reports heights for the exhaust cloud as height above ground level (AGL). For the rawinsonde data, REEDM assumes 0 m AGL = 4.9 m MSL = the height of the rawinsonde release site. However, for the Titan IV exhaust cloud, one assumes 0 m AGL = 7 m MSL = the elevation of SLC-41.

----- PROGRAM OPTIONS -----

MODEL	CONCENTRATION
RUN TYPE	OPERATIONAL
WIND-FIELD TERRAIN EFFECTS MODEL	NONE
LAUNCH VEHICLE	TITAN IV
LAUNCH TYPE	NORMAL
LAUNCH COMPLEX NUMBER	41
TURBULENCE PARAMETERS ARE DETERMINED FROM	CLIMATOLOGICAL DATA
SURFACE CHEMISTRY MODEL	absorption coefficient
SPECIES SURFACE FACTOR	HCL 0.000
CLOUD SHAPE	ELLIPTICAL
CALCULATION HEIGHT	STABILIZATION
PROPELLANT TEMPERATURE (DEG. C)	23.43
CONCENTRATION AVERAGING TIME (SEC.)	1800.00
mixing layer reflection coefficient (RNG- 0 TO 1,no reflection=0)	1.0000
DIFFUSION COEFFICIENTS	LATERAL 1.0000
	VERTICAL 1.0000
VEHICLE AIR ENTRAINMENT PARAMETER	GAMMAE 0.6400
DOWNWIND EXPANSION DISTANCE (METERS)	LATERAL 100.00
	VERTICAL 100.00

----- DATA FILES -----

INPUT FILES

RAWINSONDE FILE	rm2255.115
DATA BASE FILE	rdmbase.ksc

OUTPUT FILES

PRINT FILE	k1672255.stb
PLOT FILE	k1672255.stp

----- METEOROLOGICAL RAWINSONDE DATA -----

RAWINSONDE MSS/MSS
TIME- 2255 Z DATE- 24 APR 96
ASCENT NUMBER 0

----- T -0.7 HR SOUNDING -----

MET. LEV. NO.	ALTITUDE MSL (FT)	ALTITUDE GND (FT)	GND (M)	WIND DIR (DEG)	WIND SPEED (M/S)	WIND SPEED (KTS)	AIR TEMP (DEG C)	AIR PTEMP (DEG C)	AIR DPTEMP (DEG C)	AIR PRESS (MB)	AIR RH (%)	H M	INT-ERP
1	16	0.0	0.0	20	6.2	12.0	20.8	21.3	16.3	1018.7	76.0		
2	62	45.8	13.9	9	6.4	12.5	20.6	21.2	16.3	1017.1	76.4		**
3	108	91.5	27.9	359	6.7	13.0	20.4	21.1	16.3	1015.4	77.3		**
4	153	137.3	41.8	348	6.9	13.5	20.2	21.1	16.3	1013.8	78.3		**
5	199	183.0	55.8	337	7.2	14.0	20.0	21.0	16.3	1012.2	79.0		
6	285	268.5	81.8	344	7.2	14.0	19.7	21.0	16.3	1009.1	80.9		**
7	370	354.0	107.9	351	7.2	14.0	19.5	21.0	16.4	1006.1	82.5		**
8	456	439.5	134.0	358	7.2	14.0	19.2	21.0	16.4	1003.0	84.2		**
9	541	525.0	160.0	5	7.2	14.0	18.9	21.0	16.5	1000.0	86.0		
10	694	678.0	206.7	7	7.3	14.1	18.4	21.0	16.4	994.6	88.0		**
11	847	831.0	253.3	8	7.3	14.3	18.0	21.0	16.3	989.2	90.0		**
12	1000	984.0	299.9	10	7.4	14.4	17.5	20.9	16.2	983.9	92.0		
13	1114	1098.0	334.7	11	7.2	14.0	17.2	21.0	16.1	979.9	93.0		
14	1389	1372.5	418.3	11	7.2	14.0	17.1	21.5	14.3	970.4	83.6		**
15	1663	1647.0	502.0	10	7.2	14.0	17.0	22.0	12.5	961.0	75.0		
16	2000	1984.0	604.7	4	6.5	12.6	16.2	22.4	13.8	949.5	86.0		
17	2226	2210.0	673.6	359	6.2	12.0	15.7	22.7	14.8	941.9	94.0	*	
18	2613	2597.0	791.6	346	6.1	11.9	15.8	24.0	14.6	929.0	93.2		**
19	3000	2984.0	909.5	332	6.1	11.9	15.8	25.2	14.5	916.2	91.0		
20	3494	3478.0	1060.1	317	6.2	12.0	15.4	26.3	13.8	900.0	90.0		
21	3862	3846.0	1172.3	304	6.2	12.0	15.0	27.0	13.4	888.4	90.0		
22	4000	3984.0	1214.3	301	5.9	11.5	14.8	27.2	13.2	884.0	90.0		
23	4500	4484.0	1366.7	290	6.2	12.0	13.9	27.7	12.3	868.3	90.2		**
24	5000	4984.0	1519.1	278	6.5	12.6	13.0	28.2	11.4	852.8	90.0		
25	5082	5066.0	1544.1	278	6.7	13.0	12.9	28.4	11.3	850.0	90.0		
26	5971	5955.0	1815.1	277	7.7	15.0	11.4	29.4	9.4	823.4	88.0		

* - INDICATES THE CALCULATED TOP OF THE SURFACE MIXING LAYER
** - INDICATES THAT DATA IS LINEARLY INTERPOLATED FROM INPUT METEOROLOGY

SURFACE AIR DENSITY (GM/M**3)	1198.99
DEFAULT CALCULATED MIXING LAYER HEIGHT (M)	673.61
CLOUD COVER IN TENTHS OF CELESTIAL DOME	0.0
CLOUD CEILING (M)	9999.0

----- PLUME RISE DATA -----

EXHAUST RATE OF MATERIAL INTO GRN CLD-	(GRAMS/SEC)		4.22164E+06
TOTAL GROUND CLD MATERIAL-	(GRAMS)		3.97349E+07
HEAT OUTPUT PER GRAM-	(CALORIES)		1555.6
VEHICLE RISE HEIGHT DEFINING GROUND CLD-	(M)		199.9
VEHICLE RISE TIME PARAMETERS-	(TK=(A*Z**B)+C)	A=	0.8677
		B=	0.4500
		C=	0.0000
EXHAUST RATE OF MATERIAL INTO CONTRAIL-	(GRAMS/SEC)		4.22164E+06
CONTRAIL HEAT OUTPUT PER GRAM-	(CALORIES)		1555.6

1**********

ROCKET EXHAUST EFFLUENT DIFFUSION MODEL REEDM PAGE 5
VERSION 7.07 AT CCAS
OPERATION NUMBER 16, 1727 EDT 28 MAY 1996
launch time: 1937 EDT 24 APR 1996
RAWINSONDE ASCENT NUMBER 0, 2255 Z 24 APR 96 T -0.7 HR

****

----- EXHAUST CLOUD -----

MET. LAYER NO.	TOP OF LAYER (METERS)	CLOUD RISE TIME (SECONDS)	CLOUD RISE RANGE (METERS)	CLOUD RISE BEARING (DEGREES)	STABILIZED CLOUD RANGE (METERS)	STABILIZED CLOUD BEARING (DEGREES)
1	13.9	2.6	8.0	197.2	0.0	0.0
2	27.9	4.1	21.0	192.7	0.0	0.0
3	41.8	5.5	30.5	188.2	0.0	0.0
4	55.8	6.9	39.8	183.3	0.0	0.0
5	81.8	9.7	54.0	176.6	0.0	0.0
6	107.9	12.9	75.0	173.1	0.0	0.0
7	134.0	16.3	98.6	172.6	0.0	0.0
8	160.0	20.1	124.6	173.7	0.0	0.0
9	206.7	27.8	165.4	176.5	0.0	0.0
10	253.3	36.5	224.3	179.2	0.0	0.0
11	299.9	46.2	291.3	181.3	1876.9	187.9
12	334.7	54.0	355.3	182.9	1868.7	189.1
13	418.3	75.0	458.5	184.7	1800.1	189.2
14	502.0	99.6	621.8	186.2	1787.5	188.8
15	604.7	137.1	841.6	187.0	1693.1	187.0
16	673.6	171.4	1076.2	186.4	1645.1	184.7
17	791.6	261.6 *	1731.2	182.3	1731.2	182.3
18	909.5	261.6 *	1731.2	182.3	1731.2	182.3
19	1060.1	261.6 *	1731.2	182.3	1731.2	182.3
20	1172.3	261.6 *	1731.2	182.3	1731.2	182.3
21	1214.3	261.6 *	1731.2	182.3	1731.2	182.3
22	1366.7	261.6 *	1731.2	182.3	1731.2	182.3
23	1519.1	261.6 *	1731.2	182.3	1731.2	182.3
24	1544.1	261.6 *	1731.2	182.3	1731.2	182.3
25	1815.1	261.6 *	1731.2	182.3	1731.2	182.3

* - INDICATES CLOUD STABILIZATION TIME WAS USED

1**********

ROCKET EXHAUST EFFLUENT DIFFUSION MODEL REEDM PAGE 6
VERSION 7.07 AT CCAS
OPERATION NUMBER 16, 1727 EDT 28 MAY 1996
launch time: 1937 EDT 24 APR 1996
RAWINSONDE ASCENT NUMBER 0, 2255 Z 24 APR 96 T -0.7 HR

****

----- EXHAUST CLOUD -----

CHEMICAL SPECIES = HCL

MET. LAYER NO.	TOP OF LAYER (METERS)		LAYER SOURCE STRENGTH (GRAMS)	CLOUD UPDRAFT VELOCITY (M/S)	CLOUD RADIUS (METERS)	STD. DEVIATION MATERIAL DIST. ALONGWIND (METERS)	CROSSWIND (METERS)
1	13.9		0.00000E+00	8.6	0.0	0.0	0.0
2	27.9		0.00000E+00	9.8	0.0	0.0	0.0
3	41.8		0.00000E+00	9.9	0.0	0.0	0.0
4	55.8		0.00000E+00	9.6	0.0	0.0	0.0
5	81.8		0.00000E+00	8.8	0.0	0.0	0.0
6	107.9		0.00000E+00	7.9	0.0	0.0	0.0
7	134.0		0.00000E+00	7.2	0.0	0.0	0.0
8	160.0		0.00000E+00	6.6	0.0	0.0	0.0
9	206.7		0.00000E+00	5.7	0.0	0.0	0.0
10	253.3		0.00000E+00	5.0	0.0	0.0	0.0
11	299.9		4.03114E+04	4.6	89.7	41.8	41.8
12	334.7		1.44708E+05	4.3	238.2	111.0	111.0
13	418.3		7.32365E+05	3.7	346.0	161.2	161.2
14	502.0		1.18303E+06	3.1	439.2	204.7	204.7
15	604.7		1.90079E+06	2.3	502.6	234.2	234.2
16	673.6		1.45360E+06	1.7	535.9	249.7	249.7
17	791.6	*	2.97571E+06	0.0	550.3	256.4	256.4
18	909.5	*	3.44102E+06	0.0	538.0	250.7	250.7
19	1060.1	*	3.62368E+06	0.0	479.0	223.2	223.2
20	1172.3	*	1.78722E+06	0.0	352.9	164.4	164.4
21	1214.3	*	4.06874E+05	0.0	204.1	95.1	95.1
22	1366.7	*	9.74846E+05	0.0	127.8	59.6	59.6
23	1519.1	*	9.09282E+05	0.0	199.9	93.2	93.2
24	1544.1	*	1.44253E+05	0.0	199.9	93.2	93.2
25	1815.1	*	1.48792E+06	0.0	199.9	93.2	93.2

* - INDICATES CLOUD STABILIZATION TIME WAS USED

----- CLOUD STABILIZATION -----

CALCULATION HEIGHT	(METERS)		748.80
STABILIZATION HEIGHT	(METERS)		748.80
STABILIZATION TIME	(SECS)		261.55
FIRST MIXING LAYER HEIGHT-	(METERS)	TOP =	673.61
		BASE=	0.00
SECOND SELECTED LAYER HEIGHT-	(METERS)	TOP =	1815.08
		BASE=	673.61
SIGMAR(AZ) AT THE SURFACE	(DEGREES)		6.9555
SIGMER(EL) AT THE SURFACE	(DEGREES)		3.3604

MET. LAYER NO.	WIND SPEED (M/SEC)	WIND SPEED SHEAR (M/SEC)	WIND DIRECTION (DEG)	WIND DIRECTION SHEAR (DEG)	SIGMA OF AZI ANG (DEG)	SIGMA OF ELE ANG (DEG)
1	6.35	0.26	14.63	-10.75	6.1499	3.5971
2	6.56	0.26	3.88	-10.75	5.1653	3.9013
3	6.82	0.26	353.13	-10.75	4.8873	4.0095
4	7.07	0.26	342.38	-10.75	4.7204	4.0795
5	7.20	0.00	340.50	7.00	4.5650	4.1486
6	7.20	0.00	347.50	7.00	4.3685	4.1505
7	7.20	0.00	354.50	7.00	4.1790	4.0393
8	7.20	0.00	1.50	7.00	3.9863	3.8635
9	7.24	0.07	5.83	1.67	3.7301	3.6299
10	7.31	0.07	7.50	1.67	3.4422	3.3672
11	7.37	0.07	9.17	1.67	3.1726	3.1213
12	7.31	-0.21	10.50	1.00	2.8642	2.8400
13	7.20	0.00	10.75	-0.50	2.4417	2.4377
14	7.20	0.00	10.25	-0.50	1.9396	1.9396
15	6.84	-0.72	7.00	-6.00	1.4356	1.4356
16	6.33	-0.31	1.50	-5.00	1.0970	1.0970
17	6.16	-0.03	352.25	-13.50	1.0000	1.0000
18	6.13	-0.03	338.75	-13.50	1.0000	1.0000
19	6.15	0.05	324.50	-15.00	1.0000	1.0000
20	6.17	0.00	310.50	-13.00	1.0000	1.0000
21	6.04	-0.26	302.50	-3.00	1.0000	1.0000
22	6.06	0.28	295.25	-11.50	1.0000	1.0000
23	6.34	0.28	283.75	-11.50	1.0000	1.0000
24	6.58	0.21	278.00	0.00	1.0000	1.0000
25	7.20	1.03	277.50	-1.00	1.0000	1.0000

ALTITUDE RANGE USED IN COMPUTING TRANSITION LAYER AVERAGES
IS 206.7 TO 1815.1 METERS.

----- CALCULATED TRANSITION LAYER PARAMETERS -----

TRANSITION LAYER NUMBER- 1

VALUE AT	HEIGHT (METERS)	TEMP. (DEG K)	WIND SPEED (M/SEC)	WIND SPEED SHEAR (M/SEC)	WIND DIR. (DEG)	WIND DIR. SHEAR (DEG)	SIGMA AZI. (DEG)	SIGMA ELE. (DEG)
TOP-	673.61	295.87	6.17		359.00		1.0000	1.0000
LAYER-			7.02	0.32	8.11	2.64	2.1364	2.1213
BOTTOM-	0.00	294.43	6.17		20.00		6.9555	3.3604

TRANSITION LAYER NUMBER- 2

VALUE AT	HEIGHT (METERS)	TEMP. (DEG K)	WIND SPEED (M/SEC)	WIND SPEED SHEAR (M/SEC)	WIND DIR. (DEG)	WIND DIR. SHEAR (DEG)	SIGMA AZI. (DEG)	SIGMA ELE. (DEG)
TOP-	1815.08	302.58	7.72		277.00		1.0000	1.0000
LAYER-			5.78	0.61	303.42	19.09	1.0000	1.0000
BOTTOM-	673.61	295.87	6.17		359.00		1.0000	1.0000

----- MAXIMUM CENTERLINE CALCULATIONS -----

** DECAY COEFFICIENT (1/SEC) = 0.00000E+00 **

CONCENTRATION OF HCL AT A HEIGHT OF 748.8 METERS
DOWNWIND FROM A TITAN IV NORMAL LAUNCH
CALCULATIONS APPLY TO THE LAYER BETWEEN 673.6 AND 1815.1 METERS

RANGE FROM PAD (METERS)	BEARING FROM PAD (DEGREES)	PEAK CONCEN-TRATION (PPM)	CLOUD ARRIVAL TIME (MIN)	CLOUD DEPARTURE TIME (MIN)
2021.0989	168.2403	40.1457	4.8210	8.0012
3003.9136	152.6301	34.9158	7.9344	11.1287
4001.0652	145.0675	29.9036	10.9797	14.1996
5000.3735	140.6257	25.5090	13.9674	17.2235
6000.1558	137.7030	21.9030	16.9158	20.2181
7000.0737	135.6326	18.9823	19.8370	23.1948
8000.0386	134.0884	16.5915	22.7384	26.1607
9000.0215	132.8919	14.6000	25.6249	29.1201
10000.0127	131.9374	12.9131	28.4997	32.0756
11000.0078	131.1580	11.4643	31.3650	35.0291
12000.0049	130.5095	10.2073	34.2226	37.9815
13000.0039	129.9614	9.1093	37.0735	40.9337
14000.0020	129.4921	8.1459	39.9188	43.8860
15000.0020	129.0857	7.2983	42.7593	46.8388
16000.0010	128.7303	6.5514	45.5954	49.7922
17000.0000	128.4169	5.8925	48.4278	52.7464
18000.0000	128.1384	5.3105	51.2569	55.7015
19000.0000	127.8893	4.7961	54.0831	58.6573
20000.0000	127.6652	4.3409	56.9066	61.6141
21000.0000	127.4625	3.9375	59.7277	64.5716
22000.0000	127.2783	3.5795	62.5467	67.5300
23000.0000	127.1101	3.2614	65.3637	70.4891
24000.0000	126.9560	2.9781	68.1790	73.4490
25000.0000	126.8142	2.7254	70.9927	76.4095
26000.0000	126.6834	2.4997	73.8050	79.3707
27000.0000	126.5622	2.2975	76.6159	82.3325
28000.0000	126.4498	2.1162	79.4256	85.2949
29000.0000	126.3451	1.9532	82.2342	88.2578
30000.0000	126.2473	1.8064	85.0418	91.2212
31000.0000	126.1559	1.6740	87.8485	94.1851
32000.0000	126.0702	1.5544	90.6542	97.1494
33000.0000	125.9897	1.4460	93.4592	100.1142
34000.0000	125.9140	1.3478	96.2635	103.0794
35000.0000	125.8426	1.2586	99.0670	106.0449
36000.0000	125.7751	1.1774	101.8699	109.0107

1**********

ROCKET EXHAUST EFFLUENT DIFFUSION MODEL REEDM PAGE 10
VERSION 7.07 AT CCAS
OPERATION NUMBER 16, 1727 EDT 28 MAY 1996
launch time: 1937 EDT 24 APR 1996
RAWINSONDE ASCENT NUMBER 0, 2255 Z 24 APR 96 T -0.7 HR

****

----- MAXIMUM CENTERLINE CALCULATIONS -----

** DECAY COEFFICIENT (1/SEC) = 0.00000E+00 **

CONCENTRATION OF HCL AT A HEIGHT OF 748.8 METERS
DOWNWIND FROM A TITAN IV NORMAL LAUNCH
CALCULATIONS APPLY TO THE LAYER BETWEEN 673.6 AND 1815.1 METERS

RANGE FROM PAD (METERS)	BEARING FROM PAD (DEGREES)	PEAK CONCEN-TRATION (PPM)	CLOUD ARRIVAL TIME (MIN)	CLOUD DEPARTURE TIME (MIN)
37000.0000	125.7113	1.1034	104.6723	111.9769
38000.0000	125.6509	1.0359	107.4740	114.9434
39000.0000	125.5935	0.9741	110.2753	117.9102
40000.0000	125.5391	0.9177	113.0761	120.8773
41000.0000	125.4873	0.8659	115.8764	123.8445
42000.0000	125.4379	0.8183	118.6763	126.8121
43000.0000	125.3909	0.7746	121.4758	129.7798
44000.0000	125.3460	0.7343	124.2750	132.7478
45000.0000	125.3031	0.6972	127.0738	135.7160
46000.0000	125.2620	0.6629	129.8722	138.6844
47000.0000	125.2227	0.6312	132.6704	141.6529
48000.0000	125.1851	0.6018	135.4683	144.6216
49000.0000	125.1489	0.5745	138.2658	147.5905
50000.0000	125.1143	0.5491	141.0632	150.5595
51000.0000	125.0809	0.5255	143.8603	153.5287
52000.0000	125.0489	0.5035	146.6571	156.4980
53000.0000	125.0181	0.4830	149.4538	159.4674
54000.0000	124.9884	0.4638	152.2502	162.4370
55000.0000	124.9598	0.4458	155.0464	165.4066
56000.0000	124.9322	0.4289	157.8425	168.3764
57000.0000	124.9056	0.4130	160.6383	171.3463
58000.0000	124.8799	0.3981	163.4340	174.3163
59000.0000	124.8551	0.3840	166.2296	177.2864
60000.0000	124.8311	0.3707	169.0249	180.2566

	RANGE	BEARING
40.146 IS THE MAXIMUM PEAK CONCENTRATION	2021.1	168.2

1**********

ROCKET EXHAUST EFFLUENT DIFFUSION MODEL REEDM PAGE 11
VERSION 7.07 AT CCAS
OPERATION NUMBER 16, 1727 EDT 28 MAY 1996
launch time: 1937 EDT 24 APR 1996
RAWINSONDE ASCENT NUMBER 0, 2255 Z 24 APR 96 T -0.7 HR

****

----- MAXIMUM CENTERLINE CALCULATIONS -----

** DECAY COEFFICIENT (1/SEC) = 0.00000E+00 **

CONCENTRATION OF HCL AT A HEIGHT OF 748.8 METERS
DOWNWIND FROM A TITAN IV NORMAL LAUNCH
CALCULATIONS APPLY TO THE LAYER BETWEEN 673.6 AND 1815.1 METERS

RANGE FROM PAD (METERS)	BEARING FROM PAD (DEGREES)	30.0 MIN. MEAN CONCEN-TRATION (PPM)	CLOUD ARRIVAL TIME (MIN)	CLOUD DEPARTURE TIME (MIN)
2021.0989	168.2403	2.4808	4.8210	8.0012
3003.9136	152.6301	2.1624	7.9344	11.1287
4001.0652	145.0675	1.8617	10.9797	14.1996
5000.3735	140.6257	1.6019	13.9674	17.2235
6000.1558	137.7030	1.3904	16.9158	20.2181
7000.0737	135.6326	1.2204	19.8370	23.1948
8000.0386	134.0884	1.0824	22.7384	26.1607
9000.0215	132.8919	0.9684	25.6249	29.1201
10000.0127	131.9374	0.8723	28.4997	32.0756
11000.0078	131.1580	0.7902	31.3650	35.0291
12000.0049	130.5095	0.7191	34.2226	37.9815
13000.0039	129.9614	0.6570	37.0735	40.9337
14000.0020	129.4921	0.6023	39.9188	43.8860
15000.0020	129.0857	0.5539	42.7593	46.8388
16000.0010	128.7303	0.5109	45.5954	49.7922
17000.0000	128.4169	0.4725	48.4278	52.7464
18000.0000	128.1384	0.4381	51.2569	55.7015
19000.0000	127.8893	0.4073	54.0831	58.6573
20000.0000	127.6652	0.3795	56.9066	61.6141
21000.0000	127.4625	0.3544	59.7277	64.5716
22000.0000	127.2783	0.3317	62.5467	67.5300
23000.0000	127.1101	0.3111	65.3637	70.4891
24000.0000	126.9560	0.2924	68.1790	73.4490
25000.0000	126.8142	0.2753	70.9927	76.4095
26000.0000	126.6834	0.2597	73.8050	79.3707
27000.0000	126.5622	0.2454	76.6159	82.3325
28000.0000	126.4498	0.2323	79.4256	85.2949
29000.0000	126.3451	0.2203	82.2342	88.2578
30000.0000	126.2473	0.2093	85.0418	91.2212
31000.0000	126.1559	0.1991	87.8485	94.1851
32000.0000	126.0702	0.1897	90.6542	97.1494
33000.0000	125.9897	0.1810	93.4592	100.1142
34000.0000	125.9140	0.1729	96.2635	103.0794
35000.0000	125.8426	0.1655	99.0670	106.0449

1**********

ROCKET EXHAUST EFFLUENT DIFFUSION MODEL REEDM PAGE 12
VERSION 7.07 AT CCAS
OPERATION NUMBER 16, 1727 EDT 28 MAY 1996
launch time: 1937 EDT 24 APR 1996
RAWINSONDE ASCENT NUMBER 0, 2255 Z 24 APR 96 T -0.7 HR

****

----- MAXIMUM CENTERLINE CALCULATIONS -----

** DECAY COEFFICIENT (1/SEC) = 0.00000E+00 **

CONCENTRATION OF HCL AT A HEIGHT OF 748.8 METERS
DOWNWIND FROM A TITAN IV NORMAL LAUNCH
CALCULATIONS APPLY TO THE LAYER BETWEEN 673.6 AND 1815.1 METERS

RANGE FROM PAD (METERS)	BEARING FROM PAD (DEGREES)	30.0 MIN. MEAN CONCEN-TRATION (PPM)	CLOUD ARRIVAL TIME (MIN)	CLOUD DEPARTURE TIME (MIN)
36000.0000	125.7751	0.1585	101.8699	109.0107
37000.0000	125.7113	0.1521	104.6723	111.9769
38000.0000	125.6509	0.1462	107.4740	114.9434
39000.0000	125.5935	0.1406	110.2753	117.9102
40000.0000	125.5391	0.1355	113.0761	120.8773
41000.0000	125.4873	0.1307	115.8764	123.8445
42000.0000	125.4379	0.1262	118.6763	126.8121
43000.0000	125.3909	0.1220	121.4758	129.7798
44000.0000	125.3460	0.1181	124.2750	132.7478
45000.0000	125.3031	0.1144	127.0738	135.7160
46000.0000	125.2620	0.1110	129.8722	138.6844
47000.0000	125.2227	0.1078	132.6704	141.6529
48000.0000	125.1851	0.1048	135.4683	144.6216
49000.0000	125.1489	0.1020	138.2658	147.5905
50000.0000	125.1143	0.0994	141.0632	150.5595
51000.0000	125.0809	0.0969	143.8603	153.5287
52000.0000	125.0489	0.0945	146.6571	156.4980
53000.0000	125.0181	0.0923	149.4538	159.4674
54000.0000	124.9884	0.0902	152.2502	162.4370
55000.0000	124.9598	0.0882	155.0464	165.4066
56000.0000	124.9322	0.0864	157.8425	168.3764
57000.0000	124.9056	0.0846	160.6383	171.3463
58000.0000	124.8799	0.0829	163.4340	174.3163
59000.0000	124.8551	0.0813	166.2296	177.2864
60000.0000	124.8311	0.0798	169.0249	180.2566

	RANGE	BEARING
2.481 IS THE MAXIMUM 30.0 MIN. MEAN CONCENTRATION	2021.1	168.2

*** REEDM HAS TERMINATED

REEDM Surface Impact Report for T-0.7 hour

The following 11 pages contain the detailed REEDM report for the T–0.7 hour calculations relevant to the surface impact (i.e., 0 m AGL) of the exhaust cloud. The analyst accepted the default settings for all parameters including the heights for the first and second mixing layers. The first page of the REEDM output contains trouble shooting error codes that are beyond the scope of this report, and, therefore, that page is not included in this appendix. The REEDM report is presented in a different font so that the column headings align with the columns.

REEDM reports heights for the exhaust cloud as height above ground level (AGL). For the rawinsonde data, REEDM assumes 0 m AGL = 4.9 m MSL = the height of the rawinsonde release site. However, for the Titan IV exhaust cloud, one assumes 0 m AGL = 7 m MSL = the elevation of SLC-41.

VERSION 7.07 AT CCAS
1332 EST 25 NOV 1996
launch time: 1937 EDT 24 APR 1996
RAWINSONDE ASCENT NUMBER 0, 2255 Z 24 APR 96 T -0.7 HR

****

----- PROGRAM OPTIONS -----

MODEL	CONCENTRATION
RUN TYPE	OPERATIONAL
WIND-FIELD TERRAIN EFFECTS MODEL	NONE
LAUNCH VEHICLE	TITAN IV
LAUNCH TYPE	NORMAL
LAUNCH COMPLEX NUMBER	41
TURBULENCE PARAMETERS ARE DETERMINED FROM	CLIMATOLOGICAL DATA
SURFACE CHEMISTRY MODEL	absorption coefficient
SPECIES SURFACE FACTOR	HCL 0.000
CLOUD SHAPE	ELLIPTICAL
CALCULATION HEIGHT	SURFACE
PROPELLANT TEMPERATURE (DEG. C)	23.43
CONCENTRATION AVERAGING TIME (SEC.)	1800.00
mixing layer reflection coefficient (RNG- 0 TO 1,no reflection=0)	1.0000
DIFFUSION COEFFICIENTS	LATERAL 1.0000
	VERTICAL 1.0000
VEHICLE AIR ENTRAINMENT PARAMETER	GAMMAE 0.6400
DOWNWIND EXPANSION DISTANCE (METERS)	LATERAL 100.00
	VERTICAL 100.00

----- DATA FILES -----

INPUT FILES

RAWINSONDE FILE	k16_2255.raw
DATA BASE FILE	rdmbase.ksc

OUTPUT FILES

PRINT FILE	k1672255.sur
PLOT FILE	k1672255.sup

1**********

ROCKET EXHAUST EFFLUENT DIFFUSION MODEL REEDM PAGE 3
VERSION 7.07 AT CCAS
1332 EST 25 NOV 1996
launch time: 1937 EDT 24 APR 1996
RAWINSONDE ASCENT NUMBER 0, 2255 Z 24 APR 96 T -0.7 HR

****

----- METEOROLOGICAL RAWINSONDE DATA -----

RAWINSONDE MSS/MSS
TIME- 2255 Z DATE- 24 APR 96
ASCENT NUMBER 0

----- T -0.7 HR SOUNDING -----

MET. LEV. NO.	ALTITUDE MSL (FT)	ALTITUDE GND (FT)	WIND GND (M)	WIND DIR (DEG)	WIND SPEED (M/S)	WIND SPEED (KTS)	AIR TEMP (DEG C)	AIR PTEMP (DEG C)	AIR DPTEMP (DEG C)	AIR PRESS (MB)	AIR RH (%)	H M	INT-ERP
1	16	0.0	0.0	20	6.2	12.0	20.8	21.3	16.3	1018.7	76.0		
2	62	45.8	13.9	9	6.4	12.5	20.6	21.2	16.3	1017.1	76.4		**
3	108	91.5	27.9	359	6.7	13.0	20.4	21.1	16.3	1015.4	77.3		**
4	153	137.3	41.8	348	6.9	13.5	20.2	21.1	16.3	1013.8	78.3		**
5	199	183.0	55.8	337	7.2	14.0	20.0	21.0	16.3	1012.2	79.0		
6	285	268.5	81.8	344	7.2	14.0	19.7	21.0	16.3	1009.1	80.9		**
7	370	354.0	107.9	351	7.2	14.0	19.5	21.0	16.4	1006.1	82.5		**
8	456	439.5	134.0	358	7.2	14.0	19.2	21.0	16.4	1003.0	84.2		**
9	541	525.0	160.0	5	7.2	14.0	18.9	21.0	16.5	1000.0	86.0		
10	694	678.0	206.7	7	7.3	14.1	18.4	21.0	16.4	994.6	88.0		**
11	847	831.0	253.3	8	7.3	14.3	18.0	21.0	16.3	989.2	90.0		**
12	1000	984.0	299.9	10	7.4	14.4	17.5	20.9	16.2	983.9	92.0		
13	1114	1098.0	334.7	11	7.2	14.0	17.2	21.0	16.1	979.9	93.0		
14	1389	1372.5	418.3	11	7.2	14.0	17.1	21.5	14.3	970.4	83.6		**
15	1663	1647.0	502.0	10	7.2	14.0	17.0	22.0	12.5	961.0	75.0		
16	2000	1984.0	604.7	4	6.5	12.6	16.2	22.4	13.8	949.5	86.0		
17	2226	2210.0	673.6	359	6.2	12.0	15.7	22.7	14.8	941.9	94.0	*	
18	2613	2597.0	791.6	346	6.1	11.9	15.8	24.0	14.6	929.0	93.2		**
19	3000	2984.0	909.5	332	6.1	11.9	15.8	25.2	14.5	916.2	91.0		
20	3494	3478.0	1060.1	317	6.2	12.0	15.4	26.3	13.8	900.0	90.0		
21	3862	3846.0	1172.3	304	6.2	12.0	15.0	27.0	13.4	888.4	90.0		
22	4000	3984.0	1214.3	301	5.9	11.5	14.8	27.2	13.2	884.0	90.0		
23	4500	4484.0	1366.7	290	6.2	12.0	13.9	27.7	12.3	868.3	90.2		**
24	5000	4984.0	1519.1	278	6.5	12.6	13.0	28.2	11.4	852.8	90.0		
25	5082	5066.0	1544.1	278	6.7	13.0	12.9	28.4	11.3	850.0	90.0		
26	5971	5955.0	1815.1	277	7.7	15.0	11.4	29.4	9.4	823.4	88.0		

* - INDICATES THE CALCULATED TOP OF THE SURFACE MIXING LAYER
** - INDICATES THAT DATA IS LINEARLY INTERPOLATED FROM INPUT METEOROLOGY

SURFACE AIR DENSITY (GM/M**3)	1198.99
DEFAULT CALCULATED MIXING LAYER HEIGHT (M)	673.61
CLOUD COVER IN TENTHS OF CELESTIAL DOME	0.0
CLOUD CEILING (M)	9999.0

----- PLUME RISE DATA -----

EXHAUST RATE OF MATERIAL INTO GRN CLD-	(GRAMS/SEC)		4.22164E+06
TOTAL GROUND CLD MATERIAL-	(GRAMS)		3.97349E+07
HEAT OUTPUT PER GRAM-	(CALORIES)		1555.6
VEHICLE RISE HEIGHT DEFINING GROUND CLD-	(M)		199.9
VEHICLE RISE TIME PARAMETERS-	(TK=(A*Z**B)+C)	A=	0.8677
		B=	0.4500
		C=	0.0000
EXHAUST RATE OF MATERIAL INTO CONTRAIL-	(GRAMS/SEC)		4.22164E+06
CONTRAIL HEAT OUTPUT PER GRAM-	(CALORIES)		1555.6

----- EXHAUST CLOUD -----

MET. LAYER NO.	TOP OF LAYER (METERS)	CLOUD RISE TIME (SECONDS)	CLOUD RISE RANGE (METERS)	CLOUD RISE BEARING (DEGREES)	STABILIZED CLOUD RANGE (METERS)	STABILIZED CLOUD BEARING (DEGREES)
1	13.9	2.6	8.0	197.2	0.0	0.0
2	27.9	4.1	21.0	192.7	0.0	0.0
3	41.8	5.5	30.5	188.2	0.0	0.0
4	55.8	6.9	39.8	183.3	0.0	0.0
5	81.8	9.7	54.0	176.6	0.0	0.0
6	107.9	12.9	75.0	173.1	0.0	0.0
7	134.0	16.3	98.6	172.6	0.0	0.0
8	160.0	20.1	124.6	173.7	0.0	0.0
9	206.7	27.8	165.4	176.5	0.0	0.0
10	253.3	36.5	224.3	179.2	0.0	0.0
11	299.9	46.2	291.3	181.3	1876.9	187.9
12	334.7	54.0	355.3	182.9	1868.7	189.1
13	418.3	75.0	458.5	184.7	1800.1	189.2
14	502.0	99.6	621.8	186.2	1787.5	188.8
15	604.7	137.1	841.6	187.0	1693.1	187.0
16	673.6	171.4	1076.2	186.4	1645.1	184.7
17	791.6	261.6 *	1731.2	182.3	1731.2	182.3
18	909.5	261.6 *	1731.2	182.3	1731.2	182.3
19	1060.1	261.6 *	1731.2	182.3	1731.2	182.3
20	1172.3	261.6 *	1731.2	182.3	1731.2	182.3
21	1214.3	261.6 *	1731.2	182.3	1731.2	182.3
22	1366.7	261.6 *	1731.2	182.3	1731.2	182.3
23	1519.1	261.6 *	1731.2	182.3	1731.2	182.3
24	1544.1	261.6 *	1731.2	182.3	1731.2	182.3
25	1815.1	261.6 *	1731.2	182.3	1731.2	182.3

* - INDICATES CLOUD STABILIZATION TIME WAS USED

----- EXHAUST CLOUD -----

CHEMICAL SPECIES = HCL

MET. LAYER NO.	TOP OF LAYER (METERS)	LAYER SOURCE STRENGTH (GRAMS)	CLOUD UPDRAFT VELOCITY (M/S)	CLOUD RADIUS (METERS)	STD. DEVIATION MATERIAL DIST. ALONGWIND (METERS)	CROSSWIND (METERS)
1	13.9	0.00000E+00	8.6	0.0	0.0	0.0
2	27.9	0.00000E+00	9.8	0.0	0.0	0.0
3	41.8	0.00000E+00	9.9	0.0	0.0	0.0
4	55.8	0.00000E+00	9.6	0.0	0.0	0.0
5	81.8	0.00000E+00	8.8	0.0	0.0	0.0
6	107.9	0.00000E+00	7.9	0.0	0.0	0.0
7	134.0	0.00000E+00	7.2	0.0	0.0	0.0
8	160.0	0.00000E+00	6.6	0.0	0.0	0.0
9	206.7	0.00000E+00	5.7	0.0	0.0	0.0
10	253.3	0.00000E+00	5.0	0.0	0.0	0.0
11	299.9	4.03114E+04	4.6	89.7	41.8	41.8
12	334.7	1.44708E+05	4.3	238.2	111.0	111.0
13	418.3	7.32365E+05	3.7	346.0	161.2	161.2
14	502.0	1.18303E+06	3.1	439.2	204.7	204.7
15	604.7	1.90079E+06	2.3	502.6	234.2	234.2
16	673.6	1.45360E+06	1.7	535.9	249.7	249.7
17	791.6 *	2.97571E+06	0.0	550.3	256.4	256.4
18	909.5 *	3.44102E+06	0.0	538.0	250.7	250.7
19	1060.1 *	3.62368E+06	0.0	479.0	223.2	223.2
20	1172.3 *	1.78722E+06	0.0	352.9	164.4	164.4
21	1214.3 *	4.06874E+05	0.0	204.1	95.1	95.1
22	1366.7 *	9.74846E+05	0.0	127.8	59.6	59.6
23	1519.1 *	9.09282E+05	0.0	199.9	93.2	93.2
24	1544.1 *	1.44253E+05	0.0	199.9	93.2	93.2
25	1815.1 *	1.48792E+06	0.0	199.9	93.2	93.2

* - INDICATES CLOUD STABILIZATION TIME WAS USED

1**********

ROCKET EXHAUST EFFLUENT DIFFUSION MODEL REEDM PAGE 7
VERSION 7.07 AT CCAS
1332 EST 25 NOV 1996
launch time: 1937 EDT 24 APR 1996
RAWINSONDE ASCENT NUMBER 0, 2255 Z 24 APR 96 T -0.7 HR

****

----- CLOUD STABILIZATION -----

CALCULATION HEIGHT	(METERS)		0.00
STABILIZATION HEIGHT	(METERS)		748.80
STABILIZATION TIME	(SECS)		261.55
FIRST MIXING LAYER HEIGHT-	(METERS)	TOP =	673.61
		BASE=	0.00
SECOND SELECTED LAYER HEIGHT-	(METERS)	TOP =	1815.08
		BASE=	673.61
SIGMAR(AZ) AT THE SURFACE	(DEGREES)		6.9555
SIGMER(EL) AT THE SURFACE	(DEGREES)		3.3604

MET. LAYER NO.	WIND SPEED (M/SEC)	WIND SPEED SHEAR (M/SEC)	WIND DIRECTION (DEG)	WIND DIRECTION SHEAR (DEG)	SIGMA OF AZI ANG (DEG)	SIGMA OF ELE ANG (DEG)
1	6.35	0.26	14.63	-10.75	6.1499	3.5971
2	6.56	0.26	3.88	-10.75	5.1653	3.9013
3	6.82	0.26	353.13	-10.75	4.8873	4.0095
4	7.07	0.26	342.38	-10.75	4.7204	4.0795
5	7.20	0.00	340.50	7.00	4.5650	4.1486
6	7.20	0.00	347.50	7.00	4.3685	4.1505
7	7.20	0.00	354.50	7.00	4.1790	4.0393
8	7.20	0.00	1.50	7.00	3.9863	3.8635
9	7.24	0.07	5.83	1.67	3.7301	3.6299
10	7.31	0.07	7.50	1.67	3.4422	3.3672
11	7.37	0.07	9.17	1.67	3.1726	3.1213
12	7.31	-0.21	10.50	1.00	2.8642	2.8400
13	7.20	0.00	10.75	-0.50	2.4417	2.4377
14	7.20	0.00	10.25	-0.50	1.9396	1.9396
15	6.84	-0.72	7.00	-6.00	1.4356	1.4356
16	6.33	-0.31	1.50	-5.00	1.0970	1.0970
17	6.16	-0.03	352.25	-13.50	1.0000	1.0000
18	6.13	-0.03	338.75	-13.50	1.0000	1.0000
19	6.15	0.05	324.50	-15.00	1.0000	1.0000
20	6.17	0.00	310.50	-13.00	1.0000	1.0000
21	6.04	-0.26	302.50	-3.00	1.0000	1.0000
22	6.06	0.28	295.25	-11.50	1.0000	1.0000
23	6.34	0.28	283.75	-11.50	1.0000	1.0000
24	6.58	0.21	278.00	0.00	1.0000	1.0000
25	7.20	1.03	277.50	-1.00	1.0000	1.0000

ALTITUDE RANGE USED IN COMPUTING TRANSITION LAYER AVERAGES
IS 0.0 TO 1366.7 METERS.

1**********

ROCKET EXHAUST EFFLUENT DIFFUSION MODEL REEDM PAGE 8
VERSION 7.07 AT CCAS
1332 EST 25 NOV 1996
launch time: 1937 EDT 24 APR 1996
RAWINSONDE ASCENT NUMBER 0, 2255 Z 24 APR 96 T -0.7 HR

****

----- CALCULATED TRANSITION LAYER PARAMETERS -----

TRANSITION LAYER NUMBER- 1

VALUE AT	HEIGHT (METERS)	TEMP. (DEG K)	WIND SPEED (M/SEC)	WIND SPEED SHEAR (M/SEC)	WIND DIR. (DEG)	WIND DIR. SHEAR (DEG)	SIGMA AZI. (DEG)	SIGMA ELE. (DEG)
TOP-	673.61	295.87	6.17		359.00		1.0000	1.0000
LAYER-			6.97	0.29	4.47	5.69	2.8289	2.6699
BOTTOM-	0.00	294.43	6.17		20.00		6.9555	3.3604

TRANSITION LAYER NUMBER- 2

VALUE AT	HEIGHT (METERS)	TEMP. (DEG K)	WIND SPEED (M/SEC)	WIND SPEED SHEAR (M/SEC)	WIND DIR. (DEG)	WIND DIR. SHEAR (DEG)	SIGMA AZI. (DEG)	SIGMA ELE. (DEG)
TOP-	1815.08	302.58	7.72		277.00		1.0000	1.0000
LAYER-			5.75	0.28	321.66	15.39	1.0000	1.0000
BOTTOM-	673.61	295.87	6.17		359.00		1.0000	1.0000

----- MAXIMUM CENTERLINE CALCULATIONS -----

** DECAY COEFFICIENT (1/SEC) = 0.00000E+00 **

CONCENTRATION OF HCL AT A HEIGHT OF 0.0 METERS
DOWNWIND FROM A TITAN IV NORMAL LAUNCH
CALCULATIONS APPLY TO THE LAYER BETWEEN 0.0 AND 673.6 METERS

RANGE FROM PAD (METERS)	BEARING FROM PAD (DEGREES)	PEAK CONCEN-TRATION (PPM)	CLOUD ARRIVAL TIME (MIN)	CLOUD DEPARTURE TIME (MIN)
4000.0000	186.2558	0.1629	5.4318	9.7683
5000.0000	185.9916	1.1093	7.8189	12.1615
6000.0000	185.6972	2.3404	10.2050	14.5559
7000.0000	185.4869	3.3649	12.5893	16.9507
8000.8892	185.3291	4.0806	14.9741	19.3481
9000.7344	185.2065	4.5153	17.3550	21.7436
10000.6113	185.1083	4.7224	19.7346	24.1398
11000.5127	185.0280	4.7550	22.1130	26.5366
12000.4326	184.9611	4.6635	24.4902	28.9341
13000.3652	184.9045	4.4926	26.8664	31.3322
14000.3096	184.8560	4.2778	29.2415	33.7310
15000.2627	184.8139	4.0450	31.6157	36.1304
16000.2227	184.7771	3.8111	33.9890	38.5303
17000.1895	184.7446	3.5860	36.3615	40.9309
18000.1602	184.7158	3.3746	38.7332	43.3321
19000.1348	184.6900	3.1786	41.1043	45.7338
20000.1113	184.6667	2.9982	43.4746	48.1361
21000.0938	184.6457	2.8322	45.8444	50.5390
22000.0781	184.6265	2.6796	48.2137	52.9424
23000.0625	184.6091	2.5389	50.5824	55.3462
24000.0508	184.5931	2.4090	52.9507	57.7506
25000.0410	184.5784	2.2888	55.3185	60.1555
26000.0313	184.5648	2.1773	57.6859	62.5608
27000.0254	184.5522	2.0737	60.0529	64.9667
28000.0176	184.5405	1.9772	62.4196	67.3729
29000.3828	184.7693	1.8872	64.7821	69.7796
30000.3711	184.7595	1.8031	67.1439	72.1867
31000.3594	184.7503	1.7243	69.5056	74.5942
32000.3477	184.7417	1.6505	71.8672	77.0021
33000.3359	184.7336	1.5811	74.2288	79.4104
34000.3281	184.7260	1.5159	76.5903	81.8190
35000.3164	184.7188	1.4545	78.9518	84.2281
36000.3086	184.7120	1.3965	81.3132	86.6374
37000.3008	184.7056	1.3419	83.6746	89.0471
38000.2930	184.6995	1.2902	86.0360	91.4571

1**********

ROCKET EXHAUST EFFLUENT DIFFUSION MODEL REEDM PAGE 10
VERSION 7.07 AT CCAS
1332 EST 25 NOV 1996
launch time: 1937 EDT 24 APR 1996
RAWINSONDE ASCENT NUMBER 0, 2255 Z 24 APR 96 T -0.7 HR

****

----- MAXIMUM CENTERLINE CALCULATIONS -----

** DECAY COEFFICIENT (1/SEC) = 0.00000E+00 **

CONCENTRATION OF HCL AT A HEIGHT OF 0.0 METERS
DOWNWIND FROM A TITAN IV NORMAL LAUNCH
CALCULATIONS APPLY TO THE LAYER BETWEEN 0.0 AND 673.6 METERS

RANGE FROM PAD (METERS)	BEARING FROM PAD (DEGREES)	PEAK CONCEN-TRATION (PPM)	CLOUD ARRIVAL TIME (MIN)	CLOUD DEPARTURE TIME (MIN)
39000.2852	184.6938	1.2414	88.3974	93.8674
40000.2773	184.6883	1.1951	90.7587	96.2780
41000.2695	184.6831	1.1513	93.1200	98.6889
42000.2656	184.6781	1.1098	95.4812	101.1001
43000.2578	184.6734	1.0703	97.8425	103.5116
44000.2539	184.6689	1.0329	100.2037	105.9233
45000.2461	184.6646	0.9972	102.5649	108.3353
46000.2422	184.6604	0.9633	104.9261	110.7475
47000.2383	184.6565	0.9311	107.2873	113.1599
48000.2305	184.6527	0.9003	109.6484	115.5726
49000.2266	184.6491	0.8710	112.0095	117.9855
50000.2227	184.6456	0.8431	114.3707	120.3986
51000.2188	184.6422	0.8164	116.7318	122.8119
52000.2148	184.6390	0.7909	119.0929	125.2254
53000.2109	184.6359	0.7665	121.4539	127.6390
54000.2070	184.6329	0.7432	123.8150	130.0529
55000.2031	184.6301	0.7209	126.1761	132.4670
56000.1992	184.6273	0.6995	128.5371	134.8812
57000.1953	184.6246	0.6791	130.8982	137.2956
58000.1914	184.6220	0.6595	133.2592	139.7101
59000.1875	184.6195	0.6407	135.6202	142.1248
60000.1836	184.6171	0.6226	137.9813	144.5397

4.755 IS THE MAXIMUM PEAK CONCENTRATION

RANGE	BEARING
11000.5	185.0

1**********

ROCKET EXHAUST EFFLUENT DIFFUSION MODEL REEDM PAGE 11
VERSION 7.07 AT CCAS
1332 EST 25 NOV 1996
launch time: 1937 EDT 24 APR 1996
RAWINSONDE ASCENT NUMBER 0, 2255 Z 24 APR 96 T -0.7 HR

****

----- MAXIMUM CENTERLINE CALCULATIONS -----

** DECAY COEFFICIENT (1/SEC) = 0.00000E+00 **

CONCENTRATION OF HCL AT A HEIGHT OF 0.0 METERS
DOWNWIND FROM A TITAN IV NORMAL LAUNCH
CALCULATIONS APPLY TO THE LAYER BETWEEN 0.0 AND 673.6 METERS

RANGE FROM PAD (METERS)	BEARING FROM PAD (DEGREES)	30.0 MIN. MEAN CONCEN-TRATION (PPM)	CLOUD ARRIVAL TIME (MIN)	CLOUD DEPARTURE TIME (MIN)
4000.0000	186.2558	0.0024	5.4318	9.7683
5000.0000	185.9916	0.0251	7.8189	12.1615
6000.0000	185.6972	0.0674	10.2050	14.5559
7000.0000	185.4869	0.1121	12.5893	16.9507
8000.8892	185.3291	0.1491	14.9741	19.3481
9000.7344	185.2065	0.1751	17.3550	21.7436
10000.6113	185.1083	0.1907	19.7346	24.1398
11000.5127	185.0280	0.1974	22.1130	26.5366
12000.4326	184.9611	0.1977	24.4902	28.9341
13000.3652	184.9045	0.1937	26.8664	31.3322
14000.3096	184.8560	0.1872	29.2415	33.7310
15000.2627	184.8139	0.1793	31.6157	36.1304
16000.2227	184.7771	0.1711	33.9890	38.5303
17000.1895	184.7446	0.1630	36.3615	40.9309
18000.1602	184.7158	0.1553	38.7332	43.3321
19000.1348	184.6900	0.1481	41.1043	45.7338
20000.1113	184.6667	0.1415	43.4746	48.1361
21000.0938	184.6457	0.1354	45.8444	50.5390
22000.0781	184.6265	0.1298	48.2137	52.9424
23000.0625	184.6091	0.1246	50.5824	55.3462
24000.0508	184.5931	0.1198	52.9507	57.7506
25000.0410	184.5784	0.1153	55.3185	60.1555
26000.0313	184.5648	0.1112	57.6859	62.5608
27000.0254	184.5522	0.1074	60.0529	64.9667
28000.0176	184.5405	0.1038	62.4196	67.3729
29000.0137	184.5296	0.1004	64.7821	69.7796
30000.0098	184.5195	0.0973	67.1439	72.1867
31000.3594	184.7503	0.0943	69.5056	74.5942
32000.3477	184.7417	0.0916	71.8672	77.0021
33000.3359	184.7336	0.0890	74.2288	79.4104
34000.3281	184.7260	0.0865	76.5903	81.8190
35000.3164	184.7188	0.0841	78.9518	84.2281
36000.3086	184.7120	0.0819	81.3132	86.6374
37000.3008	184.7056	0.0798	83.6746	89.0471

----- MAXIMUM CENTERLINE CALCULATIONS -----

** DECAY COEFFICIENT (1/SEC) = 0.00000E+00 **

CONCENTRATION OF HCL AT A HEIGHT OF 0.0 METERS
DOWNWIND FROM A TITAN IV NORMAL LAUNCH
CALCULATIONS APPLY TO THE LAYER BETWEEN 0.0 AND 673.6 METERS

RANGE FROM PAD (METERS)	BEARING FROM PAD (DEGREES)	30.0 MIN. MEAN CONCEN-TRATION (PPM)	CLOUD ARRIVAL TIME (MIN)	CLOUD DEPARTURE TIME (MIN)
38000.2930	184.6995	0.0778	86.0360	91.4571
39000.2852	184.6938	0.0759	88.3974	93.8674
40000.2773	184.6883	0.0741	90.7587	96.2780
41000.2695	184.6831	0.0724	93.1200	98.6889
42000.2656	184.6781	0.0708	95.4812	101.1001
43000.2578	184.6734	0.0692	97.8425	103.5116
44000.2539	184.6689	0.0677	100.2037	105.9233
45000.2461	184.6646	0.0662	102.5649	108.3353
46000.2422	184.6604	0.0649	104.9261	110.7475
47000.2383	184.6565	0.0635	107.2873	113.1599
48000.2305	184.6527	0.0623	109.6484	115.5726
49000.2266	184.6491	0.0610	112.0095	117.9855
50000.2227	184.6456	0.0599	114.3707	120.3986
51000.2188	184.6422	0.0587	116.7318	122.8119
52000.2148	184.6390	0.0577	119.0929	125.2254
53000.2109	184.6359	0.0566	121.4539	127.6390
54000.2070	184.6329	0.0556	123.8150	130.0529
55000.2031	184.6301	0.0546	126.1761	132.4670
56000.1992	184.6273	0.0537	128.5371	134.8812
57000.1953	184.6246	0.0528	130.8982	137.2956
58000.1914	184.6220	0.0519	133.2592	139.7101
59000.1875	184.6195	0.0510	135.6202	142.1248
60000.1836	184.6171	0.0502	137.9813	144.5397

	RANGE	BEARING
0.198 IS THE MAXIMUM 30.0 MIN. MEAN CONCENTRATION	12000.4	185.0

*** REEDM HAS TERMINATED

Appendix B—Cape Canaveral Air Station Meteorological Data

[Tower data was provided by Randy Evans of ENSCO Inc. in the NASA Applied Meteorology Unit. Rawinsonde data was provided by Karl Overbeck, ACTA, and R.N. Abernathy, The Aerospace Corp.]

This appendix contains both rawinsonde and tower data collected for the subject launch. The tower data presented was recorded at 2330Z on 24 April 1996 to 0000Z on 25 April 1996, in 10-min intervals. Relative to the launch time of 2337Z, this data is from T–7 min to T+23 min. The columns are as follows:

DAY	Year (1996) and day of year (115th)
TIME	ZULU (Greenwich Mean) time
LAT	Latitude
LON	Longitude
Z	Elevation above ground level
DIR	Compass direction from which the wind originates
SPD	Wind speed in knots
T	Ambient temperature, °F
TD	Dew Point Temperature, °F
TIDN	Tower identification number

Rawinsonde data taken at T–0.7, T–0.5, and T–0.2 hours is presented as formatted for input to the REEDM program. In this data, all wind directions are reported in the convention of rawinsonde wind vectors; the angle clockwise from true north from which the wind originates.

The launch window opened at 2245 Zulu but, due to the rupture of a rawinsonde balloon and unacceptable REEDM predictions, the launch was delayed.

DAY	TIME	LAT	LON	Z	DIR	SPD	T	TD	TIDN
96115	233000	28.4338	80.5734	6			68		1
96115	233000	28.4338	80.5734	12	4	4.1			1
96115	233000	28.4338	80.5734	54	355	5.1	67		1
96115	233000	28.4443	80.5621	6			69	64	2
96115	233000	28.4443	80.5621	12	3	2.9			2
96115	233000	28.4443	80.5621	54	7	7.0	69	64	2
96115	233000	28.4443	80.5621	90	10	8.9			2
96115	233000	28.4443	80.5621	162	7	11.1			2
96115	233000	28.4443	80.5621	204	5	11.1	68	64	2
96115	233000	28.4443	80.5621	6			69	64	2
96115	233000	28.4443	80.5621	12	3	2.9			2
96115	233000	28.4443	80.5621	54	2	7.0	68	63	2
96115	233000	28.4443	80.5621	90	6	8.9			2
96115	233000	28.4443	80.5621	162	6	11.1			2
96115	233000	28.4443	80.5621	204	360	11.1	68	64	2
96115	233000	28.4598	80.5267	6			68		3
96115	233000	28.4598	80.5267	12	2	11.1			3
96115	233000	28.4598	80.5267	54	358	14.0	68		3
96115	233000	28.4466	80.5652	6					17
96115	233000	28.7435	80.7005	6					19
96115	233000	28.7435	80.7005	54					19
96115	233000	28.7975	80.7378	6			68	63	22
96115	233000	28.7975	80.7378	54	359	14.0			22
96115	233000	28.4721	80.5393	6					36
96115	233000	28.4721	80.5393	90	1	9.9			36
96115	233000	28.5622	80.5785	6					40
96115	233000	28.5622	80.5785	54	5	8.0			40
96115	233000	28.5836	80.5842	6					41
96115	233000	28.5836	80.5842	54	351	9.9			41
96115	233000	28.5130	80.5613	6			68	64	61
96115	233000	28.5130	80.5613	12	10	1.9			61
96115	233000	28.5130	80.5613	54	4	7.0	68	63	61
96115	233000	28.5130	80.5613	162	6	11.1			61
96115	233000	28.5130	80.5613	204	10	13.0	67	64	61
96115	233000	28.5130	80.5613	6			67	62	62
96115	233000	28.5130	80.5613	12	5	1.9			62
96115	233000	28.5130	80.5613	54	352	6.0	67	63	62
96115	233000	28.5130	80.5613	162	359	12.1			62
96115	233000	28.5130	80.5613	204	360	12.1	67	63	62
96115	233000	28.5358	80.5747	6			67		108
96115	233000	28.5358	80.5747	12	359	2.9			108
96115	233000	28.5358	80.5747	54	354	8.0	67		108
96115	233000	28.6141	80.6203	6			67		112
96115	233000	28.6141	80.6203	12	1	5.1			112
96115	233000	28.6141	80.6203	54	359	8.9	67		112
96115	233000	28.4048	80.6519	6			70	65	300
96115	233000	28.4048	80.6519	54	13	14.0			300
96115	233000	28.4600	80.5711	6			67		303
96115	233000	28.4600	80.5711	12	354	2.9			303
96115	233000	28.4600	80.5711	54	357	6.0	66		303
96115	233000	28.6027	80.6414	6			67		311

96115	233000	28.6027	80.6414	12	359	4.1			311
96115	233000	28.6027	80.6414	54	358	8.0	67		311
96115	233000	28.6105	80.6069	6					393
96115	233000	28.6105	80.6069	60	354	9.9	68	62	393
96115	233000	28.6057	80.6016	6			68	61	394
96115	233000	28.6057	80.6016	60	1	11.1	67	62	394
96115	233000	28.6294	80.6235	6					397
96115	233000	28.6294	80.6235	60	353	11.1	67	62	397
96115	233000	28.6248	80.6182	6			68	60	398
96115	233000	28.6248	80.6182	60	351	13.0	67	62	398
96115	233000	28.4586	80.5923	6			68		403
96115	233000	28.4586	80.5923	12	10	7.0			403
96115	233000	28.4586	80.5923	54	10	9.9	67		403
96115	233000	28.6062	80.6739	6			67		412
96115	233000	28.6062	80.6739	12	19	2.9			412
96115	233000	28.6062	80.6739	54	360	8.0	67		412
96115	233000	28.6586	80.6998	6			66		415
96115	233000	28.6586	80.6998	12	350	4.1			415
96115	233000	28.6586	80.6998	54	359	8.9	66		415
96115	233000	28.7055	80.7265	6			67	62	418
96115	233000	28.7055	80.7265	54	4	8.0			418
96115	233000	28.7755	80.8043	6			68	61	421
96115	233000	28.7755	80.8043	54	357	7.0			421
96115	233000	28.5158	80.6400	6			67		506
96115	233000	28.5158	80.6400	12	354	6.0			506
96115	233000	28.5158	80.6400	54	359	8.0	67		506
96115	233000	28.5623	80.6694	6			67		509
96115	233000	28.5623	80.6694	12	2	6.0			509
96115	233000	28.5623	80.6694	54	360	8.0	65		509
96115	233000	28.5986	80.6817	6					511
96115	233000	28.5986	80.6817	30	357	8.0			511
96115	233000	28.6160	80.6930	6			68	61	512
96115	233000	28.6160	80.6930	30	6	8.9			512
96115	233000	28.6307	80.7027	6					513
96115	233000	28.6307	80.7027	30	6	9.9			513
96115	233000	28.6431	80.7482	6			67		714
96115	233000	28.6431	80.7482	12	358	5.1			714
96115	233000	28.6431	80.7482	54	357	8.9	66		714
96115	233000	28.4632	80.6702	6			67		803
96115	233000	28.4632	80.6702	12	14	4.1			803
96115	233000	28.4632	80.6702	54	9	6.0	67		803
96115	233000	28.5184	80.6962	6					805
96115	233000	28.5184	80.6962	12					805
96115	233000	28.5184	80.6962	54					805
96115	233000	28.7464	80.8707	6			67	59	819
96115	233000	28.7464	80.8707	54	0	5.1			819
96115	233000	28.4079	80.7604	6			68	62	1000
96115	233000	28.4079	80.7604	54	29	6.0			1000
96115	233000	28.5272	80.7742	6			69	62	1007
96115	233000	28.5272	80.7742	54	6	8.9			1007
96115	233000	28.6056	80.8248	6			68	60	1012
96115	233000	28.6056	80.8248	54	6	4.1			1012

96115	233000	28.5697	80.5864	6			69	64	1101
96115	233000	28.5697	80.5864	12	359	1.9			1101
96115	233000	28.5697	80.5864	54	4	8.9	68	64	1101
96115	233000	28.5697	80.5864	162	3	11.1			1101
96115	233000	28.5697	80.5864	204	2	12.1	67	63	1101
96115	233000	28.5697	80.5864	6			68	64	1102
96115	233000	28.5697	80.5864	12	1	1.9			1102
96115	233000	28.5697	80.5864	54	2	8.0	68	63	1102
96115	233000	28.5697	80.5864	162	359	11.1			1102
96115	233000	28.5697	80.5864	204	359	12.1	67	62	1102
96115	233000	28.4843	80.7856	6			68	62	1204
96115	233000	28.4843	80.7856	54	8	6.0			1204
96115	233000	28.6445	80.9034	6					1215
96115	233000	28.4114	80.9284	6			68	63	1500
96115	233000	28.4114	80.9284	54	26	5.1			1500
96115	233000	28.4475	80.8538	6					1502
96115	233000	28.4960	80.8843	6			68	64	1605
96115	233000	28.4960	80.8843	54	12	11.1			1605
96115	233000	28.5583	80.9132	6					1609
96115	233000	28.6173	80.9581	6					1612
96115	233000	28.6173	80.9581	54					1612
96115	233000	28.6762	80.9987	6			67	58	1617
96115	233000	28.6762	80.9987	54	24	6.0			1617
96115	233000	28.5231	81.0100	6			68	60	2008
96115	233000	28.5231	81.0100	54	21	8.0			2008
96115	233000	28.6489	81.0693	6			68	58	2016
96115	233000	28.6489	81.0693	54	6	8.0			2016
96115	233000	28.4417	81.0291	6			69	61	2202
96115	233000	28.4417	81.0291	54	25	11.1			2202
96115	233000	28.6256	80.6571	6			67	62	3131
96115	233000	28.6256	80.6571	12	349	6.0			3131
96115	233000	28.6256	80.6571	54	354	8.9	67	63	3131
96115	233000	28.6256	80.6571	162	355	12.1			3131
96115	233000	28.6256	80.6571	204	357	12.1	66	61	3131
96115	233000	28.6256	80.6571	295	360	13.0			3131
96115	233000	28.6256	80.6571	394	356	14.0			3131
96115	233000	28.6256	80.6571	492	356	14.0	67	63	3131
96115	233000	28.6256	80.6571	6			68	62	3132
96115	233000	28.6256	80.6571	12	350	6.0			3132
96115	233000	28.6256	80.6571	54	1	8.9	67	62	3132
96115	233000	28.6256	80.6571	162	359	12.1			3132
96115	233000	28.6256	80.6571	204	3	12.1	67	63	3132
96115	233000	28.6256	80.6571	295	5	13.0			3132
96115	233000	28.6256	80.6571	394	3	14.0			3132
96115	233000	28.6256	80.6571	492	4	14.0	65	62	3132
96115	233000	28.3932	80.8211	6			70	63	9001
96115	233000	28.3932	80.8211	54	15	5.1			9001
96115	233000	28.3382	80.7321	6			69	61	9404
96115	233000	28.3382	80.7321	54	7	5.1			9404

□
□□□□

DAY	TIME	LAT	LON	Z	DIR	SPD	T	TD	TIDN
96115	234000	28.4338	80.5734	6			67		1
96115	234000	28.4338	80.5734	12	1	4.1			1
96115	234000	28.4338	80.5734	54	353	5.1	67		1
96115	234000	28.4443	80.5621	6			68	64	2
96115	234000	28.4443	80.5621	12	1	2.9			2
96115	234000	28.4443	80.5621	54	1	7.0	68	64	2
96115	234000	28.4443	80.5621	90	3	8.9			2
96115	234000	28.4443	80.5621	162	3	11.1			2
96115	234000	28.4443	80.5621	204	1	12.1	68	64	2
96115	234000	28.4443	80.5621	6			68	64	2
96115	234000	28.4443	80.5621	12	357	4.1			2
96115	234000	28.4443	80.5621	54	357	7.0	68	63	2
96115	234000	28.4443	80.5621	90	358	9.9			2
96115	234000	28.4443	80.5621	162	1	11.1			2
96115	234000	28.4443	80.5621	204	357	13.0	68	64	2
96115	234000	28.4598	80.5267	6			68		3
96115	234000	28.4598	80.5267	12	2	12.1			3
96115	234000	28.4598	80.5267	54	359	13.0	67		3
96115	234000	28.4466	80.5652	6					17
96115	234000	28.7435	80.7005	6			68	64	19
96115	234000	28.7435	80.7005	54	359	15.0			19
96115	234000	28.7975	80.7378	6					22
96115	234000	28.7975	80.7378	54					22
96115	234000	28.4721	80.5393	6					36
96115	234000	28.4721	80.5393	90	356	8.9			36
96115	234000	28.5622	80.5785	6					40
96115	234000	28.5622	80.5785	54	2	6.0			40
96115	234000	28.5836	80.5842	6					41
96115	234000	28.5836	80.5842	54	348	9.9			41
96115	234000	28.5130	80.5613	6			68	64	61
96115	234000	28.5130	80.5613	12	15	1.9			61
96115	234000	28.5130	80.5613	54	2	7.0	68	63	61
96115	234000	28.5130	80.5613	162	2	12.1			61
96115	234000	28.5130	80.5613	204	8	14.0	67	64	61
96115	234000	28.5130	80.5613	6			67	62	62
96115	234000	28.5130	80.5613	12	2	2.9			62
96115	234000	28.5130	80.5613	54	350	7.0	67	63	62
96115	234000	28.5130	80.5613	162	357	12.1			62
96115	234000	28.5130	80.5613	204	359	13.0	67	63	62
96115	234000	28.5358	80.5747	6			67		108
96115	234000	28.5358	80.5747	12	4	2.9			108
96115	234000	28.5358	80.5747	54	360	8.0	67		108
96115	234000	28.6141	80.6203	6			67		112
96115	234000	28.6141	80.6203	12	358	5.1			112
96115	234000	28.6141	80.6203	54	356	11.1	67		112
96115	234000	28.4048	80.6519	6					300
96115	234000	28.4048	80.6519	54					300
96115	234000	28.4600	80.5711	6			67		303
96115	234000	28.4600	80.5711	12	352	2.9			303
96115	234000	28.4600	80.5711	54	356	6.0	66		303
96115	234000	28.6027	80.6414	6			67		311

96115	234000	28.6027	80.6414	12	2	5.1		311
96115	234000	28.6027	80.6414	54	2	9.9	67	311
96115	234000	28.6105	80.6069	6				393
96115	234000	28.6105	80.6069	60	352	11.1	68	62 393
96115	234000	28.6057	80.6016	6			68	62 394
96115	234000	28.6057	80.6016	60	358	14.0	67	62 394
96115	234000	28.6294	80.6235	6				397
96115	234000	28.6294	80.6235	60	352	12.1	67	61 397
96115	234000	28.6248	80.6182	6			67	60 398
96115	234000	28.6248	80.6182	60	350	13.0	67	62 398
96115	234000	28.4586	80.5923	6			68	403
96115	234000	28.4586	80.5923	12	14	7.0		403
96115	234000	28.4586	80.5923	54	12	8.9	67	403
96115	234000	28.6062	80.6739	6			66	412
96115	234000	28.6062	80.6739	12	16	2.9		412
96115	234000	28.6062	80.6739	54	356	8.0	66	412
96115	234000	28.6586	80.6998	6			66	415
96115	234000	28.6586	80.6998	12	347	4.1		415
96115	234000	28.6586	80.6998	54	357	8.9	66	415
96115	234000	28.7055	80.7265	6			67	62 418
96115	234000	28.7055	80.7265	54	6	8.0		418
96115	234000	28.7755	80.8043	6			67	61 421
96115	234000	28.7755	80.8043	54	1	7.0		421
96115	234000	28.5158	80.6400	6			67	506
96115	234000	28.5158	80.6400	12	354	4.1		506
96115	234000	28.5158	80.6400	54	358	5.1	67	506
96115	234000	28.5623	80.6694	6			67	509
96115	234000	28.5623	80.6694	12	7	6.0		509
96115	234000	28.5623	80.6694	54	2	8.0	65	509
96115	234000	28.5986	80.6817	6				511
96115	234000	28.5986	80.6817	30	355	7.0		511
96115	234000	28.6160	80.6930	6			68	61 512
96115	234000	28.6160	80.6930	30	0	8.0		512
96115	234000	28.6307	80.7027	6				513
96115	234000	28.6307	80.7027	30	3	8.9		513
96115	234000	28.6431	80.7482	6			66	714
96115	234000	28.6431	80.7482	12	355	5.1		714
96115	234000	28.6431	80.7482	54	355	8.9	66	714
96115	234000	28.4632	80.6702	6			67	803
96115	234000	28.4632	80.6702	12	359	2.9		803
96115	234000	28.4632	80.6702	54	353	6.0	67	803
96115	234000	28.5184	80.6962	6				805
96115	234000	28.5184	80.6962	12				805
96115	234000	28.5184	80.6962	54				805
96115	234000	28.7464	80.8707	6			67	58 819
96115	234000	28.7464	80.8707	54	359	6.0		819
96115	234000	28.4079	80.7604	6			68	62 1000
96115	234000	28.4079	80.7604	54	25	8.0		1000
96115	234000	28.5272	80.7742	6			69	62 1007
96115	234000	28.5272	80.7742	54	2	11.1		1007
96115	234000	28.6056	80.8248	6			67	60 1012
96115	234000	28.6056	80.8248	54	6	6.0		1012

96115	234000	28.5697	80.5864	6			69	64	1101
96115	234000	28.5697	80.5864	12	340	1.9			1101
96115	234000	28.5697	80.5864	54	358	8.9	68	64	1101
96115	234000	28.5697	80.5864	162	1	12.1			1101
96115	234000	28.5697	80.5864	204	1	13.0	67	63	1101
96115	234000	28.5697	80.5864	6			68	64	1102
96115	234000	28.5697	80.5864	12	350	1.9			1102
96115	234000	28.5697	80.5864	54	355	8.9	68	63	1102
96115	234000	28.5697	80.5864	162	356	13.0			1102
96115	234000	28.5697	80.5864	204	358	13.0	67	62	1102
96115	234000	28.4843	80.7856	6			68	62	1204
96115	234000	28.4843	80.7856	54	11	8.0			1204
96115	234000	28.6445	80.9034	6					1215
96115	234000	28.4114	80.9284	6			68	63	1500
96115	234000	28.4114	80.9284	54	16	4.1			1500
96115	234000	28.4475	80.8538	6					1502
96115	234000	28.4960	80.8843	6			68	64	1605
96115	234000	28.4960	80.8843	54	10	8.9			1605
96115	234000	28.5583	80.9132	6					1609
96115	234000	28.6173	80.9581	6			67	59	1612
96115	234000	28.6173	80.9581	54	15	5.1			1612
96115	234000	28.6762	80.9987	6			66	58	1617
96115	234000	28.6762	80.9987	54	14	5.1			1617
96115	234000	28.5231	81.0100	6			68	60	2008
96115	234000	28.5231	81.0100	54	28	6.0			2008
96115	234000	28.6489	81.0693	6			67	58	2016
96115	234000	28.6489	81.0693	54	15	8.9			2016
96115	234000	28.4417	81.0291	6			68	60	2202
96115	234000	28.4417	81.0291	54	35	11.1			2202
96115	234000	28.6256	80.6571	6			67	62	3131
96115	234000	28.6256	80.6571	12	357	6.0			3131
96115	234000	28.6256	80.6571	54	356	8.0	67	63	3131
96115	234000	28.6256	80.6571	162	353	11.1			3131
96115	234000	28.6256	80.6571	204	355	12.1	66	61	3131
96115	234000	28.6256	80.6571	295	358	14.0			3131
96115	234000	28.6256	80.6571	394	357	14.0			3131
96115	234000	28.6256	80.6571	492	357	14.0	65	62	3131
96115	234000	28.6256	80.6571	6			67	62	3132
96115	234000	28.6256	80.6571	12	357	5.1			3132
96115	234000	28.6256	80.6571	54	1	8.9	67	63	3132
96115	234000	28.6256	80.6571	162	355	11.1			3132
96115	234000	28.6256	80.6571	204	3	12.1	67	63	3132
96115	234000	28.6256	80.6571	295	4	14.0			3132
96115	234000	28.6256	80.6571	394	4	14.0			3132
96115	234000	28.6256	80.6571	492	5	15.0	65	62	3132
96115	234000	28.3932	80.8211	6			70	63	9001
96115	234000	28.3932	80.8211	54	25	4.1			9001
96115	234000	28.3382	80.7321	6			68	62	9404
96115	234000	28.3382	80.7321	54	7	5.1			9404

□

□□□□

DAY	TIME	LAT	LON	Z	DIR	SPD	T	TD	TIDN
96115	235000	28.4338	80.5734	6			67		1
96115	235000	28.4338	80.5734	12	360	4.1			1
96115	235000	28.4338	80.5734	54	353	6.0	67		1
96115	235000	28.4443	80.5621	6			68	64	2
96115	235000	28.4443	80.5621	12	0	4.1			2
96115	235000	28.4443	80.5621	54	358	7.0	68	64	2
96115	235000	28.4443	80.5621	90	0	8.9			2
96115	235000	28.4443	80.5621	162	2	11.1			2
96115	235000	28.4443	80.5621	204	360	12.1	67	64	2
96115	235000	28.4443	80.5621	6			68	64	2
96115	235000	28.4443	80.5621	12	356	4.1			2
96115	235000	28.4443	80.5621	54	355	8.0	68	62	2
96115	235000	28.4443	80.5621	90	357	8.9			2
96115	235000	28.4443	80.5621	162	0	11.1			2
96115	235000	28.4443	80.5621	204	356	12.1	67	64	2
96115	235000	28.4598	80.5267	6			68		3
96115	235000	28.4598	80.5267	12	359	12.1			3
96115	235000	28.4598	80.5267	54	356	15.0	68		3
96115	235000	28.4466	80.5652	6					17
96115	235000	28.7435	80.7005	6			68	64	19
96115	235000	28.7435	80.7005	54	3	15.0			19
96115	235000	28.7975	80.7378	6			67	63	22
96115	235000	28.7975	80.7378	54	359	15.9			22
96115	235000	28.4721	80.5393	6					36
96115	235000	28.4721	80.5393	90	356	11.1			36
96115	235000	28.5622	80.5785	6					40
96115	235000	28.5622	80.5785	54	3	7.0			40
96115	235000	28.5836	80.5842	6					41
96115	235000	28.5836	80.5842	54	352	9.9			41
96115	235000	28.5130	80.5613	6			68	64	61
96115	235000	28.5130	80.5613	12	359	1.9			61
96115	235000	28.5130	80.5613	54	358	7.0	68	63	61
96115	235000	28.5130	80.5613	162	358	9.9			61
96115	235000	28.5130	80.5613	204	5	12.1	67	64	61
96115	235000	28.5130	80.5613	6			67	62	62
96115	235000	28.5130	80.5613	12	360	2.9			62
96115	235000	28.5130	80.5613	54	344	7.0	67	63	62
96115	235000	28.5130	80.5613	162	353	11.1			62
96115	235000	28.5130	80.5613	204	355	12.1	67	63	62
96115	235000	28.5358	80.5747	6			67		108
96115	235000	28.5358	80.5747	12	355	2.9			108
96115	235000	28.5358	80.5747	54	350	8.0	67		108
96115	235000	28.6141	80.6203	6			67		112
96115	235000	28.6141	80.6203	12	5	5.1			112
96115	235000	28.6141	80.6203	54	1	11.1	67		112
96115	235000	28.4048	80.6519	6			70	65	300
96115	235000	28.4048	80.6519	54	3	13.0			300
96115	235000	28.4600	80.5711	6			66		303
96115	235000	28.4600	80.5711	12	350	2.9			303
96115	235000	28.4600	80.5711	54	356	6.0	65		303
96115	235000	28.6027	80.6414	6			67		311

96115	235000	28.6027	80.6414	12	358	4.1			311
96115	235000	28.6027	80.6414	54	1	8.9	67		311
96115	235000	28.6105	80.6069	6					393
96115	235000	28.6105	80.6069	60	351	9.9	67	63	393
96115	235000	28.6057	80.6016	6			67	62	394
96115	235000	28.6057	80.6016	60	3	11.1	67	63	394
96115	235000	28.6294	80.6235	6					397
96115	235000	28.6294	80.6235	60	355	12.1	67	62	397
96115	235000	28.6248	80.6182	6			67	60	398
96115	235000	28.6248	80.6182	60	350	13.0	67	63	398
96115	235000	28.4586	80.5923	6			67		403
96115	235000	28.4586	80.5923	12	7	6.0			403
96115	235000	28.4586	80.5923	54	5	8.9	67		403
96115	235000	28.6062	80.6739	6			66		412
96115	235000	28.6062	80.6739	12	11	2.9			412
96115	235000	28.6062	80.6739	54	359	8.9	66		412
96115	235000	28.6586	80.6998	6			66		415
96115	235000	28.6586	80.6998	12	352	4.1			415
96115	235000	28.6586	80.6998	54	360	8.9	66		415
96115	235000	28.7055	80.7265	6			67	62	418
96115	235000	28.7055	80.7265	54	4	8.0			418
96115	235000	28.7755	80.8043	6			67	61	421
96115	235000	28.7755	80.8043	54	358	7.0			421
96115	235000	28.5158	80.6400	6			66		506
96115	235000	28.5158	80.6400	12	351	6.0			506
96115	235000	28.5158	80.6400	54	354	8.0	66		506
96115	235000	28.5623	80.6694	6			67		509
96115	235000	28.5623	80.6694	12	8	4.1			509
96115	235000	28.5623	80.6694	54	2	5.1	65		509
96115	235000	28.5986	80.6817	6					511
96115	235000	28.5986	80.6817	30	358	6.0			511
96115	235000	28.6160	80.6930	6			67	61	512
96115	235000	28.6160	80.6930	30	3	7.0			512
96115	235000	28.6307	80.7027	6					513
96115	235000	28.6307	80.7027	30	6	8.9			513
96115	235000	28.6431	80.7482	6			66		714
96115	235000	28.6431	80.7482	12	3	5.1			714
96115	235000	28.6431	80.7482	54	1	8.0	66		714
96115	235000	28.4632	80.6702	6			66		803
96115	235000	28.4632	80.6702	12	358	2.9			803
96115	235000	28.4632	80.6702	54	354	5.1	66		803
96115	235000	28.5184	80.6962	6					805
96115	235000	28.5184	80.6962	12					805
96115	235000	28.5184	80.6962	54					805
96115	235000	28.7464	80.8707	6			66	58	819
96115	235000	28.7464	80.8707	54	5	5.1			819
96115	235000	28.4079	80.7604	6			68	62	1000
96115	235000	28.4079	80.7604	54	23	8.9			1000
96115	235000	28.5272	80.7742	6			68	62	1007
96115	235000	28.5272	80.7742	54	1	11.1			1007
96115	235000	28.6056	80.8248	6			67	60	1012
96115	235000	28.6056	80.8248	54	6	6.0			1012

96115	235000	28.5697	80.5864	6			69	64	1101
96115	235000	28.5697	80.5864	12	357	1.9			1101
96115	235000	28.5697	80.5864	54	2	9.9	68	64	1101
96115	235000	28.5697	80.5864	162	3	11.1			1101
96115	235000	28.5697	80.5864	204	1	12.1	67	63	1101
96115	235000	28.5697	80.5864	6			68	64	1102
96115	235000	28.5697	80.5864	12	359	2.9			1102
96115	235000	28.5697	80.5864	54	359	8.9	68	63	1102
96115	235000	28.5697	80.5864	162	359	12.1			1102
96115	235000	28.5697	80.5864	204	1	12.1	68	63	1102
96115	235000	28.4843	80.7856	6			67	62	1204
96115	235000	28.4843	80.7856	54	1	7.0			1204
96115	235000	28.6445	80.9034	6					1215
96115	235000	28.4114	80.9284	6			67	63	1500
96115	235000	28.4114	80.9284	54	19	5.1			1500
96115	235000	28.4475	80.8538	6					1502
96115	235000	28.4960	80.8843	6			67	64	1605
96115	235000	28.4960	80.8843	54	11	8.9			1605
96115	235000	28.5583	80.9132	6					1609
96115	235000	28.6173	80.9581	6			67	59	1612
96115	235000	28.6173	80.9581	54	11	8.0			1612
96115	235000	28.6762	80.9987	6			66	57	1617
96115	235000	28.6762	80.9987	54	15	6.0			1617
96115	235000	28.5231	81.0100	6			67	60	2008
96115	235000	28.5231	81.0100	54	21	6.0			2008
96115	235000	28.6489	81.0693	6			67	58	2016
96115	235000	28.6489	81.0693	54	16	8.0			2016
96115	235000	28.4417	81.0291	6			67	60	2202
96115	235000	28.4417	81.0291	54	33	8.9			2202
96115	235000	28.6256	80.6571	6			67	62	3131
96115	235000	28.6256	80.6571	12	356	6.0			3131
96115	235000	28.6256	80.6571	54	358	9.9	67	63	3131
96115	235000	28.6256	80.6571	162	357	13.0			3131
96115	235000	28.6256	80.6571	204	358	14.0	66	61	3131
96115	235000	28.6256	80.6571	295	359	15.0			3131
96115	235000	28.6256	80.6571	394	355	15.0			3131
96115	235000	28.6256	80.6571	492	355	15.0	65	62	3131
96115	235000	28.6256	80.6571	6			67	62	3132
96115	235000	28.6256	80.6571	12	353	5.1			3132
96115	235000	28.6256	80.6571	54	4	9.9	67	63	3132
96115	235000	28.6256	80.6571	162	1	12.1			3132
96115	235000	28.6256	80.6571	204	4	14.0	67	63	3132
96115	235000	28.6256	80.6571	295	3	15.0			3132
96115	235000	28.6256	80.6571	394	3	15.9			3132
96115	235000	28.6256	80.6571	492	3	15.9	65	62	3132
96115	235000	28.3932	80.8211	6			69	63	9001
96115	235000	28.3932	80.8211	54	14	4.1			9001
96115	235000	28.3382	80.7321	6			68	62	9404
96115	235000	28.3382	80.7321	54	14	6.0			9404

□
□□□□

DAY	TIME	LAT	LON	Z	DIR	SPD	T	TD	TIDN
96116	0	28.4338	80.5734	6			67		1
96116	0	28.4338	80.5734	12	358	2.9			1
96116	0	28.4338	80.5734	54	350	6.0	67		1
96116	0	28.4443	80.5621	6			67	64	2
96116	0	28.4443	80.5621	12	350	2.9			2
96116	0	28.4443	80.5621	54	352	8.0	67	63	2
96116	0	28.4443	80.5621	90	355	8.9			2
96116	0	28.4443	80.5621	162	357	11.1			2
96116	0	28.4443	80.5621	204	355	12.1	67	64	2
96116	0	28.4443	80.5621	6			67	64	2
96116	0	28.4443	80.5621	12	348	4.1			2
96116	0	28.4443	80.5621	54	348	8.0	68	63	2
96116	0	28.4443	80.5621	90	351	9.9			2
96116	0	28.4443	80.5621	162	355	11.1			2
96116	0	28.4443	80.5621	204	351	12.1	67	64	2
96116	0	28.4598	80.5267	6			68		3
96116	0	28.4598	80.5267	12	358	13.0			3
96116	0	28.4598	80.5267	54	352	15.9	68		3
96116	0	28.4466	80.5652	6					17
96116	0	28.7435	80.7005	6			68	64	19
96116	0	28.7435	80.7005	54	1	15.9			19
96116	0	28.7975	80.7378	6			67	63	22
96116	0	28.7975	80.7378	54	1	15.0			22
96116	0	28.4721	80.5393	6					36
96116	0	28.4721	80.5393	90	353	9.9			36
96116	0	28.5622	80.5785	6					40
96116	0	28.5622	80.5785	54	5	7.0			40
96116	0	28.5836	80.5842	6					41
96116	0	28.5836	80.5842	54	351	9.9			41
96116	0	28.5130	80.5613	6			67	64	61
96116	0	28.5130	80.5613	12	354	1.9			61
96116	0	28.5130	80.5613	54	360	7.0	67	63	61
96116	0	28.5130	80.5613	162	360	11.1			61
96116	0	28.5130	80.5613	204	6	14.0	67	64	61
96116	0	28.5130	80.5613	6			67	62	62
96116	0	28.5130	80.5613	12	352	1.9			62
96116	0	28.5130	80.5613	54	345	7.0	67	63	62
96116	0	28.5130	80.5613	162	355	12.1			62
96116	0	28.5130	80.5613	204	357	13.0	67	63	62
96116	0	28.5358	80.5747	6			67		108
96116	0	28.5358	80.5747	12	1	2.9			108
96116	0	28.5358	80.5747	54	352	8.9	67		108
96116	0	28.6141	80.6203	6			66		112
96116	0	28.6141	80.6203	12	5	5.1			112
96116	0	28.6141	80.6203	54	1	8.9	67		112
96116	0	28.4048	80.6519	6			69	64	300
96116	0	28.4048	80.6519	54	2	14.0			300
96116	0	28.4600	80.5711	6			66		303
96116	0	28.4600	80.5711	12	349	2.9			303
96116	0	28.4600	80.5711	54	358	6.0	65		303
96116	0	28.6027	80.6414	6			67		311

96116	0	28.6027	80.6414	12	357	4.1			311
96116	0	28.6027	80.6414	54	358	8.0	67		311
96116	0	28.6105	80.6069	6					393
96116	0	28.6105	80.6069	60	353	11.1	67	63	393
96116	0	28.6057	80.6016	6			67	62	394
96116	0	28.6057	80.6016	60	1	13.0	68	63	394
96116	0	28.6294	80.6235	6					397
96116	0	28.6294	80.6235	60	353	11.1	67	62	397
96116	0	28.6248	80.6182	6			67	60	398
96116	0	28.6248	80.6182	60	351	14.0	67	63	398
96116	0	28.4586	80.5923	6			67		403
96116	0	28.4586	80.5923	12	10	8.0			403
96116	0	28.4586	80.5923	54	7	11.1	67		403
96116	0	28.6062	80.6739	6			66		412
96116	0	28.6062	80.6739	12	13	1.9			412
96116	0	28.6062	80.6739	54	354	8.0	66		412
96116	0	28.6586	80.6998	6			66		415
96116	0	28.6586	80.6998	12	349	4.1			415
96116	0	28.6586	80.6998	54	358	9.9	66		415
96116	0	28.7055	80.7265	6			67	62	418
96116	0	28.7055	80.7265	54	360	8.0			418
96116	0	28.7755	80.8043	6			67	61	421
96116	0	28.7755	80.8043	54	358	7.0			421
96116	0	28.5158	80.6400	6			66		506
96116	0	28.5158	80.6400	12	352	6.0			506
96116	0	28.5158	80.6400	54	352	8.0	66		506
96116	0	28.5623	80.6694	6			66		509
96116	0	28.5623	80.6694	12	3	5.1			509
96116	0	28.5623	80.6694	54	357	6.0	65		509
96116	0	28.5986	80.6817	6					511
96116	0	28.5986	80.6817	30	349	5.1			511
96116	0	28.6160	80.6930	6			67	61	512
96116	0	28.6160	80.6930	30	0	8.0			512
96116	0	28.6307	80.7027	6					513
96116	0	28.6307	80.7027	30	4	8.0			513
96116	0	28.6431	80.7482	6			66		714
96116	0	28.6431	80.7482	12	6	5.1			714
96116	0	28.6431	80.7482	54	359	8.0	66		714
96116	0	28.4632	80.6702	6			66		803
96116	0	28.4632	80.6702	12	5	1.9			803
96116	0	28.4632	80.6702	54	360	5.1	66		803
96116	0	28.5184	80.6962	6					805
96116	0	28.5184	80.6962	12					805
96116	0	28.5184	80.6962	54					805
96116	0	28.7464	80.8707	6			65	58	819
96116	0	28.7464	80.8707	54	348	2.9			819
96116	0	28.4079	80.7604	6			67	62	1000
96116	0	28.4079	80.7604	54	26	8.9			1000
96116	0	28.5272	80.7742	6			68	62	1007
96116	0	28.5272	80.7742	54	3	12.1			1007
96116	0	28.6056	80.8248	6			67	60	1012
96116	0	28.6056	80.8248	54	0	4.1			1012

96116	0	28.5697	80.5864	6			68	64	1101
96116	0	28.5697	80.5864	12	355	1.9			1101
96116	0	28.5697	80.5864	54	2	8.9	68	64	1101
96116	0	28.5697	80.5864	162	3	12.1			1101
96116	0	28.5697	80.5864	204	3	13.0	67	63	1101
96116	0	28.5697	80.5864	6			68	64	1102
96116	0	28.5697	80.5864	12	359	1.9			1102
96116	0	28.5697	80.5864	54	1	8.0	68	63	1102
96116	0	28.5697	80.5864	162	358	12.1			1102
96116	0	28.5697	80.5864	204	2	13.0	67	62	1102
96116	0	28.4843	80.7856	6			67	62	1204
96116	0	28.4843	80.7856	54	3	6.0			1204
96116	0	28.6445	80.9034	6					1215
96116	0	28.4114	80.9284	6			67	63	1500
96116	0	28.4114	80.9284	54	17	6.0			1500
96116	0	28.4475	80.8538	6					1502
96116	0	28.4960	80.8843	6			67	64	1605
96116	0	28.4960	80.8843	54	10	11.1			1605
96116	0	28.5583	80.9132	6					1609
96116	0	28.6173	80.9581	6			67	59	1612
96116	0	28.6173	80.9581	54	7	8.0			1612
96116	0	28.6762	80.9987	6			65	57	1617
96116	0	28.6762	80.9987	54	21	5.1			1617
96116	0	28.5231	81.0100	6			67	60	2008
96116	0	28.5231	81.0100	54	13	8.0			2008
96116	0	28.6489	81.0693	6			67	58	2016
96116	0	28.6489	81.0693	54	17	8.9			2016
96116	0	28.4417	81.0291	6			67	60	2202
96116	0	28.4417	81.0291	54	34	8.0			2202
96116	0	28.6256	80.6571	6			67	62	3131
96116	0	28.6256	80.6571	12	352	6.0			3131
96116	0	28.6256	80.6571	54	356	8.9	67	63	3131
96116	0	28.6256	80.6571	162	355	12.1			3131
96116	0	28.6256	80.6571	204	356	13.0	67	61	3131
96116	0	28.6256	80.6571	295	358	14.0			3131
96116	0	28.6256	80.6571	394	355	15.0			3131
96116	0	28.6256	80.6571	492	357	15.9	65	62	3131
96116	0	28.6256	80.6571	6			67	62	3132
96116	0	28.6256	80.6571	12	352	5.1			3132
96116	0	28.6256	80.6571	54	2	8.0	67	63	3132
96116	0	28.6256	80.6571	162	358	12.1			3132
96116	0	28.6256	80.6571	204	5	12.1	67	63	3132
96116	0	28.6256	80.6571	295	3	14.0			3132
96116	0	28.6256	80.6571	394	2	15.0			3132
96116	0	28.6256	80.6571	492	4	15.9	65	63	3132
96116	0	28.3932	80.8211	6			68	63	9001
96116	0	28.3932	80.8211	54	19	2.9			9001
96116	0	28.3382	80.7321	6			68	62	9404
96116	0	28.3382	80.7321	54	9	5.1			9404

□

□□□□

T-0.7 hour Rawinsonde Data Formatted as Input for REEDM

```
RS011152255
TEST NBR A1756 WS-9A                    402
RAWINSONDE MSS/MSS
CAPE CANAVERAL AFS, FLORIDA
2255Z  24 APR 96

  ALT   DIR   SPD  SHR  TEMP  DPT   PRESS   RH ABHUM DENSITY I/R V/S  VPS  PW
GEOMFT DEG   KTS /SEC DEG C DEG C   MBS    PCT  G/M3   G/M3   N  KTS  MBS  MM

    16  20  12.0 .000  20.8  16.3 1018.70  76 13.70 1198.99 349 671 18.58  0
  1000  10  14.4 .006  17.5  16.2  983.90  92 13.74 1170.83 344 667 18.44  4
  2000   4  12.6 .004  16.2  13.8  949.51  86 11.89 1135.89 325 665 15.87  8
  3000 332  11.9 .011  15.8  14.5  916.21  91 12.35 1096.96 320 665 16.48 12
  4000 301  11.5 .011  14.8  13.2  884.02  90 11.41 1062.76 307 664 15.15 15
  5000 278  12.6 .008  13.0  11.4  852.80  90 10.25 1031.96 293 661 13.53 18
  6000 999 999.0 .999  11.4   9.4  822.49  87  8.96 1001.61 279 659 11.77 21
  7000 999 999.0 .999   9.9   7.7  793.10  86  8.04  971.29 266 657 10.50 24
TERMINATION        7280 GEOPFT   2219 GEOPM  784.7 MBS
TROPOPAUSE        0  FEET       .00 MB     .0 C     .0 C

MANDATORY LEVELS
GEOPFT DIR KTS  TEMP   DPT PRESS   RH

   541   5  14  18.9  16.5 1000.0  86
  1982   4  13  16.3  13.8  950.0  86
  3494 317  12  15.4  13.8  900.0  90
  5082 278  13  12.9  11.3  850.0  90
  6751 999 999  10.7   8.3  800.0  85
SIGNIFICANT LEVELS
GEOMFT DIR KTS  TEMP   DPT PRESS   IR  RH

    16  20  12  20.8  16.3 1018.7 349  76
   199 337  14  20.0  16.3 1012.2 348  79
   565   7  15  18.8  16.5  999.2 348  87
  1114  11  14  17.2  16.1  979.9 343  93
  1663  10  14  17.0  12.5  961.0 321  75
  2226 359  12  15.7  14.8  941.9 328  94
  3862 304  12  15.0  13.4  888.4 308  90
  5971 277  15  11.4   9.4  823.4 279  88
  6817 999 999  10.7   8.2  798.4 269  85
  7293 999 999   8.6   6.7  784.7 262  88
TERMINATION
146 146
NNNN
```

T-0.5 hour Rawinsonde Data Formatted as Input for REEDM

```
RS011152310
TEST NBR A1756 RS9B                0630
RAWINSONDE MSS/MSS
CAPE CANAVERAL AFS, FLORIDA
2310Z  24 APR 96

  ALT  DIR   SPD  SHR  TEMP  DPT   PRESS   RH ABHUM DENSITY I/R V/S  VPS  PW
GEOMFT DEG   KTS /SEC DEG C DEG C   MBS   PCT  G/M3   G/M3   N  KTS  MBS  MM

    16 360   3.0 .000  20.5  17.0 1018.80  81 14.33 1199.95 353 670 19.42  0
  1000  14  13.7 .018  17.5  16.4  983.99  94 13.94 1171.05 345 667 18.69  4
  2000  11  11.4 .004  16.4  15.4  949.62  94 13.11 1134.73 333 666 17.52  8
  3000 333   8.0 .012  15.4  14.4  916.30  94 12.36 1098.68 320 664 16.45 12
  4000 286  10.2 .013  14.6  13.1  884.08  91 11.33 1063.61 306 663 15.04 16
  5000 278  13.1 .006  12.7  11.1  852.83  90 10.02 1033.27 292 661 13.22 19
  6000 279  15.8 .005  10.9   9.3  822.47  90  8.94 1003.38 279 659 11.71 22
  7000 278  18.4 .004   9.3   7.2  793.02  87  7.79  973.45 265 657 10.16 24
  8000 279  20.7 .004   7.5   5.4  764.43  86  6.95  944.61 254 655  9.00 27
  9000 278  21.6 .002   5.3   2.2  736.68  80  5.58  918.27 240 652  7.17 28
 10000 277  19.3 .004   3.3  -2.4  709.70  68  4.14  891.91 225 649  5.27 30
 11000 999 999.0 .999   4.8 -16.0  683.65  20  1.36  856.17 199 650  1.75 31
TERMINATION       11574 GEOPFT   3528 GEOPM  668.6 MBS
TROPOPAUSE        0  FEET      .00 MB     .0 C     .0 C

MANDATORY LEVELS
GEOPFT DIR KTS  TEMP   DPT PRESS   RH

   544  11  14  18.8  16.5 1000.0  87
  1986  11  11  16.4  15.4  950.0  94
  3496 301   9  15.3  13.8  900.0  91
  5083 278  13  12.5  11.0  850.0  91
  6748 279  18   9.8   7.6  800.0  86
  8501 279  21   6.5   3.5  750.0  81
 10348 278  18   3.8 -10.0  700.0  39
SIGNIFICANT LEVELS
GEOMFT DIR KTS  TEMP   DPT PRESS   IR  RH

    16 360   3  20.5  17.0 1018.8 353  81
   198   2  13  20.0  16.7 1012.3 350  81
  1134  15  14  17.1  16.4  979.3 344  96
  3238 314   8  15.6  14.3  908.5 317  92
  7721 279  20   8.0   6.6  772.3 259  91
  8845 278  22   5.7   2.5  740.9 241  80
  9396 277  21   4.3   1.4  725.9 236  81
  9939 277  20   3.2  -1.1  711.3 227  73
 10482 279  18   3.9 -12.4  697.0 207  29
 11023 999 999   4.8 -16.2  683.1 199  20
 11597 999 999   3.5 -16.1  668.6 196  22
TERMINATION
100 100
NNNN
```

T-0.2 hour Rawinsonde Data Formatted as Input for REEDM

RS011152325
TEST NBR A1756 WS-9C R-3 2610
RAWINSONDE MSS/MSS
CAPE CANAVERAL AFS, FLORIDA
2325Z 24 APR 96

ALT GEOMFT	DIR DEG	SPD KTS	SHR /SEC	TEMP DEG C	DPT DEG C	PRESS MBS	RH PCT	ABHUM G/M3	DENSITY G/M3	I/R N	V/S KTS	VPS MBS	PW MM
16	10	9.0	.000	20.3	17.0	1018.80	81	14.31	1200.79	353	670	19.37	0
1000	17	12.9	.007	17.3	16.3	983.97	94	13.80	1171.94	345	667	18.49	4
2000	12	10.4	.005	16.5	15.3	949.55	93	12.99	1134.19	332	666	17.36	8
3000	339	7.9	.010	15.9	14.8	916.29	93	12.61	1096.51	321	665	16.82	12
4000	293	9.4	.012	14.9	13.3	884.11	90	11.46	1062.46	307	664	15.23	16
5000	278	12.5	.007	13.3	11.4	852.91	89	10.22	1031.21	293	662	13.51	19
6000	277	15.8	.005	11.2	9.9	822.60	91	9.27	1002.18	281	659	12.16	22
7000	277	18.7	.005	9.5	7.7	793.16	88	8.04	972.79	267	657	10.49	24
8000	277	20.2	.003	7.6	6.1	764.59	90	7.28	944.20	256	655	9.44	27
9000	278	21.0	.001	5.9	3.3	736.87	83	6.00	916.35	242	652	7.73	29
10000	275	19.8	.003	3.5	-.1	709.95	78	4.79	891.00	229	649	6.12	30
11000	281	16.1	.007	5.4	-15.6	683.96	20	1.42	854.67	199	651	1.82	31
12000	294	17.4	.007	3.4	-16.6	658.87	21	1.31	829.22	193	649	1.67	31
13000	298	18.0	.003	1.2	-17.9	634.53	22	1.18	804.95	187	646	1.49	32
14000	298	16.6	.002	.0	-19.0	610.94	22	1.08	778.51	180	645	1.36	32
15000	300	16.5	.001	-2.3	-20.6	588.09	23	.94	755.85	174	642	1.18	32
16000	305	18.9	.005	-4.4	-22.4	565.91	23	.81	733.12	169	639	1.01	33
17000	304	20.8	.003	-7.0	-24.9	544.40	22	.66	712.22	163	636	.81	33
18000	298	20.7	.004	-9.3	-26.9	523.51	22	.55	690.98	158	633	.67	33
19000	291	20.7	.004	-11.7	-29.0	503.24	22	.46	670.36	152	630	.55	33
20000	288	21.9	.002	-14.1	-31.0	483.59	22	.38	650.23	147	627	.46	33
21000	289	24.1	.004	-16.8	-32.5	464.52	24	.33	630.96	143	624	.39	34
22000	291	27.1	.005	-19.6	-34.7	446.01	25	.27	612.63	138	621	.32	34
23000	293	31.1	.007	-22.3	-36.9	428.05	25	.22	594.27	134	617	.25	34
24000	294	34.8	.006	-25.0	-38.8	410.63	26	.18	576.32	130	614	.21	34
25000	293	36.9	.004	-27.4	-40.5	393.75	27	.15	558.16	125	611	.18	34
26000	289	38.0	.005	-29.9	-42.7	377.41	27	.12	540.36	121	608	.14	34
27000	283	38.5	.006	-32.5	-44.8	361.58	28	.10	523.48	117	605	.11	34
28000	277	39.3	.007	-35.1	-46.9	346.27	29	.08	506.62	113	601	.09	34
29000	271	42.7	.009	-37.5	-49.7	331.44	27	.06	490.04	110	598	.06	34
30000	265	48.5	.013	-39.7	-51.8	317.11	26	.05	473.24	106	596	.05	34
31000	260	54.3	.012	-40.9	-52.7	303.31	26	.04	454.97	102	594	.04	34
32000	259	59.9	.009	-43.6	-54.2	290.00	29	.03	440.09	98	591	.04	34
33000	262	65.8	.011	-45.7	-56.3	277.15	28	.03	424.40	95	588	.03	34
34000	264	73.9	.014	-47.2	-57.9	264.77	28	.02	408.25	91	586	.02	34
35000	262	79.9	.011	-48.4	-58.8	252.88	28	.02	392.02	87	584	.02	34
36000	260	83.1	.008	-50.2	-60.1	241.45	29	.02	377.19	84	582	.02	34
37000	257	85.7	.007	-52.6	-62.3	230.43	29	.01	364.05	81	579	.01	34
38000	257	89.5	.007	-54.9	-64.3	219.81	30	.01	350.83	78	576	.01	34
39000	257	95.7	.010	-56.6	-65.8	209.59	30	.01	337.14	75	574	.01	34
40000	257	100.4	.008	-58.1	-67.1	199.77	30	.01	323.64	72	572	.01	34
41000	257	101.5	.002	-59.0	99.9	190.36	999	99.99	309.66	69	570	.01999	
42000	257	100.4	.002	-60.8	99.9	181.34	999	99.99	297.49	66	568	.00999	
43000	257	100.7	.001	-61.8	99.9	172.69	999	99.99	284.62	63	567	.00999	
44000	259	99.8	.007	-61.4	99.9	164.44	999	99.99	270.59	60	567	.00999	
45000	263	97.8	.010	-61.6	99.9	156.60	999	99.99	257.83	57	567	.00999	
46000	266	94.1	.011	-63.4	99.9	149.10	999	99.99	247.68	55	564	.00999	
47000	267	89.1	.009	-64.8	99.9	141.90	999	99.99	237.23	53	563	.00999	
48000	266	82.5	.012	-66.1	99.9	135.01	999	99.99	227.17	51	561	.00999	
49000	261	78.4	.013	-65.8	99.9	128.43	999	99.99	215.80	48	561	.00999	
50000	256	80.5	.012	-65.7	99.9	122.18	999	99.99	205.21	46	561	.00999	
51000	256	83.4	.005	-67.0	99.9	116.23	999	99.99	196.41	44	560	.00999	
52000	259	82.3	.009	-67.8	99.9	110.53	999	99.99	187.51	42	559	.00999	
53000	999	999.0	.999	-67.0	99.9	105.11	999	99.99	177.63	40	560	.00999	

TERMINATION 53421 GEOPFT 16283 GEOPM 101.8 MBS
TROPOPAUSE 0 FEET .00 MB .0 C .0 C

MANDATORY LEVELS

GEOPFT	DIR	KTS	TEMP	DPT	PRESS	RH
543	13	13	18.5	16.4	1000.0	88
1984	12	10	16.5	15.3	950.0	93
3497	313	8	15.6	14.0	900.0	90
5086	278	13	13.1	11.1	850.0	88
6753	277	18	9.8	8.2	800.0	89
8507	278	21	6.9	4.5	750.0	85
10358	274	17	4.6	-9.5	700.0	38
12336	296	18	2.7	-17.1	650.0	22
14444	299	16	-1.1	-19.7	600.0	23
16699	305	20	-6.3	-24.2	550.0	23
19118	290	21	-12.1	-29.3	500.0	22
21728	290	26	-19.0	-34.1	450.0	25
24562	294	36	-26.5	-39.8	400.0	27
27676	279	39	-34.5	-46.4	350.0	28
31154	259	56	-41.5	-53.0	300.0	27
35138	262	81	-48.8	-59.0	250.0	29
39842	257	100	-58.1	-67.0	200.0	30
42580	257	101	-61.6	99.9	175.0	999
45711	265	95	-63.1	99.9	150.0	999
49354	257	79	-65.3	99.9	125.0	999

SIGNIFICANT LEVELS

GEOMFT	DIR	KTS	TEMP	DPT	PRESS	IR	RH
16	10	9	20.3	17.0	1018.8	353	81
195	3	14	19.7	16.6	1012.4	350	82
1061	17	13	17.1	16.2	981.8	344	95
1578	16	12	16.2	15.5	963.9	337	96
3238	327	8	15.9	14.5	908.5	318	92
4273	286	10	14.4	13.0	875.5	304	92
6046	277	16	11.1	9.8	821.2	280	92
7178	277	19	9.2	7.3	788.0	264	88
7754	277	20	7.9	6.9	771.6	260	94
9391	278	21	5.0	2.0	726.3	237	81
9967	275	20	3.5	.7	710.8	231	82
10158	273	18	3.7	-4.0	705.8	220	57
10543	276	16	5.2	-13.6	695.7	204	24
11102	282	16	5.4	-16.0	681.4	198	19
15723	304	18	-3.7	-21.8	572.0	170	23
23681	294	34	-24.2	-38.4	416.1	131	25
29184	270	44	-38.0	-50.4	328.8	109	26
38229	257	90	-55.4	-64.7	217.4	78	30
40939	257	102	-58.8	-67.7	190.9	69	30
42005	257	100	-60.8	99.9	181.3	66	999
45326	264	97	-61.6	99.9	154.1	57	999
47807	267	84	-65.7	99.9	136.3	51	999
51630	258	83	-67.9	99.9	112.6	43	999
53635	999	999	-68.1	99.9	101.8	39	999

TERMINATION
044 044
NNNN

Appendix C—Description of Sampling Aircraft

Cloud sampling was performed using a Piper Seminole aircraft Model PA-44-180. The following pages present a photo of this model, with performance specification data, downloaded from the New Piper Aircraft Inc. Internet Web page and used by permission. Also presented are sketches of the installation of the Geomet instrument probe. These sketches were prepared to document the external aircraft modifications for FAA approval. Note that the external length of the probe is 18 in. The end of the probe is 6 in. forward of the aircraft's nose, 11.5 in. to the starboard side of the aircraft centerline, and 8 in. from the nearest aircraft surface.

Piper Seminole

Piper Seminole - PA-44-180

Performance Specifications

Engine

Manufacturer: Lycoming
Model: 0-360-A1H6/LO-360-A1H6
Horsepower: 180 hp

Weights

Gross Weight: 3800 lbs/1724 kgs
Standard Empty/Equipped Weight (*b,c): 2586 lbs/1173 kgs
Standard Useful Load (*a): 1230 lbs/558 kgs

Dimensions

Wing Span: 38.6 feet/11.8 meters
Length: 27.6 feet/8.4 meters
Height: 8.5 feet/2.6 meters
Wing Area: 183.8 square feet/17.08 square meters

Fuel Capacity

Usable Fuel: 108 gallons/409 litres

Maximum Speed

TAS at Gross Weight: 168 kts/311 kmh

Cruising Speeds

Normal Cruise Speed: 162 kts/300 kmh

Cruising Range

Cruising Range: 610 nm/1130 km
(45 minute reserves at 75% power)

Stall Speed

Flaps Down Full 40 degrees: IAS 55 kts/IAS 102 kmh

Service Ceiling

Twin Engine (100 fpm): 15,000 feet/4572 meters
Single Engine (50 fpm): 3,800 feet/1158 meters

Take-Off Distance

Total over 50-foot obstacle: 2200 feet/671 meters

Landing Distance

Total over 50-foot obstacle: 1490 feet/454 meters

*a. Standard Useful load is ramp weight minus standard equipped weight.
*b. The standard empty weight and standard equipped weight are the same.
*c. Standard aircraft per marketing.

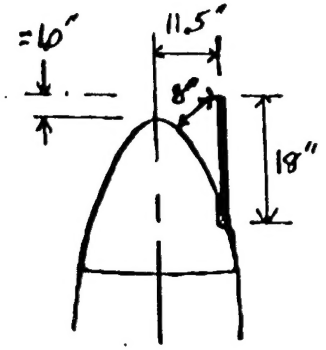

GEOMET .
Probe Location

Piper Seminole lightweight twin-engined four-seat cabin monoplane (*Pilot Press*)